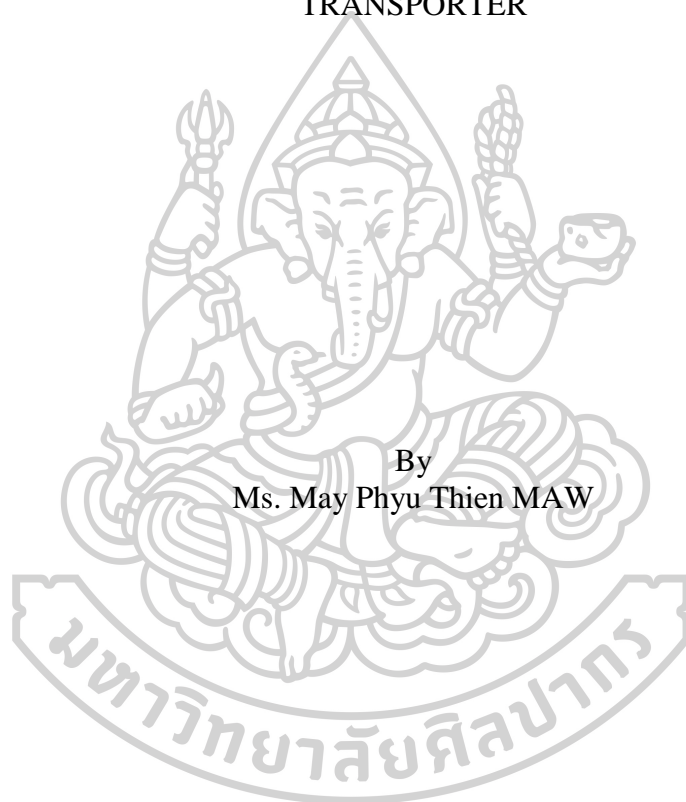




THE EFFECTS OF *CITRUS HYSTRIX* FRUIT ON P-GLYCOPROTEIN EFFLUX
TRANSPORTER



By
Ms. May Phyu Thien MAW

A Thesis Submitted in Partial Fulfillment of the Requirements
for Doctor of Philosophy (PHARMACEUTICAL SCIENCES)
Graduate School, Silpakorn University
Academic Year 2019
Copyright of Graduate School, Silpakorn University

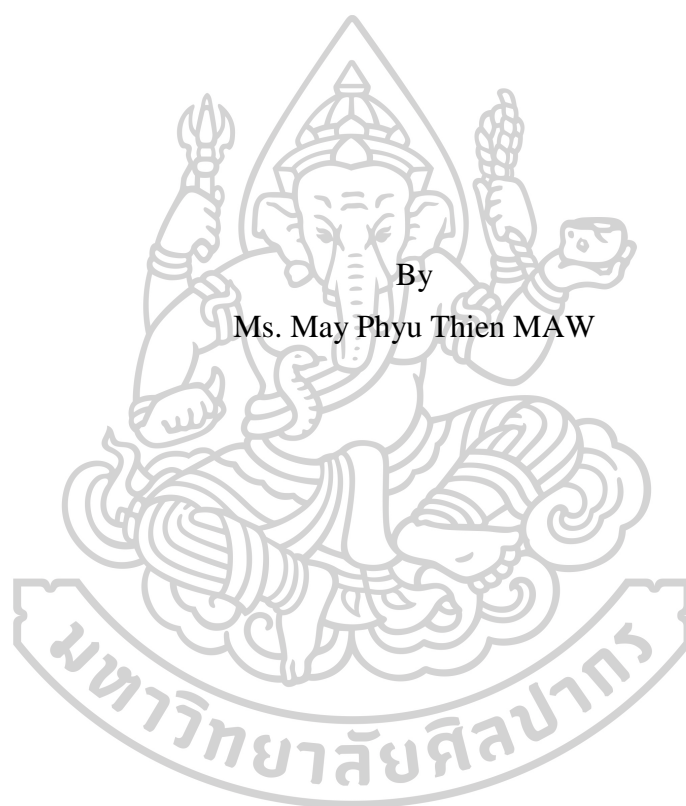


The effects of *Citrus hystrix* fruit on P-glycoprotein efflux transporter



วิทยานิพนธ์นี้เป็นส่วนหนึ่งของการศึกษาตามหลักสูตรปริญญาคุุณบัณฑิต
สาขาวิชาวิทยาการทางเภสัชศาสตร์ แบบ 1.1 ปริญญาคุุณบัณฑิต
บัณฑิตวิทยาลัย มหาวิทยาลัยศิลปากร
ปีการศึกษา 2562
ลิขสิทธิ์ของบัณฑิตวิทยาลัย มหาวิทยาลัยศิลปากร

THE EFFECTS OF *CITRUS HYSTRIX* FRUIT ON P-GLYCOPROTEIN
EFFLUX TRANSPORTER



A Thesis Submitted in Partial Fulfillment of the Requirements
for Doctor of Philosophy (PHARMACEUTICAL SCIENCES)
Graduate School, Silpakorn University
Academic Year 2019
Copyright of Graduate School, Silpakorn University

Title	The effects of <i>Citrus hystrix</i> fruit on P-glycoprotein efflux transporter
By	May Phyu Thien MAW
Field of Study	(PHARMACEUTICAL SCIENCES)
Advisor	Associate Professor Nusara Piyapolrunroj , Ph.D.

Graduate School Silpakorn University in Partial Fulfillment of the Requirements for the Doctor of Philosophy

.....Dean of graduate school
(Associate Professor Jurairat Nunthanid, Ph.D.)

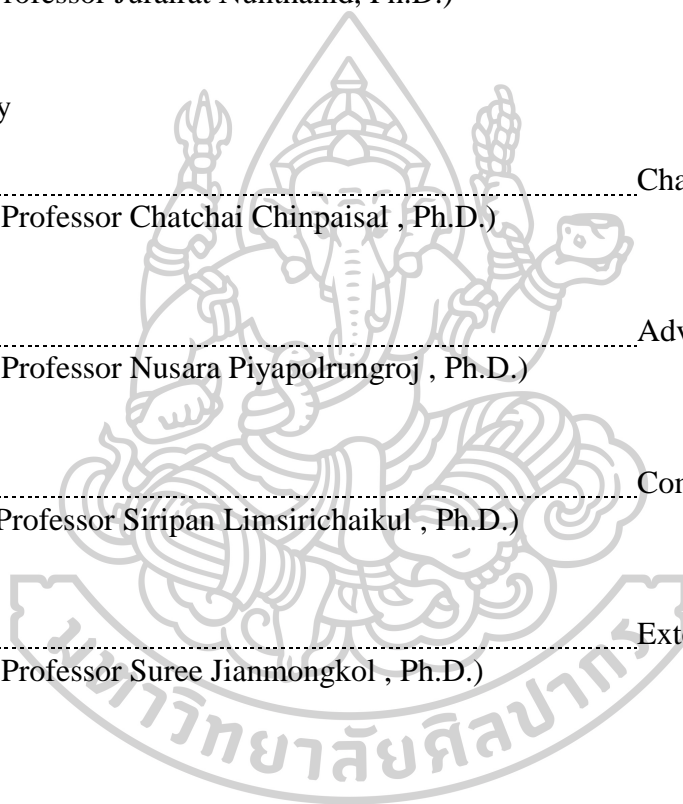
Approved by

.....Chair person
(Associate Professor Chatchai Chinpaisal , Ph.D.)

.....Advisor
(Associate Professor Nusara Piyapolrunroj , Ph.D.)

.....Committee
(Assistant Professor Siripan Limsirichaikul , Ph.D.)

.....External Examiner
(Associate Professor Suree Jianmongkol , Ph.D.)



58356803 : Major (PHARMACEUTICAL SCIENCES)

MS. MAY PHYU THIEN MAW : THE EFFECTS OF *CITRUS HYSTRIX* FRUIT ON P-GLYCOPROTEIN EFFLUX TRANSPORTER THESIS ADVISOR : ASSOCIATE PROFESSOR NUSARA PIYAPOLRUNGROJ, Ph.D.

Oral route is one of the most commonly routes of drug administration. However, there are various factors influencing the absorption of orally administered drugs into systemic circulation. P-glycoprotein, an efflux transporter expressed at the intestinal membrane, is crucial for intestinal drug absorption. Drugs taken orally may have interaction with fruits or vegetables commonly consumed in normal diet. The objective of this study was to investigate the possibility of P-gp mediated drug interactions of *C. hystrix*. The effects of extracts and/or active compounds on P-gp function and protein expression were evaluated *in vitro* using Caco-2, LLC-PK₁ and overexpressed human P-gp LLC-GA5-COL300. The results show that the flavedo extract significantly inhibited P-gp function. The furanocoumarins were isolated as the P-gp inhibitors with the order of inhibitory potency as follows: epoxybergamottin > dihydroxybergamottin > oxypeucedanin > bergamottin > oxypeucedanin hydrate. The mechanistic study of dihydroxybergamottin and oxypeucedanin revealed that both compounds reversibly inhibited P-gp function. Dihydroxybergamottin was likely to be P-gp inhibitor but not P-gp substrate. The IC₅₀ values were $39.8 \pm 0.8 \mu\text{M}$ and $41.5 \pm 2.1 \mu\text{M}$ from the uptake and transport studies, respectively. Interestingly, oxypeucedanin was possibly both substrate and reversible inhibitor of P-gp. The IC₅₀ values of oxypeucedanin from uptake and transport studies were $60.3 \pm 1.0 \mu\text{M}$ and $50.7 \pm 5.1 \mu\text{M}$, respectively. Both dihydroxybergamottin and oxypeucedanin could down-regulate the protein expression of P-gp in a concentration dependent manner. In summary, *C. hystrix* fruit and its constituent furanocoumarins could inhibit P-gp function and protein expression, implying that there is a potential for P-gp mediated drug interactions with P-gp substrate drugs. On the other hand, the P-gp inhibition effect could be employed as the potential bioenhancer to improve the bioavailability of P-gp substrate drugs. However, the *in vivo* study should be considered to confirm their effects.

ACKNOWLEDGEMENTS

First and foremost, I would like to express my deepest gratitude to my thesis advisor, Associate Professor Nusara Piyapolrungrroj for her supervision, patience, tremendous guidance, kindness and encouragement throughout my study. She provided me with various opportunities and supported me in every way. She has been a great mentor and helped me to improve my knowledge and to accomplish my research effectively.

My appreciation and deepest gratitude go to Associate Professor Auayporn Apirakaramwong, Assistant Professor Siripan Limsirichaikul, Assistant Professor Chanokporn sukonpan and Associate Professor Panadda Phatanawasin for their time, guidance and helpful advice throughout the years. I would also like to extend my sincere gratitude to Associate Professor Chatchai Chinpaisal and Associate Professor Suree Jianmongkol for their valuable comments and suggestions.

My outmost appreciation also goes to Associate Professor Tanasait Ngawhirunpat, Associate Professor Jurairat Nunthanid, Professor Pornsak Srimornsak and Lecturer Waranee Bunchuailua, for assisting me to get an opportunity for studying at Faculty of Pharmacy, Silpakorn University. I would like to express my special gratitude to the Faculty of Pharmacy, Silpakorn University, Nakhom pathom, Thailand for the scholarships, laboratory equipments and other facilities to perform research work efficiently. I would like to express my much appreciation and gratitude to every teachers and staffs in Faculty of Pharmacy, Silpakorn University for their tremendous guidance, assistance and support.

I am grateful to Ministry of Health, Myanmar and University of Pharmacy, Mandalay, Myanmar for granting permission to study Doctor of Philosophy Program in Pharmaceutical Sciences at Faculty of Pharmacy, Silpakorn University. Finally, I would like to express my deepest gratitude and sincere appreciation to my family for their love, support and encouragement throughout my life.

May Phyu Thien MAW

TABLE OF CONTENTS

	Page
ABSTRACT.....	D
ACKNOWLEDGEMENTS.....	E
TABLE OF CONTENTS.....	F
LIST OF TABLES	J
LIST OF FIGURES	K
LIST OF ABBREVIATIONS.....	M
Chapter I.....	1
Background information and Purpose of the study.....	1
Background information.....	2
1.1 Transfer of solutes across cell membrane.....	2
Cell Membrane.....	2
Transport processes.....	3
Paracellular transport.....	3
Passive diffusion.....	3
Facilitated diffusion.....	4
Active transport.....	4
<i>Primary active transport</i>	4
<i>Secondary active transport</i>	5
Endocytosis and exocytosis.....	6
1.2 Membrane transporters	6
SLC transporters.....	6
ABC transporters.....	7
1.3 P-glycoprotein.....	14
1.3.1 Structure and substrate	14
1.3.2 Distribution and function.....	16

1.4 Drug interactions	20
Metabolism-mediated drug interactions	22
Transporter-mediated drug interactions	22
1.5 Transporter-mediated plant-drug interactions	23
1.5.1 Herb-drug interactions.....	24
1.5.2 Fruit-drug interactions	25
1.6 <i>Citrus hystrix</i> (<i>C. hystrix</i>)	28
2. Purpose of the study.....	29
Chapter 2.....	31
Materials and methods	31
1. Materials	31
1.1 Apparatus and instruments	31
1.2 Chemicals and reagents	32
1.3 Cell lines	33
2. Methods	34
2.1 Preparation of crude extracts from <i>C. hystrix</i> fruits	34
2.2 Isolation of active compounds from flavedo extract of <i>C. hystrix</i>	34
2.3. Chromatographic and Spectroscopic analysis of the extracts and active compounds.....	36
TLC analysis.....	36
HPLC analysis	36
LC-MS analysis	36
¹ H-NMR analysis.....	37
2.4 P-gp function assay.....	39
2.4.1 Cell Culture	39
2.4.2 Preparation of extracts, fractions and isolated compounds	39
2.4.3 Uptake study.....	40
Calcein-AM uptake assay.....	40
Doxorubicin uptake assay	40

2.4.4 Transport study.....	41
Transport study of doxorubicin	41
Transport study of dihydroxybergamottin and oxypeucedanin.....	42
2.5 Western blotting.....	42
2.5.1 Cell lysis and sample preparation.....	43
2.5.2 Running the gel	43
2.5.3 Protein blotting	43
2.5.4 Antibody staining and Detection	44
Data analysis	44
Chapter 3	45
Results and discussions.....	45
1. Effects of <i>C. hystrix</i> fruit extracts on P-gp function.....	45
1.1 Extraction of <i>C. hystrix</i> fruits	45
1.2 Calcein-AM uptake in Caco-2, LLC-PK ₁ and LLC-GA5-COL300	47
2. Effects of the flavedo extract on P-gp function	50
2.1 Concentration dependent study.....	50
2.2 Fractionation of the flavedo extract and their effects on calcein-AM uptake in Caco-2, LLC-PK ₁ and LLC-GA5-COL300	52
3. Isolation of active compounds from flavedo extract	53
4. Identification of the active compounds and their activities on P-gp function	56
4.1 Identification of the isolated pure compounds.....	56
4.2 Effects of the isolated furanocoumarins on P-gp function	63
5. Effects of dihydroxybergamottin and oxypeucedanin on P-gp function and expression	67
5.1 Evaluation of dihydroxybergamottin and oxypeucedanin as P-gp substrate.....	67
5.2 Evaluation of dihydroxybergamottin and oxypeucedanin as P-gp inhibitor	69
5.2.1 Doxorubicin uptake assay	69
5.2.2 Doxorubicin transport assay	70
5.2.3 Inhibition mechanisms	73
5.3 Effects of dihydroxybergamottin and oxypeucedanin on P-gp expression	74

Chapter 4	77
Conclusion	77
REFERENCES	80
VITA.....	113



LIST OF TABLES

	Page
Table 1. Biological profiles of SLC and ABC transporters	8
Table 2. P-gp inhibitors and inducers	18
Table 3. Clinically significant P-gp mediated drug-drug interactions	19
Table 4. Examples of pharmacodynamic and pharmacokinetic interactions.....	21
Table 5. P-gp mediated herb-drug interactions addressed by case reports or clinical studies	25
Table 6. Clinically significant fruit-drug interactions.....	26
Table 7. Clinically significant citrus species-drug interactions	28
Table 8. Effects of the flavedо fractions on calcein-AM uptake in Caco-2, LLC-PK ₁ and LLC-GA5-COL300.....	53
Table 9. PTLC conditions used to isolate pure compounds.....	55
Table 10. Preliminary screening of the compounds on P-gp function in Caco-2, LLC-PK ₁ and LLC-GA5-COL300	56
Table 11. The content of furanocoumarins found in the flavedо of <i>C. hystrix</i> fruit....	62
Table 12. Concentration dependent effects of epoxybergamottin, dihydroxybergamottin and oxypeucedanin on calcein-AM uptake in LLC-GA5-COL300.....	65
Table 13. Apparent permeability coefficients and efflux ratio of dihydroxybergamottin and oxypeucedanin in bidirectional transport study.....	68
Table 14. P _{app, b-a} values of doxorubicin and the percentage of the control transport activity in the absence and presence of dihydroxybergamottin and oxypeucedanin performed in LLC-GA5-COL300.....	72
Table 15. The IC ₅₀ values of the dihydroxybergamottin and oxypeucedanin calculated from doxorubicin uptake and transport studies.....	73

LIST OF FIGURES

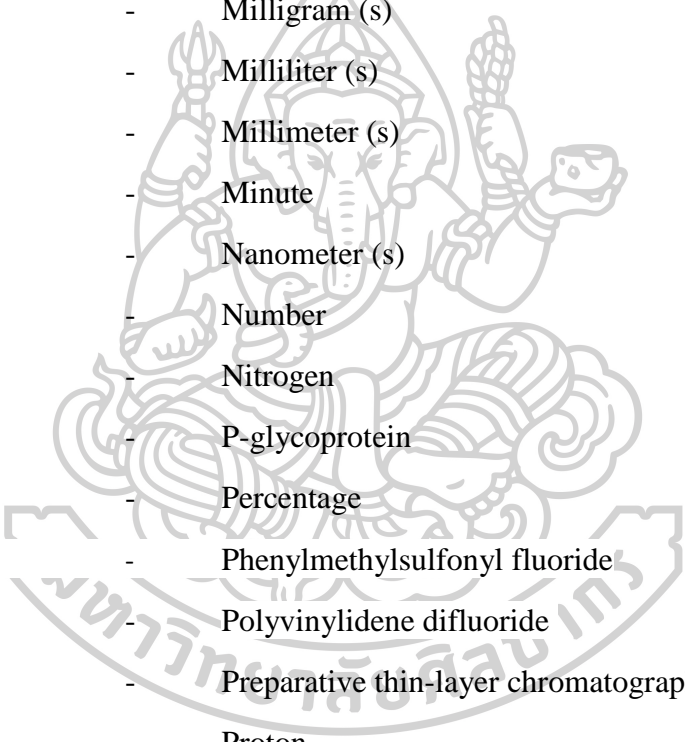
	Page
Figure 1. Schematic diagram of cell membrane	3
Figure 2. Classification of membrane transport mechanisms	5
Figure 3. Structure of P-glycoprotein	14
Figure 4. Catalytic cycle of P-glycoprotein drug efflux	15
Figure 5. Isolation of active compounds from the flavedo extract of <i>C. hystrix</i>	38
Figure 6. TLC profiles of methanolic extracts obtained from <i>C. hystrix</i> fruits	45
Figure 7. HPLC profiles of methanolic extracts (1 mg/ml) obtained from <i>C. hystrix</i> fruits	46
Figure 8. Effects of the <i>C. hystrix</i> methanolic extracts (80 µg/ml) on calcein-AM uptake in (a) Caco-2, (b) LLC-PK ₁ and (c) LLC-GA5-COL300.....	49
Figure 9. Concentration dependent effects of the flavedo extract on calcein-AM uptake in Caco-2, LLC-PK ₁ and LLC-GA5-COL300	51
Figure 10. TLC profiles of the fractions obtained from the column chromatography	52
Figure 11. TLC chromatogram of sub-fractions obtained from column chromatography of E1, E2, E3 and E5	55
Figure 12. TLC chromatogram of standard bergamottin (B) and compound <u>1</u>	57
Figure 13. TLC chromatogram of compound <u>2</u> and oxypeucedanin <u>3</u>	58
Figure 14. TLC chromatogram of standard dihydroxybergamottin (D) and compound <u>4</u>	59
Figure 15. TLC chromatogram of standard oxypeucedanin hydrate (OH) and compound <u>5</u>	60
Figure 16. TLC chromatogram of the isolated pure compounds	61
Figure 17. HPLC chromatogram of furanocoumarins found in flavedo extract of <i>C. hystrix</i> fruit.....	61
Figure 18. Structures of isolated furanocoumarins from <i>C. hystrix</i> flavedo	63
Figure 19. Effects of furanocoumarins (100 µM) on calcein-AM uptake in LLC-PK ₁ and LLC-GA5-COL300.....	64

Figure 20. Effect of cyclosporine (10 μ M) on oxypeucedanin transport in LLC-GA5-COL300.....	68
Figure 21. Effects of dihydroxybergamottin and oxypeucedanin on intracellular accumulation of doxorubicin in LLC-GA5-COL300	70
Figure 22. Effect of incubation conditions on calcein-AM uptake in LLC-GA5-COL300 in the presence of dihydroxybergamottin and oxypeucedanin	74
Figure 23. MDR1 expression in LLC-PK ₁ and LLC-GA5-COL300.....	75
Figure 24. Effects of dihydroxybergamottin and oxypeucedanin on P-gp protein expression in LLC-GA5-COL300	76



LIST OF ABBREVIATIONS

APCI	-	Atmospheric pressure chemical ionization
<i>C. hystrix</i>	-	<i>Citrus hystrix</i>
°C	-	Degree celsius
δ	-	Delta chemical shift scale
calcein-AM	-	Calcein acetoxymethyl ester
Caco-2	-	Human colonic adenocarcinoma cell line
CD ₃ OD	-	Deuterated methanol
DAD	-	Diode array HPLC detector
DMEM	-	Dulbecco's modified Eagle medium
ESI	-	Electrospray ionization
eV	-	Electron volt
EtOAc	-	Ethyl acetate
EDTA	-	Ethylenediaminetetraacetic acid
EMA	-	European medicines agency
FBS	-	Fetal bovine serum
FDA	-	Food and drug administration
G	-	Gram (s)
HBSS	-	Hanks' balanced salt solution
HPLC	-	High performance liquid chromatography
hr	-	Hour
Int	-	Intensity
kV	-	Kilovolt (s)
LC-MS	-	Liquid chromatography–mass spectrometry
l	-	Litre
LLC-PK ₁	-	Porcine kidney epithelial cell line



M199	-	Medium 199
m/z	-	Mass to charge ratio
MDR1	-	Multidrug resistance
MHz	-	Megahertz
MS	-	Mass spectrometry
MW	-	Molecular weight
μl	-	Microliter (s)
μm	-	Micrometer (s)
mg	-	Milligram (s)
ml	-	Milliliter (s)
mm	-	Millimeter (s)
min	-	Minute
nm	-	Nanometer (s)
no.	-	Number
N ₂	-	Nitrogen
P-gp	-	P-glycoprotein
%	-	Percentage
PMSF	-	Phenylmethanolsulfonyl fluoride
PVDF	-	Polyvinylidene difluoride
PTLC	-	Preparative thin-layer chromatography
¹ H	-	Proton
¹ H-NMR	-	Proton nuclear magnetic resonance spectroscopy
R _f	-	Retention factor
RFU	-	Relative fluorescence unit
rpm	-	Revolution per minute
S	-	Second
SDS	-	Sodium lauryl sulfate
TLC	-	Thin-layer chromatography
THF	-	Tetrahydrofuran

Tris-HCl	-	Tris hydrochloride
UV	-	Ultra violet
V	-	Volt
v/v	-	Volume by volume
w/w	-	Weight by weight



Chapter I

Background information and Purpose of the study

The oral route of drug administration is the most commonly used since it is convenient, relatively safe and economical. The orally administered drug must pass through the gastrointestinal epithelia to be absorbed into the systemic circulation and exert its biological effect. Various factors are affecting the rate and extent of absorption of orally administered drugs which, in turn, governed their bioavailability. Absorption from the GI tract is regulated by physicochemical properties of drugs such as lipid solubility, intestinal permeability, particle size, degradation in the gastrointestinal tract, physical state of the drug (solution, suspension, or solid dosage form) and physiological factors such as gastrointestinal pH, alteration of gut flora, altering motility, and transporter proteins (1).

Transporter proteins that are expressed in the intestine mediate the selective absorption and excretion of both endogenous compounds and xenobiotics. Transporters are generally classified into two major superfamilies, the ATP binding cassette (ABC) and solute carrier (SLC) transporters. They play a critical role in the pharmacokinetics and pharmacodynamics processes of drugs which in turn regulate the therapeutic and adverse effects (2). Among the ABC transporters, P-glycoprotein (P-gp), an efflux transporter, has been recognized as one of the important transporters that regulate the intestinal absorption of orally administered drugs. P-gp located at the apical surface of epithelial cells exports a variety of orally administered drugs, such as cyclosporin, into the intestinal lumen by utilizing ATP thereby serve as the intestinal barrier (3).

P-gp plays an important role in inhibiting optimal drug delivery of orally administered drugs since it is located at the apical surface of the intestinal cells. Modulation of P-gp function would affect the absorption of many P-gp substrate drugs (4, 5). Drugs taken orally may have interaction with herbal products, fruits or vegetables commonly consumed in normal diet. This may give rise to clinically significant pharmacokinetic interactions (6). Although the effects of fruits on P-gp mediated efflux have been reported, there is limited study available on certain fruits

that may modulate the bioavailability of drugs. This study was conducted to investigate the effect of *C. hystrix* fruits on the function of P-gp.

Background information

1.1 Transfer of solutes across cell membrane

A drug can be administered into the human body by various routes of administration. Apart from introducing directly into the systemic circulation, drug must pass through cell membrane in order to process absorption, distribution, metabolism, excretion, and subsequently to exert an action of a drug.

Cell Membrane

The cell membrane is made up of phospholipid bilayer of lipid which consists of hydrophobic hydrocarbon chains (fatty acid) oriented inward and hydrophilic heads (glycerol and phosphorylated alcohol) oriented outward. Cell membrane can move laterally and the lipid molecules present endorsed cell membrane with fluidity, flexibility, organization, high electrical resistance, and relative impermeability to highly polar molecules. Membrane proteins embedded in the bilayer serve as structural anchors, receptors, ion channels, or transporters to transduce electrical or chemical signaling pathways and provide selective targets for drug actions (1). Carbohydrates are also present in the membrane as glycoproteins or glycolipids linked to either proteins or lipids (Figure 1) (7).

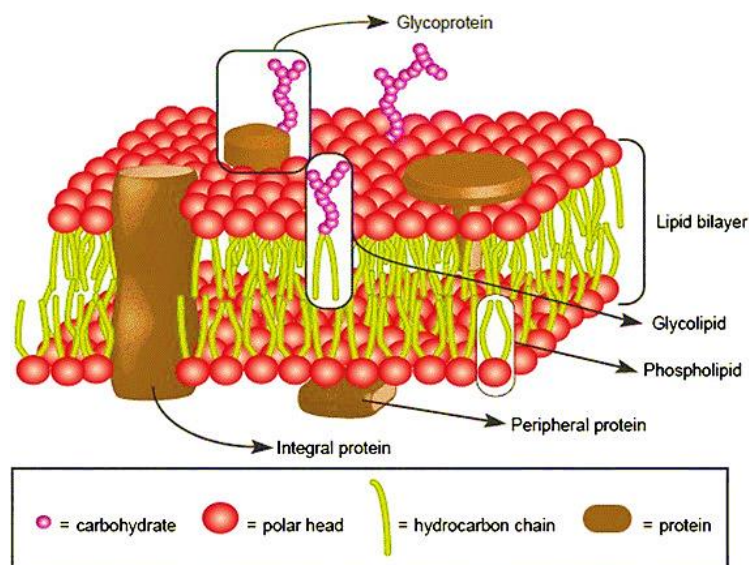


Figure 1. Schematic diagram of cell membrane

(7)

Transport processes

The solute can be transported across cell membrane by the following mechanisms: paracellular transport and transcellular transport such as passive diffusion, facilitated diffusion and active transport, endocytosis and exocytosis (Figure 2) (2, 8, 9).

Paracellular transport

In paracellular transport, small molecules such as Na^+ or Cl^- can pass through the tight junctions between the epithelial cells of the cellular membrane according to their electrochemical gradient (9, 10). The extent of absorptivity through paracellular transport depends on the different epithelia. Generally, molecules larger than 11-15 Å cannot pass the cell membrane through paracellular transport.

Passive diffusion

Diffusion of solute across cell membrane according to their concentration gradient is called passive diffusion. The rate of diffusion depends on the magnitude of

the concentration gradient across the membrane, the lipid-water partition coefficient of the drug and membrane surface area exposed to the drug. The greater the partition coefficient, the higher is the concentration of drug in the membrane and the faster is its diffusion. After a steady state is attained, the concentration of the unbound drug is the same on both sides of the membrane if the drug is a non-electrolyte. For ionic compounds, the steady-state concentrations depend on the electrochemical gradient for the ion and on differences in pH across the membrane (2). Passive diffusion does not saturate, does not require energy and cannot be inhibited by analogues which use similar transport (11). Orally administered drugs that are absorbed rapidly and completely are transported by passive diffusion (12).

Facilitated diffusion

Facilitated diffusion is a transport of solute across cell membrane which is facilitated by membrane transporter. Since solute can cross the cell membrane according to electrochemical gradient as in the passive diffusion, no energy is required e.g. permeation of glucose across a muscle cell membrane mediated by the insulin-sensitive glucose transporter GLUT4. This type of transport is illustrated by selective, saturable and competitively inhibited by analogues that use the same transport system (2).

Active transport

Active transport is a transport of solute against their electrochemical gradient by utilizing energy. Active transport is characterized by movement of solute against electrochemical gradient, requirement of energy, selectivity, saturation at high concentration and competitive inhibition by co-transported compounds. Active transport can be divided into two types, primary and secondary active transport (2).

Primary active transport

Primary active transport is a type of membrane transport that utilizes energy directly from hydrolysis of ATP. ABC transporters and Na^+/K^+ -ATPase are examples of primary active transport (2). They consist of ATP binding domain and a highly

conserved domain that exhibits ATPase activity. In mammalian, primary active transporter effluxes out of the solute from the cell in a unidirectional manner (9).

Secondary active transport

Secondary active transport is the transport of solute (S1) against its concentration gradient by utilizing energy obtained from the passage of another solute (S2) across cell membrane according to its concentration gradient (9) e.g. Na^+ -dependent glucose transporters SGLT1 and SGLT2 move glucose across membranes of gastrointestinal (GI) epithelium and renal tubules by coupling glucose transport to downhill Na^+ flux. Secondary active transporter can be classified into two groups according to the direction of passage of two solutes across cell membrane. If the transport of the two solutes (S1 and S2) across cell membrane is in the same direction, it is called symporters or cotransporters (2). Examples of symporters are the sodium dependent glucose transporter or the sodium dependent amino acid transporters. Whereas, transport of the two solutes (S1 and S2) in opposite direction, it is called antiporters e.g. $\text{Na}^+/\text{Ca}^{2+}$ exchanger in cardiac muscle cells or the Na^+/H^+ exchanger involved in regulation of cytosolic pH (9).

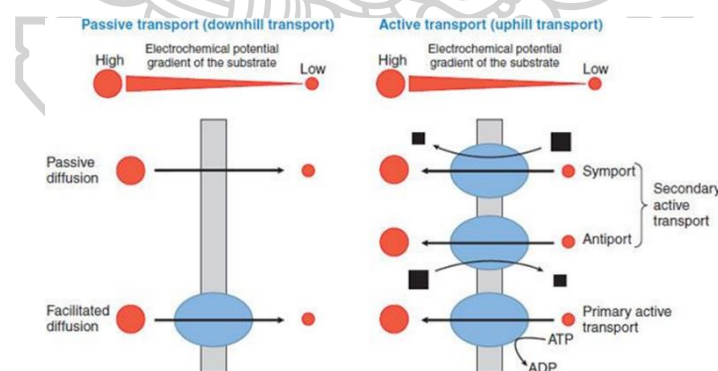


Figure 2. Classification of membrane transport mechanisms

(2). Light blue circles; the substrate (Size of the circles is proportional to the concentration of the substrate, arrows show the direction of flux). Black squares; the ion that supplies the driving force for transport (size is proportional to the concentration of the ion). Dark blue ovals; transport proteins.

Endocytosis and exocytosis

Large molecular weight polypeptides such as peptide antigens move across cell membrane by means of endocytosis and exocytosis mechanism by utilizing energy (9). There are two types of endocytosis, namely phagocytosis and pinocytosis. In endocytosis, uptake of foreign substance, either a solid or a liquid, occur through the formation of endocytic vesicle. Ingestion of solid particles such as food particles, cell debris, dead cells, bacteria and viruses is called phagocytosis. Pinocytosis is the uptake of fluids along with the dissolved solutes (e.g. nutrients). Exocytosis is the process of elimination of cellular waste and secretion of contents into the external environment from the cell by forming secretory vesicles which is fused with the plasma membrane (13).

1.2 Membrane transporters

Transporters are membrane bound proteins varying from 40–200 kDa that are expressed in membranes of all organisms. They regulate the transport of essential nutrient, ions, cellular waste, environmental toxins and other xenobiotics into and out of the cells (9). The basic mechanisms of membrane transporters may be facilitated or active transport. Transporters are generally classified into two major superfamilies, the ATP binding cassette (ABC) and solute carrier (SLC) transporters.

SLC transporters

The SLC transporter family consists of 395 transporters and grouped into 52 distinct subfamilies, including proton-dependent oligopeptide transporters (POT), organic anion transporters (OAT), organic cation transporters (OCT), nucleoside transporters (CNT), monocarboxylate transporters (MCT) and the multidrug and toxin extrusion proteins (MATE) (14). The SLC transporters import substrates into the cells except MATE transporters which efflux their substrates out of the cells (15). They can be classified as either facilitative diffusion transporters, which transport substrates according to their concentration gradient across the membrane, or secondary active transporters, which transport substrates against the concentration gradient across the membrane driven by a transport of another substrate (16). The SLC transporters

transport various substrates including essential nutrients and metabolites such as glucose, amino acids, vitamins, neurotransmitters, and inorganic/metal ions (17).

ABC transporters

The ABC transporter family consists of 48 genes and can be categorized into seven subfamilies ranging from ABCA (12 members), ABCB (11 members), ABCC (13 members), ABCD (4 members), ABCE (1 member), ABCF (3 members) and ABCG (5 members). The ABC transporters are primary active transporters which utilize energy obtained from ATP hydrolysis to transport the substrate against their electrochemical gradient. These transporters mediate the transport of endogenous compounds such as conjugated bile salts, steroid hormones, cholesterol, unconjugated bilirubin and exogenous compounds (18, 19).

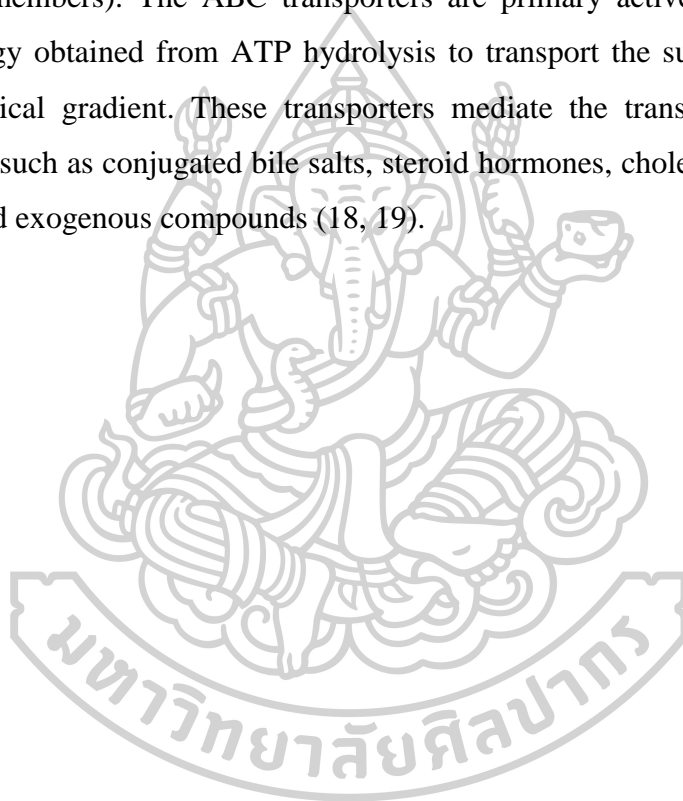


Table 1. Biological profiles of SLC and ABC transporters

(20-22)

Gene	Protein (alias)	Tissue	Physiological roles	Physiological substrate	Drug substrate
<i>SLC transporters</i>					
<i>SLC10A1</i>	NTCP	Liver	Uptake of bile acids into the hepatocytes from the sinusoids	Bile salts, sulfo-conjugated bile acids, sulfated steroids, sulfated thyroid hormones, Bromosulphthalein	Rosuvastatin, fluvastatin atorvastatin, pitavastatin
<i>SLC10A2</i>	ASBT	Intestine, kidney, gallbladder	Bile acids absorption	Bile acids, taurine- and glycine-conjugated bile acids	Naphtol derivatives Dimeric bile acid analogues Benzothiazepine derivatives
<i>SLC22A1</i>	OCT1	Liver	Uptake of cationic compounds across the sinusoidal membrane into hepatocytes; reabsorption of cationic compounds in kidney	Thiamine, choline, acetylcholine, monoamine neurotransmitters	Metformin, oxaliplatin, aciclovir, ganciclovir, lamivudine, berberine, picoplatin, irinotecan, palitacel
<i>SLC22A2</i>	OCT2	Major: kidney; others: brain small intestine, lung, placenta, skin	Uptake of organic cationic compounds for renal excretion; reabsorption of choline, dopamine etc	Creatinine, bile acids, acetylcholine, dopamine, norepinephrine, epinephrine, serotonin, histamine	Metformin, cimetidine, procainamide, amiloride, cisplatin, debrisoquine, propranolol, ranitidine, pancuronium, berberine

Gene	Protein (alias)	Tissue	Physiological roles	Physiological substrate	Drug substrate
<i>SLC22A3</i>	OCT3	Ubiquitously expressed. Major: kidney, liver, placenta, heart, and skeletal muscle	Uptake of organic cationic compounds into brain, heart and liver; involved in the distribution of cationic compounds in the brain	Creatinine, serotonin acetylcholine, dopamine, steroids, histamine, epinephrine	Lidocaine, atropine, lamivudine, phenoxybenzamine, prazosin, verapamil, metformin, nicotine, cimetidine, amantadine, ranitidine, ketamine, quinidine, procainamide
<i>SLC22A4</i>	OCTN1	Ubiquitously expressed	Involved in the reabsorption of zwitterions and the secretion of cations in the proximal tubule	Ergothioneine, carnitine, acetylcholine, glycinebetaine	Pregabalin, ipratropium, pyrilamine, gabapentin, quinidine, quinine, verapamil, doxorubicin, ipratropium
<i>SLC22A5</i>	OCTN2	Ubiquitously Expressed Major: intestine, kidney	Uptake of carnitine into small intestine, kidney, adipocytes, cardiac myocytes, skeletal muscle cells, neurons, brain, lymphocytes, spermatozoa, and across the blood-retinal barrier	Carnitine, choline	Etoposide, cephaloridine, ipratropium, tiotropium, emetine, oxaliplatin, mildronate, verapamil, spironolactone, pyrilamine
<i>SLC22A6</i>	OAT1	Major: kidney; others: choroid plexus in brain, skeletal muscle and placenta	Uptake of urate and other anionic compounds for renal excretion	Medium chain fatty acids, cAmp, cGmp, prostaglandin E2, F2, urate	Adefovir, zidovudine, ciprofloxacin, statins, cephaloridin, methotrexate, pravastatin, diuretics, antibiotics, antivirals

Gene	Protein (alias)	Tissue	Physiological roles	Physiological substrate	Drug substrate
<i>SLC22A7</i>	OAT2	Liver, Kidney	Efflux of glutamate into the sinusoids and uptake of various organic anion compounds into hepatocyte; tubular secretion of urate and organic anion compounds; possibly involved in regulation of intracellular cGMP content	Glutamate, glutarate, urate, ascorbate, hypoxanthine, GMP, GDP, GTP, cGMP, cAMP, prostaglandin E2, F2, α -ketoglutarate	Salicylate, bumetanide, erythromycin, tetracycline, zidovudine, ranidine, 5-fluorouracil, paclitaxel, allopurinol, methothrexate, taxol
<i>SLC22A8</i>	OAT3	Kidney, brain, skeletal muscle, developing bone	Involved in renal secretion of urate and indoxyl sulfate and anion drug metabolites; involved in removal of neurotransmitter and anion drug metabolites from brain	cAMP, cortisol, prostaglandin E2, F2a, estrone sulfate, estradiol-17 β -glucuronide, taurocholate, cholate, urate, indoxyl sulfate	Benzylpenicillin, tetracycline, valacyclovir, zidovudine, adefovir, tenofovir, oseltamivir, cimetidine, famotidine, ranitidine, fexofenadine, furosemide, pravastatin, indomethacin, salicylate, ketoprofen, ibuprofen, rosuvastatin, topotecan
<i>SLC47A1</i>	MATE1	Major: Liver and kidney; Others: adrenal gland, testes, heart and skeletal muscle	Renal and biliary excretion of endogenous and exogenous organic cations	Peptides and nucleosides, creatinine, guanidine, thiamine, E3S	Metformin, cephalixin, acyclovir, gancyclovir, fexofenadine, oxaliplatin
<i>SLC01A2</i>	OATP1A2	Major: brain, kidney, liver,	Transportation of organic anionic, neutral and cationic	Cholic acid, DHEAS, prostaglandin E2,	Erythromycin, atenolol, fexofenadine, celiprolol,

Gene	Protein (alias)	Tissue	Physiological roles	Physiological substrate	Drug substrate
		intestine	compounds; delivery and removal of thyroid hormones	taurocholate, , bilirubin thyroxine, triiodothyronine,	fluoroquinolones, rosuvastatin lopinavir
<i>SLCO1B1</i>	OATP1B1	Liver	Involved in drug disposition and is responsible for the hepatic uptake of drugs and endogenous compounds	Bile acids, bilirubin, steroid hormones, thyroid hormones	Statins, repaglinide, olmesartan, enalapril, temocaprilat, valsartan, Phalloidin
<i>SLCO1B3</i>	OATP1B3	Liver	Involved in drug disposition and is responsible for the hepatic uptake of drugs and endogenous compounds	Bilirubin, bile acids, conjugated steroids, eicosanoids and thyroid hormones	Statins, fexofenadine, enalapril, erythromycin, valsartan, docetaxel, digoxin, paclitaxel
ABC transporters					
<i>ABCB1</i>	MDR1/ Pgp/ ABCB1	Ubiquitously expressed Major: intestine, brain, liver, kidney	Export of xenobiotics from cells into extracellular spaces (e.g. at the BBB) or out of the body (e.g. in the gut) and for renal and hepatic clearance	Steroids, lipids, bilirubin, bile acids	Digoxin, loperamide, berberine, irinotecan, doxorubicin, vinblastine, paclitaxel, fexofenadine, seliciclib
<i>ABCB11</i>	BSEP/ ABCB11	Major: liver; others: intestine, kidney, brain, placenta, testis	Disposition of bile salts from the liver, into the bile canaliculi for export into the gut	Bile acids	Pravastatin, vinblastine
<i>ABCC1</i>	MRP1	Ubiquitously expressed testis, cardiomyocytes, placenta, lung, prostate, thymus	Efflux of xenobiotic and endogenous metabolites; transport of inflammatory mediators (e.g. LTC4)	Leukotrienes, prostaglandins, folic acid, leucovorin, glucuronide conjugates of: 17 β -estradiol	Adefovir, indinavir, saquinavir, ritonavir, methotrexate, etoposide, doxorubicin, vincristine, daunorubicin, vinblastine

Gene	Protein (alias)	Tissue	Physiological roles	Physiological substrate	Drug substrate
		and kidney, with lower expression in small intestine, colon, brain			
<i>ABCC2</i>	MRP2	Major: liver, kidney, intestine; Others: gallbladder, bronchi, and placenta	Terminal excretion and detoxification of endogenous and xenobiotic anionic compounds	Bilirubin, leukotriene C ₄ , 17 β -estradiol, cholecystokinin peptide	Glutathione and glucuronide conjugates, methotrexate, etoposide, valsartan, olmesartan
<i>ABCC3</i>	MRP3	Ubiquitously expressed Major: Liver and intestine	Physiological regulation of bile salt enterohepatic circulation, as well as the disposition of phytoestrogens	Bile salts, estradiol-17 β -glucuronide, leukotriene C ₄	Fexofenadine, etoposide methotrexate, vincristine, acetaminophen
<i>ABCC5</i>	MRP5	Ubiquitously expressed	May be involved in cellular signaling by eliminating camp and cgmp from the cells, protective function against xenobiotics	cAmp, cGmp, folate, hyaluronan	Methotrexate, 6-, 6-thioguanine, 9-(2-phosphonylmethoxyethyl)-adenine (PMEA), 5-fluorouracil, rosuvastatin, atorvastatin
<i>ABCG2</i>	BCRP/ ABCG2	Intestine, liver, kidney, brain, placenta,	Regulation of intestinal absorption, biliary and renal secretion of substrates and	Dietary flavonoids, uric acid estrone 3-sulfate	Anthracyclines, daunorubicin, doxorubicin, topotecan,

Gene	Protein (alias)	Tissue	Physiological roles	Physiological substrate	Drug substrate
		mammary glands	protection of the fetus and brain from toxins; a major role in the multidrug resistance		SN-38, irinotecan, methotrexate, imatinib, irinotecan, mitoxantrone, nucleoside analogs, prazosin, pantoprazole, statins, topotecan

1.3 P-glycoprotein

P-glycoprotein (P-gp), human multidrug resistance protein 1, is an efflux transporter which is encoded by multidrug resistance (*MDR*) 1 gene (also known as *ABCB1*) and belongs to ATP-binding cassette (ABC) transporter superfamily (3).

1.3.1 Structure and substrate

P-gp is a 170 kDa membrane protein consisting of 1280 amino acids and composed of two homologous halves (610 amino acids each) joined by linker region (~ 60 amino acids). The basic structure consists of two transmembrane domains (TMD1 and TMD2) and two intracellular nucleotide binding domains (NBD1 and NBD2) (Figure 3). Transmembrane domains function as substrate binding sites and contain six membrane spanning (TM) segments for each domain. Nucleotide binding domains include Walker A, Walker B, a glutamine loop (Q-loop) and a switch motif which are responsible for ATP binding, hydrolysis and conformational changes (20-23). It has been reported that there are two binding sites for ATP but hydrolysis of ATP occurs one by one. P-gp substrate drugs activate adenosine triphosphate (ATPase) activity which then hydrolyzes ATP (23).

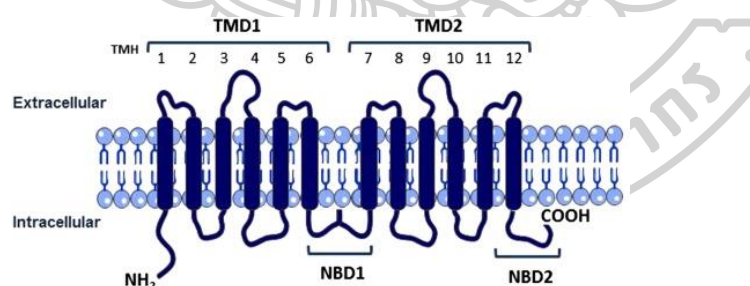


Figure 3. Structure of P-glycoprotein

(20)

Study of X-ray crystal structure of mouse P-gp, which has 87% sequence similarity with the human P-gp described that the protein has inward facing conformation owing to the two halves of six TMDs. This conformation results in a large internal cavity, which is open to the cytoplasm and the inner leaflet of the membrane. TMs 4/6 and 10/12 form two portals through which hydrophobic

molecules can enter into the cavity directly from the inner leaflet. By this way the entry of the substrates from the inner membrane leaflet is allowed and entry from outer leaflet and extracellular is limited (18, 20).

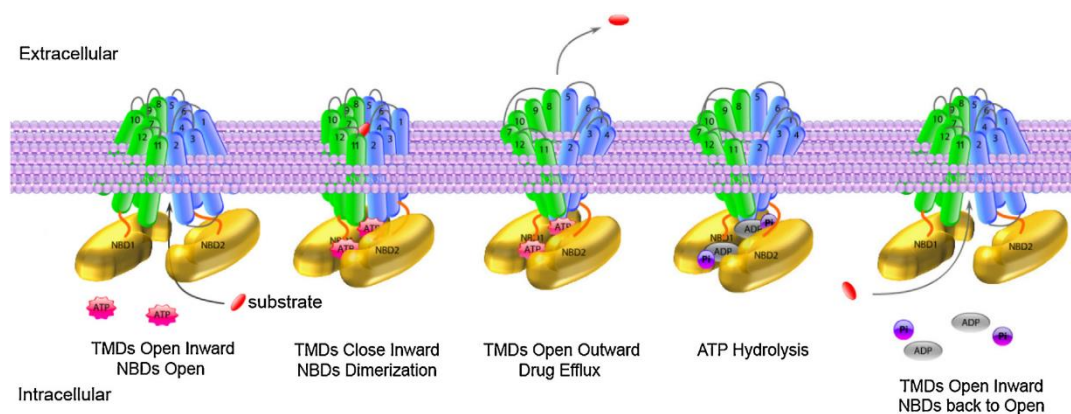


Figure 4. Catalytic cycle of P-glycoprotein drug efflux
(22)

There are different models namely pore, flippase and hydrophobic vacuum cleaner model which explain the catalytic cycle of P-gp drug efflux. In the hydrophobic vacuum cleaner model, substrates pass through the lipid bilayer and then enter into the binding cavity of the P-gp. Following this the pump exports substrates directly to the external aqueous phase. While in the flippase model, a substrate passes through the inner leaflet of the membrane and subsequently enters into the drug binding cavity of P-gp. The pump flips substrate into the outer membrane instead of transporting directly to the extracellular medium. Then the substrate diffuses into the external phase by means of concentration gradient. The pore model is described as an interaction of P-gp with drugs within the boundaries of the cytosol, followed by efflux out of the cell via protein channels (24, 25).

The transport process of substrate by P-gp consists of substrate binding, conformational changes from inward-facing to outward-facing, binding and hydrolysis of ATP, dissociation of substrate and rearranging the pump to the basal state. When the substrate binds to the TMD from inner membrane, the dimerization of the NBD occurs. Binding of ATP to NBD induces conformation changes from inward opening to outward opening position. This outward facing conformation facilitates the

translocation process of substrate. Then substrates is released into the extracellular by the hydrolysis of ATP to ADP and phosphate. The NBDs dissociate and return to the basal position to start new transport cycle (Figure 4) (20, 22, 23).

Physicochemical characteristics such as log P and hydrogen-bond donor/acceptor atoms are important for substrates to be recognized by P-gp. In addition, the basic nitrogen atom and two planar aromatic rings are required for the substrates to be exported out of the cells by P-gp (26, 27). It was later reported that compounds which do not have a basic protein nitrogen atom are also transported by P-glycoprotein (27). These substrates are usually hydrophobic, amphipathic with molecular weight of 200-300 kDa (28). However, neutral compounds such as cyclosporine A and digoxin, negatively charged molecules such as atorvastatin and fexofenadine, and some hydrophilic drugs such as methotrexate are also substrates of P-gp (14).

1.3.2 Distribution and function

In 1976, Juliano and Ling found that there was a cross-resistant between colchicine resistant chinese hamster ovary cells and other structurally and functionally unrelated drugs such as vancomycin, daunomycin. They found that drug resistance is due to the reduced permeability of drugs which was governed by the carbohydrate containing protein in the membrane. They termed this protein as permeability glycoprotein or P-glycoprotein (P-gp) (29).

High expression of P-gp is found on the multidrug resistant (MDR) tumour. It effluxes out various clinically useful anticancer drugs such as anthracyclines (e.g. doxorubicin), vinca alkaloids (e.g. vincristine), podophyllotoxins (e.g. etoposide) and taxanes (e.g. taxol) (30). Lower intracellular drug concentration results in sub-optimal treatment and treatment failure. P-gp is one of the barriers to successful clinical drug therapy (31). Cancer such as leukemias, multiple myeloma, and several pediatric cancers develop multidrug resistance (MDR) during the course of treatment. Patients with renal and colon cancer are prone to MDR even at initial treatment because there is intrinsic P-gp action in kidney and colon (32).

Interestingly, P-gp is highly expressed in the normal tissues such as apical surface of epithelial cells of liver, kidney and intestine, etc. It functions as a barrier to the toxicity of endogenous and exogenous substances by facilitating their excretion (33). P-gp limits the absorption of toxic molecules by pumping out of the enterocytes into the lumen and facilitates the elimination of toxin and metabolites into bile in the hepatocyte. In kidney, P-gp mediates the transports of substrates from the blood into the urine. Thus, this efflux transporter plays an important role in absorption and elimination processes (18, 20, 28, 34). It is also expressed in the brain and limits the entry of substrates from the blood thus protecting the brain from toxic compounds. At the placenta, high level of P-gp expression is found for preventing the fetus from toxins. P-gp at the adrenal gland and uterine endometrium transports hormones such as steroid hormones. At hematopoietic progenitor cells, P-gp prevents the bone marrow from the toxicity of chemotherapeutic drugs. It also expresses at low level in skeletal muscle, skin, prostate, lungs, heart, spleen and ovary (14, 18, 20, 28, 31, 34).

Induction or inhibition of this transporter can result in drug interactions. Drug which induces P-gp can decrease the bioavailability of susceptible drug. On the other hand, drug which inhibits P-gp can increase the bioavailability of another drug. Several therapeutic drugs, natural products and pharmaceutical excipients are reported to inhibit and induce P-gp. The examples of P-gp inhibitors and P-gp inducers are summarized in table 2.

In summary, the location of P-gp suggests that its primary physiological role is to protect organs and the fetus from toxic substances. However, it can affect the treatment efficacy by modifying the absorption, excretion and limits the access of xenobiotics to the brain and the fetus (31).

Table 2. P-gp inhibitors and inducers

(35, 36)

Inhibitors				Inducers
1 st generation	2 nd generation	3 rd generation	Others	
Amiodarone, Quinidine, Verapamil, Felodipine, Nifedipine, Diltiazem Vinblastine, Erythromycin, Clarithromycin Omeprazole, Esomeprazole, Pantoprazole, Cyclosporine A, Ritonavir, Chlorpromazine	Dexverapamil, Gallopamil, PSC 833 (valspodar), MS-209, Reversin 121, Reversin 125	XR 9576 (tariquidar), VX-710 (biricodar), GF 120918 (elacridar), OC 144-093, LY335979 (zosuquidar), Mitotane (NSC-38721), Annamycin	Natural product, Pharmaceutical excipients	Rifampin, Phenytoin, reserpine, carbamazepine St. John's wort Rifabutin, Quercetin,

1.3.3 Role of P-gp in intestinal absorption

Oral route is one of the most common routes of drug administration because it is economic, relatively safe and better compliance (37). However, there are various factors affecting the rate and extent of absorption of orally administered drugs into systemic circulation. These factors can be categorized into 1) physicochemical properties of a drug e.g. solubility, lipophilicity, intestinal permeability, pKa, particle size, etc., 2) physiological factors e.g. gastrointestinal pH, gastric emptying, intestinal

transit time and intestinal transporters, etc., 3) formulations e.g. solution, capsule, tablet, suspension, etc. (14, 24, 38).

After oral administration, drug molecules have to pass through the intestinal membrane by means of passive diffusion or active transport. One of the factors that affects oral drug absorption is efflux transporter P-gp located at the intestinal membrane. P-gp exports a variety of structurally and pharmacologically unrelated substances. A narrow therapeutic range e.g. digoxin (39) was also reported to be affected by P-gp. Anticancer agent paclitaxel, which is widely used in the treatment of breast and ovarian cancer has poor bioavailability after oral administration. It is found that P-gp in the intestinal membrane pumps the drug directly into the intestinal lumen causing low absorption (40). P-gp mediated clinically significant drug interactions of various drugs including drugs with narrow therapeutic range drugs are shown in table 3. Therefore, P-gp efflux transporter is recognized as a determining factor of oral bioavailability and intestinal efflux of drugs (41).

Table 3. Clinically significant P-gp mediated drug-drug interactions
(42)

Interacting drug	Affected drug	Clinical pharmacokinetic impact (fold change)				
		AUC	C _{max}	CL _R	CL/ F	t _{1/2}
Cyclosporin	Docetaxel	7.3	5.7	ND	ND	ND
Cyclosporin	Paclitaxel	8.5	2.0	ND	ND	ND
Dronedaron	Digoxin	2.3	1.7	0.5	ND	ND
Elacridar	Topotecan	2.4	2.8	ND	ND	NS
Erythromycin	Simvastatin	6.2	3.5	ND	ND	NS
Indinavir/ Ritonavir	Fexofenadine	4.8	2.5	ND	0.2	0.7
Itraconazole	Digoxin	1.7	NS	0.8	ND	NS

Interacting drug	Affected drug	Clinical pharmacokinetic impact (fold change)				
		AUC	C _{max}	CL _R	CL/ F	t _{1/2}
Itraconazole	Quinidine	2.4	1.6	0.5	ND	1.6
Lovastatin	Verapamil	1.6	1.3	ND	ND	NS
Quinidine	Digoxin	ND	ND	0.7	0.6	ND
Ranolazine	Digoxin	1.6	1.5	ND	ND	ND
Ritonavir	Digoxin	1.9	ND	0.6	0.6	2.6
Ritonavir	Saquinavir	29.9	22.5	ND	ND	ND
Valsopodar	Digoxin	3.0	2.4	0.2	0.3	ND
Verapamil	(R)-Fexofenadine	2.9	2.2	ND	0.4	NS
Verapamil	(S)- Fexofenadine	2.2	2.2	ND	0.5	NS
Verapamil	Simvastatin	4.6	2.6	ND	ND	NS

ND = not determined

NS = not significant

1.4 Drug interactions

There is an increasing frequency of people using more than one drug at a time. As a result unanticipated, unrecognized or mismanaged interactions can occur. Drug interactions can lead to have desired, reduced or unwanted effects (43). In addition to drug-drug interactions, concurrent ingestion of food, beverages, dietary supplements or alternative medicine (drug-nutrient/food/herb interactions) could also alter systemic exposure of drugs. Underlying disease condition can also cause drug-disease interactions (44). Therefore it is important to evaluate drug interactions scientifically to know the potential of interactions and prevent the risk concerning with drug-interactions (45).

Drug interactions can be classified into two broad categories: interactions altering pharmacodynamics and interactions altering pharmacokinetic mechanisms. There is a potential for pharmacodynamic interactions when drugs compete with each other at the pharmacological target and/or have similar (therapeutic) or opposite (adverse) pharmacodynamic effects (46). Pharmacokinetic drug interactions occur at absorption, distribution, metabolism and excretion processes (39). Examples of pharmacodynamic and pharmacokinetic interactions are shown in table 4. Recently, drug interaction concerning with pharmacokinetic processes has been one of the important reasons of drug withdrawal from the market (47). One of the major mechanisms of pharmacokinetic drug interactions involves inhibition or induction of metabolizing enzymes and/or drug transporters.

Table 4. Examples of pharmacodynamic and pharmacokinetic interactions
(39, 43, 48)

Drug I	Drug II	Possible effects
Pharmacodynamic interactions		
Nonsteroidal anti-inflammatory drug	Selective serotonin reuptake inhibitor	Increased risk of bleeding
Warfarin	Aspirin	Increased risk of gastric bleeding
Nonsteroidal anti-inflammatory drug	Glucocorticoids	Increased risk of gastric Bleeding
ACE inhibitors	Spironolactone, amiloride	Hyperkalemia
ACE inhibitors	Nonsteroidal anti-inflammatory drug	Reduced effect
Phenprocoumon	Vitamin K	Reduced effect
Pharmacokinetic interactions		
Levothyroxine	Antacids	Decreased absorption of levothyroxine
Warfarin	Diclofenac	Displacement of warfarin from its binding site and cause bleeding

Omeprazole	Clopidogrel	Decreased the antiplatelet activity of clopidogrel by inhibiting of prodrug into active metabolite
Methotrexate	Nonsteroidal anti-inflammatory drug	Increased toxicity by inhibiting methotrexate excretion

Metabolism-mediated drug interactions

Drug-metabolizing enzymes metabolize and facilitate elimination of xenobiotics or drugs introduced into the body. Drug metabolizing enzymes can be classified into phase I and phase II. Phase I metabolizing enzymes involve cytochrome P450 (CYP) superfamily enzymes. Among the CYP enzymes, CYP3A4 metabolizes about 50–60% of all clinically used drugs. This was followed by CYP2B6 which metabolizes about 25% of the xenobiotics. Phase II metabolizing enzymes consist mainly of sulfotransferases (SULT), UDP-glucuronosyltransferases (UGT), and glutathione transferases. Of all the organs the liver and intestine are the predominant sites for drug metabolizing enzymes. Orally administered drugs mostly encounter first-pass metabolism by enzymes located at the intestine and/or liver, before it reaches the systemic circulation (49, 50). As reported, the activity of the enzymes can be modified through inhibition or induction, when a drug is coadministered with the enzyme inhibitors or inducers. This may modulate the bioavailability of the drug leading to metabolism mediated drug interactions (51).

Transporter-mediated drug interactions

Although less well recognized than metabolizing enzymes, membrane transporters can have clinically relevant effect on efficacy and safety of drugs by modulating absorption, distribution and excretion processes (52). For orally administered drugs, the ABC and SLC transporters expressed in the membrane of enterocyte regulate the transport of endogenous (e.g. creatinine and glucose) and exogenous including drugs and xenobiotics (41). Because there have been clinically significant drug interactions reported with P-gp, breast cancer resistance protein

(BCRP), organic anion transporting polypeptide (OATP1B1/OATP1B3), organic anion transporter (OAT1/OAT3), multidrug and toxin extrusion (MATE) proteins, organic cation transporter 2 (OCT2) transporters, FDA regulatory guidance suggests that interaction associated with these transporters should be studied (53).

Among the ABC transporters, P-gp is well characterized and plays a vital role in pharmacokinetic mechanisms of several clinically important drugs (42, 54). Because of its localization as a barrier to various organs and wide substrate spectrum, drug interactions can occur by modulation of this protein. This especially concerns with narrow therapeutic drug such as digoxin because even small variations in plasma concentration may modify its efficacy and/or toxicity. Therefore regulatory agencies including US Food and Drug Administration (FDA) and the European Medicines Agency (EMA) recommend to evaluate the inhibitory potential of drugs on P-gp (55).

1.5 Transporter-mediated plant-drug interactions

Nowadays, the consumptions of medicinal plants have been increased. World Health Organization estimated that about 70% of world population currently utilized medicinal plants as complementary and alternative medicine (56). When patients taking medicines concomitantly ingested certain fruits, vegetables, herbal products, etc., there is a high potential for drug interactions (6). In addition, herbal products consist of various phytochemicals which in turn increase the risk of herb-drug interactions (57).

One of the major mechanisms responsible for herb-drug interactions is either induction or inhibition of membrane transporter (57). By modulating the function and expression of transporter, phytochemicals influence the pharmacokinetics of the drug by modulating absorption, distribution and excretion. These plant-drug interactions have been major concerns with narrow-therapeutic drugs such as anticancer agents (e.g. irinotecan), cardiovascular agents (e.g. digoxin), and immunosuppressants (e.g. cyclosporine).

1.5.1 Herb-drug interactions

Efflux transporter P-gp mediated herb-drug interaction is one of the main clinical concerns, which reportedly involve St John's wort, ginger, garlic, ginkgo, ginseng and many other plants (57-60). The extracts of *Bacopa monniera*, *Schisandra lignans*, *Vernonia amygdalina*, *Morinda lucida* Benth, *Carica papaya*, *Mangifera indica* significantly inhibited P-gp function both *in vitro* and rat (61-64). Bitter melon, soybean, dokudami and welsh onion also reported to inhibit P-gp function *in vitro* (65).

It was reported that plant secondary metabolites such as anthraquinone, emodin, carnosic acid from rosemary, polyphenols derived from *Mangifera indica* such as mangiferin, norathyriol, quercetin and naphthoquinone ester rhinacanthin-c inhibited P-gp activity (61, 66-68). Naringin increased antiplatelet and antithrombotic agent clopidogrel intestinal absorption and its oral bioavailability by inhibiting intestinal P-gp (38). Kim *et al.* reported that the absorption of phenytoin, propranolol, theophylline and fexofenadine was increased when given together with piperine (69). Capsaicin also enhanced plasma concentration of cyclosporine, a P-gp substrate, in rats (70). It has been found that quercetin inhibited digoxin efflux which increased the absorption of digoxin (71). Popular beverage green tea constituent, epigallocatechin-3-gallate inhibited P-gp mediated transport of digoxin in human adenocarcinoma cell line (72). In 1989, it was reported that grapefruit juice can enhance the plasma concentration of felodipine by inhibiting P-gp (73). Grapefruit juice was also reported to inhibit colchicine (74), talinolol (75), and digoxin transport mediated by P-gp in *in vitro* study (14). These finding suggests that P-gp substrate drugs when taken together with phytochemical constituents may modify the absorption and/or plasma concentration of drugs.

Herbal products can also alter P-gp expression and modulate the pharmacokinetics of conventional medicine. For example; St. John's wort decreased the plasma concentration of digoxin, indinavir and fexofenadine by inducing mRNA expression and activating pregnane X receptor which controls the transcription of *MDR1* gene. It has been reported that plant flavonoids tangeritin and naringenin induce mRNA expression by stimulating the constitutive androstane receptor (CAR) and

pregnane X receptor mediated pathways (71). Contrastly, alkaloid sinapine down-regulated *MDR1* expression through suppression of fibroblast growth factor receptor (FGFR)4/FRS2 α -ERK1/2 mediated NF- κ B activation in MCF-7/dox cancer cells (76). Alkaloid sinomenine decreased P-gp expression by inhibiting NF- κ B signaling pathway (77). Dioxin also significantly reduced mRNA and protein expression through nuclear factor κ -B (NF- κ B) mechanism in Caco-2 cells (78). Ginsenoside 20(S)-Rh2 repressed adriamycin-induced *MDR1* expression by inhibiting mitogen-activated protein kinase (MAPK)/nuclear factor (NF)- κ B pathway in MCF-7/Adr cells (79). Anthraquinone derivative emodin inhibited the mitogen-activated protein kinase (MAPK)/AP-1 pathway thereby decreased P-gp expression (66).

Herb-drug interaction can impact on clinical outcome. Examples of herb-drug interactions addressed by case reports or clinical studies are listed in table 5.

Table 5. P-gp mediated herb-drug interactions addressed by case reports or clinical studies

(80)

Herb	Drug	Result of interaction	Possible mechanism
St John's wort	Digoxin	Decreased plasma digoxin concentration	Induction of P-gp
St John's wort	Simvastatin	Decreased plasma digoxin concentration	Induction of P-gp and CYP enzymes
St John's wort	Amitriptyline	Decreased plasma levels of amitriptyline	Induction of both CYP2C19 and P-gp
St John's wort	Cyclosporine	Decreased plasma levels in some cases, with acute rejection episodes	Induction of CYP2C19 and P-gp

1.5.2 Fruit-drug interactions

Grapefruits (*Citrus paradise*) is well-known example of fruit that interacts with various drugs. Other fruits such as orange, pomelo, pomegranate, cranberry, grape, apple are also described to have interactions with drugs. Not only juice but also

whole fruit, fruit pulp and fruit extracts also interact with various pharmacological agents. Phytochemical constituents of the fruits modify intestinal cytochrome P450 and phase II conjugation enzymes, as well as uptake and efflux transport proteins (81). Clinically significant fruit-drug interactions are shown in table 6.

Table 6. Clinically significant fruit-drug interactions

(82)

Fruit	Drug	Result of interaction	Possible mechanism
Pomegranate juice	Intravenous iron during hemodialysis	Attenuated oxidative stress and inflammation induced by intravenous iron	Antioxidant activity
Cranberry juice	Triple therapy medications for H. pylori	Increased eradication rate of H. pylori eradication in females	Underlying mechanism unclear
Wheat grass juice	Fluorouracil, adriamycin and Cytosan	Reduced side effects of chemotherapy such as myelotoxicity	Antioxidant activity
Apple juice	Fexofenadine	Decreased in drug bioavailability and potential lower efficacy	Inhibition of intestinal OATP2B1
Grape juice	Cyclosporine	Significantly decreased bioavailability and potential risk of subtherapeutic concentrations of cyclosporine	Induction of CYP3A4

Grapefruit juice drug interactions are widely recognized as compared to other nutrients. Grapefruit juice inhibits CYP3A4, CYP1A2, MRP2, OATP and P-glycoprotein. A wide variety of drugs such as calcium channel antagonist, central nervous system modulators, HMG-CoA reductase, immunosuppressants, antivirals, phosphodiesterases-5 inhibitor, antihistamines, antiarrhythmics and antibiotics are known to interact with grapefruit. The constituents in grapefruit naringin, naringenin,

furanokumarin, bergapten (5-methoxypsoralen) and flavonoids are responsible for such interactions (81).

Apart from grapefruit, fruit-drug interactions involving citrus fruits are also common. For example, tangerine stimulates CYP3A4 activity and inhibits P-gp resulting in interactions with nifedipine, digoxin, etc. Bitter orange inhibits CYP3A4, OATP-A and OATP-B and has interaction with various drugs such as vinblastine, fexofenadine, glibenclamide, atenolol, ciprofloxacin, cyclosporine, celiprolol, levofloxacin and pravastatin (81).

Grapefruit, pomelo and orange juice inhibited P-gp mediated transport of digoxin in L-MDR1 cells (83). The results from Honda *et al.* study showed that 6,7-dihydroxybergamottin, bergamottin from grapefruit and tangeretin, heptamethoxy flavone and nobiletin from orange juice co-inhibited the P-gp and MRP2 transporter (84). Limonin, isolated from *Citrus jambhiri* and *Citrus pyriformis* significantly augmented cytotoxicity of doxorubicin in Caco-2 and CEM/ADR5000 cell lines (85). Nobiletin, polymethoxylated flavone, inhibited P-gp activity without modulating mRNA and protein expression (86). In contrast oxypeucedanin, a common constituent of citrus species, inhibited P-gp activity, mRNA and protein expression in MDCK-MDR1 cell line (87). On the other hand, bergapten increased the P-gp efflux function by inducing mRNA and P-gp protein expression (88).

Interactions of drugs with citrus species can have impact on the clinical outcome. Grapefruit juice increases plasma concentration of some statins and calcium channel blockers by inhibiting CYP3A4 and P-gp, leading to adverse effects such as muscle pain with some statins and severe hypotension with some calcium channel blockers (89). Grapefruit and Seville orange juice can increase the plasma concentration of dextromethorphan in healthy volunteers (90). Table 7 represents significant citrus-drugs interactions.

Table 7. Clinically significant citrus species-drug interactions

(82)

Fruit	Drug	Result of interaction	Possible mechanism
Grapefruit	Felodipine	Increased plasma concentration of felodipine	Inhibition of CYP3A4
Orange juice	Aliskiren	Reduced plasma concentration of aliskiren	Inhibition of OATP2B1
Seville orange juice	Felodipine	Increased plasma concentration of felodipine	Inhibition of CYP3A4
Pomelo pulp	Cyclosporine	Increased bioavailability of cyclosporine	Inhibition of CYP3A and P-gp activity
Lime juice	Artemether, camoquine	Increased eradication of acute uncomplicated malaria in children	Antioxidant property
Grape juice	Cyclosporine	Significantly decreased bioavailability of cyclosporine	Induction of CYP3A4

1.6 *Citrus hystrix* (*C. hystrix*)

C. hystrix, commonly known as kaffir lime or leech lime, is a citrus belonging to Rutaceae family. It is called makrut in Thai. In Myanmar, it is called Shauk-cho, Shauk-nu or Shauk-waing. It is edible plant and widely grows in south East Asia (91, 92). It is a small evergreen tree, 3 to 6 m tall. It has shrubby aromatic and distinctive “double” shaped leaves. Petals are white with reddish or pink on the outside and consists of 4 to 5 petals with around 30 stamens (93). The fruits are subglobose to oblate-globose shape, with thick rind, knobby and wrinkled in nature (94).

C. hystrix fruit contains phytoconstituents such as vitamin C, folic acid, potassium, flavonoids (naringin and hesperidin), glyceroglycolipids, α -tocopherol, limonoids, furanocoumarins (dihydroxybergamottin, oxypeucedanin), benzenoid derivatives and alkaloids (95-97). Its peel contains cellulose, pectin and lignin which are important source of dietary fiber and functional compounds (98).

It has been reported that *C. hystrix* fruit is widely consumed and exhibits a wide range of medicinal properties. The green and mature fruit is used as an ingredient in cooking and pickle preparation. Traditionally, the whole fruit is used for treating headache, flu, fever, sore throat, bad breath and indigestion (93, 95, 99).

Scientifically, *C. hystrix* fruit is reported to have antioxidant, antimicrobial, anti-inflammatory and antiproliferative activities (95, 99). It was also reported that ethanolic extract of *C. hystrix* peel protected cardiac toxicity induced by doxorubicin in rats (100). It was reported that coumarins (bergamottin, oxypeucedanin and 5-[(6',7-dihydroxy-3',7'-dimethyl-2-octenyl) oxy-]-psoralen) from the methanolic extract of fruits inhibited lipopolysaccharide and interferon induced nitric oxide generation in RAW 264.7 cells. Limonene, citronellal, sabinene and β -pinene from the peel had antimicrobial activity. The isolated citrusosides A-D and furanocoumarin compounds from the hexane and methanolic extract of peel exhibited anti-acetylcholinesterase activity (95). The flavonoid hesperidin from the juice showed antioxidant activity (101).

2. Purpose of the study

There are many reports concerning with the role of citrus species on fruit-drug interactions. *C. hystrix* fruit is commonly found in Thailand and Myanmar. Many people consume it as an ingredient in food or a part of beverage so it might cause interaction with conventional medicine. It has been reported that this fruit inhibits the CYP3A4 and CYP2C9 activities (102). Since CYP3A4 and P-gp share substrates, inhibitors and inducers (103, 104), ingestion of *C. hystrix* fruits may modify the efflux transporter P-gp. However, there is no information about the effect of *C. hystrix* on P-gp activity. Therefore, this study focused on P-gp mediated drug interactions of *C. hystrix*. The investigation was performed in Caco-2 cell line, and LLC-PK₁ versus LLC-GA5-COL300.

This study was conducted with the following objectives;

1. To investigate the effects of *C. hystrix* fruit on P-gp function and expression.
2. To elucidate its active compounds from *C. hystrix*

The information obtained from this study may be beneficial for understanding fruit-drug interactions.



Chapter 2

Materials and methods

1. Materials

1.1 Apparatus and instruments

1. Centrifuge
2. TLC developing tank (10 cm × 10 cm), (20 cm × 20 cm)
3. Refrigerator, Freezer -80°C, -20°C and 4°C
4. Glass Column (3 x 60 cm)
5. Silica Gel 60 (0.015-0.040 mm mesh), Merck (Germany)
6. TLC Plate (20 cm × 20 cm), Silica gel 60 F254 aluminium plates, Merck (Germany)
7. PTLC (20 cm × 20 cm), Silica gel 60 F254 aluminium plates, Merck (Germany)
8. Rotary Evaporator, Buchi, F-100/F-105 (Switzerland)
9. Zorbax SB-C18 column (4.6 x 150 mm, 3.5 µm), Agilent (USA)
10. HPLC (Agilent 1260 infinity (USA)
11. LC-MS (1100 series/Trap SL with ESI Source (G2440DA) (USA)
12. Microplate reader, Victor Nivo, PerkinElmer (USA)
13. Biological safety cabinet, BHA 120, Gelman Sciences Pty Ltd (Australia)
14. CO₂ incubator
15. Autoclave
16. Hot air oven
17. Dry Bath Incubator (MK2000-1), Allsheng (China)
18. Western blotting equipment, Bio-rad (USA)
19. Gel documentation, Alliance Q9 Advanced, Uvitec (UK)
20. Polycarbonate insert of Transwell® cluster (0.45 µm pore size, Costar, Cambridge, MA, USA)

21. Qubit® 2.0 fluorometer, Invitrogen, Thermo Fisher Scientific (USA)

1.2 Chemicals and reagents

1. Acetonitrile, Methanol, Tetrahydrofuran (HPLC grade)
2. Chloroform, Ethyl acetate, Formic acid, Methanol, n-Hexane, Toluene (Analytical grade)
3. Dulbecco's modified Eagle medium (DMEM), Gibco BRL (Grand Island, NY, USA)
4. Medium 199 (M199), Gibco BRL (Grand Island, NY, USA)
5. L-glutamine, Gibco BRL (Grand Island, NY, USA)
6. Non-essential amino acids, Gibco BRL (Grand Island, NY, USA)
7. Penicillin (10,000 units/ml)-streptomycin (10 mg/ml), Gibco BRL (Grand Island, NY, USA)
8. Fetal bovine serum (FBS), Gibco BRL (Grand Island, NY, USA)
9. 0.25% trypsin-1 mM EDTA, Gibco BRL (Grand Island, NY, USA)
10. Hanks' balanced salt solution pH 7.4 (HBSS), Gibco BRL (Grand Island, NY, USA)
11. Phosphate buffered Saline pH 7.4 (PBS), Gibco BRL (Grand Island, NY, USA)
12. 0.4% trypan blue, Sigma Chemical Company (St. Louis, MO, USA)
13. Calcein acetoxymethyl ester (calcein-AM), Fluka Chemie GmbH (Switzerland)
14. Verapamil, Sigma Chemical Company (St. Louis, MO, USA)
15. Doxorubicin hydrochloride (2mg/ml), Pharmachemie BV (Netherlands)
16. Cyclosporine (Sandimmune®, 50mg/ml), Novartis (Switzerland)
17. Pierce ECL western blotting substrate, Thermo Fisher Scientific (USA)
18. Mdr-1 (D-11): sc-5510 mouse monoclonal antibody, Santacruz (USA)

19. Beta Actin loading control mouse monoclonal antibody (MA5-15739), Invitrogen, Thermo Fisher Scientific (USA)
20. 0.45 μ m polyvinylidene difluoride (PVDF) membrane (Millipore 45 Corp., Bedford, MA)
21. Qubit[®] 2.0 fluorometer protein assay kit, Invitrogen, Thermo Fisher Scientific (USA)
22. Triton X-100, Fisher chemicals (UK)
23. Pierce BCA protein assay kit, Thermo Fisher Scientific (USA)
24. BLUltra Prestained Protein Ladder, GeneDireX (USA)
25. Polyvinylidene difluoride membrane, Amersham Pharmacia Biotech Ltd (UK)
26. Sodium dodecyl sulfate
27. Ammonium persulphate
28. Sodium Lauryl sulphate, Ajax Finechem Pty Ltd (Australia)
29. Tris (hydroxymethyl) aminomethane, Merck (Germany)
30. Glycine, Ajax Finechem Pty Ltd (Australia)
31. 2-Mercaptoethanol 99%, Acros organics (UK)
32. Tris-HCl, Vivantis (Malaysia)
33. Skim milk powder, Morinaga (Japan)
34. Glycerol
35. Bromophenol blue dye
36. Acrylamide
37. Peroxidase-labeled affinity purified antibody to mouse IgG (γ), Sera care KPL (USA)
38. Bergamottin (Apin Chemicals, Code: 06450b)

1.3 Cell lines

1. Caco-2, a human colonic adenocarcinoma cell line (ATCC, sale order no. S0249019)
2. LLC-GA5-COL300, a human P-gp overexpressed-LLC-PK₁ cell line (Riken Cell Bank, air waybill no: 8462-5956-2849)

2. Methods

2.1 Preparation of crude extracts from *C. hystrix* fruits

The *C. hystrix* fruits (2 kg) were purchased from a fresh market in Nakhon Pathom, Thailand in April, 2018. The fresh fruits were thoroughly washed with water. Then they were separated into four parts (flavedo, albedo, segment membrane & juice). Flavedo, albedo and segment membrane were dried at 50°C for 24 hr and grounded into powder by using blender. In the case of juice, it was concentrated by using rotary evaporator.

The extraction of crude extracts from the dried flavedo (86 g), albedo (25 g) and segment membrane (50 g) were done by maceration method. The dried powdered samples were macerated with methanol (1.5 L) at room temperature for 3 days with frequent agitation and the macerate was filtered. This extraction was repeated twice to complete the extraction process. Rotary evaporator was employed to evaporate the solvent from the combined filtrates and dried on water bath at 40 °C to obtain crude extracts. All extracts were kept at -20°C until used.

Concentrated juice (5 g) was extracted with methanol for three times and the combined mixtures were centrifuged (2,500 x g for 30 min) to separate organic layer from aqueous layer. The organic layer was then evaporated by means of rotary evaporator and dried at 40 °C on water bath. The dried extract was kept at -20°C until used.

All the extracts were checked with thin layer chromatography (TLC) and High performance liquid chromatography (HPLC) to obtain the fingerprints of the extracts.

2.2 Isolation of active compounds from flavedo extract of *C. hystrix*

The dried methanolic flavedo extract (21 g) was partitioned between ethyl acetate and deionized water (1:1). The ethyl acetate layer was evaporated by rotary evaporator to obtain greenish residue as ethyl acetate extract (9 g, 7 % of dried weight). Ethyl acetate extract (8 g) was loaded into the glass column (3 x 60 cm) which contain silica gel 60 (200 g) as stationary phase. The gradient elution of n-hexane:ethyl acetate, starting with 10% ethyl acetate in n-hexane followed by 20% of

ethyl acetate and finally 80% of ethyl acetate in n-hexane was used as mobile phase. The fractions were continuously collected and combined according to the chromatographic pattern on TLC. Five fractions, E1 (145 mg), E2 (356 mg), E3 (393 mg), E4 (432 mg) and E5 (390 mg), were obtained from the separation. All these 5 fractions were further separated by column chromatography and preparative thin layer chromatography (PTLC) to obtain pure compounds.

Fraction E1 (145 mg) and E2 (356 mg) were further separated by column chromatography. Each fraction was loaded into the glass column (1 x 40 cm) containing silica gel 60 as stationary phase. The gradients of n-hexane:ethyl acetate (9:1), n-hexane:ethyl acetate (8:2) were used as mobile phase. Two major fractions, E11 (16 mg) and E12 (15 mg) were collected from the separation of fraction E1. Separation of fraction E2 provided four major fractions namely, E21 (43 mg), E22 (31 mg), E23 (2 mg) and E24 (2 mg). Then fractions E11, E21 and E22 were further purified by PTLC, using n-hexane:ethyl acetate (8:2) as a mobile phase. White powder was attained and named as compound **1** (8 mg).

Fraction E3 (393 mg) was fractionated on silica gel 60 (25 g) column (1 x 40 cm) which was eluted with toluene:ethyl acetate (10:1.5). Five major fractions, E31 (11 mg), E32 (111 mg), E33 (13 mg), E34 (7 mg) and E35 (15 mg), were obtained. Purification of fraction E32 by PTLC with mobile phase composed of n-hexane:ethyl acetate (7:3) (x 2 migration) provided two compounds which was named as compound **2** (3 mg) and **3** (15 mg).

Fraction E5 (390 mg) was separated by on silica gel 60 column chromatography, utilizing the gradient elution of toluene:ethyl acetate (10:1.5), toluene:ethyl acetate (8:2), toluene:ethyl acetate (1:1) as mobile phase. Four major fractions, E51 (10 mg), E52 (29 mg), E53 (32 mg) and E54 (45 mg), were obtained. Fraction E51 gave a pure compound, denoted as compound **4** (10 mg). Fraction E54 was purified by PTLC utilizing the mobile phase which was composed of toluene:ethyl acetate (10:1.5) (x2 migration) followed by chloroform:methanol (12:1). Pure compound **4** (4 mg) and **5** (4 mg) were obtained.

The schematic of compound isolation is shown in figure 5. All five compounds were further analyzed by LC-MS and ¹H NMR to elucidate the structure.

2.3. Chromatographic and Spectroscopic analysis of the extracts and active compounds

TLC analysis

The extract or each isolated compound was dissolved in methanol and spotted on TLC plate (5 cm × 7 cm). Then it was developed in the mobile phase containing toluene:ethyl acetate (10:1.5), toluene:ethyl acetate (10:1.5), chloroform:methanol (12:1). Then TLC plate was visualized under UV lamp (356 nm and 254 nm).

HPLC analysis

An Agilent 1260 infinity liquid chromatography system, provided with a quaternary solvent delivery system, an autosampler and DAD detector, was used for HPLC analysis. A Zorbax SB-C18 column (4.6 x 150 mm, 3.5 µm) was utilized. Detection wavelength was set at 310 nm. The mobile phase was composed of solvent A: water-acetonitrile-tetrahydrofuran (85:10:5 v/v) and solvent B: acetonitrile-methanol-tetrahydrofuran (65:30:5 v/v) using a gradient elution with a flow rate of 0.3 ml/min. Gradient conditions were as follow: 5 min, 0% B, 20 min 32% B, 24 min 32% B, 38 min 55% B, 40 min 90% B, 50 min 90% B, 60 min 0% B. The samples were dissolved in methanol and filtered through a 0.45 µm PVDF membrane. The injection volume of all samples was 5 µl.

LC-MS analysis

Identification of the active compounds was carried out by LC-MS system. MS parameters were set as follows: ionization mode, ESI; dry Temp, 350 °C; nebulizer 30 psi; dry Gas, 8 L/min; scan range, m/z 100-500. A Zorbax SB-C18 column (4.6 x 150 mm, 3.5 µm) was utilized. Detection wavelength was set at 250 and 310 nm. The gradient of 0.05% v/v aqueous formic acid (Solvent A) and 0.05 % v/v formic acid in acetonitrile (Solvent B) was used as mobile phase at a flow rate of 0.4 ml/min. The gradient started at 0 min, 60% B; 5 min, 80% B; 10 min, 80% B; 12 min, 95% B; 17 min, 95% B; 21 min, 60% B; 23 min, 60% B. All samples were dissolved in methanol

and filtered through a 0.45 μm PVDF membrane. The injection volume used was 10 μl .

^1H -NMR analysis

^1H (300 MHz) NMR spectra were recorded by using Bruker Bio (300 MHz) NMR spectrometer with tetramethylsilane as an internal standard. Deuterated methanol (CD_3OD) was used as operating solvent. Chemical shifts are expressed in δ values. This analysis was performed by a scientist at Faculty of Science, Silpakorn University.



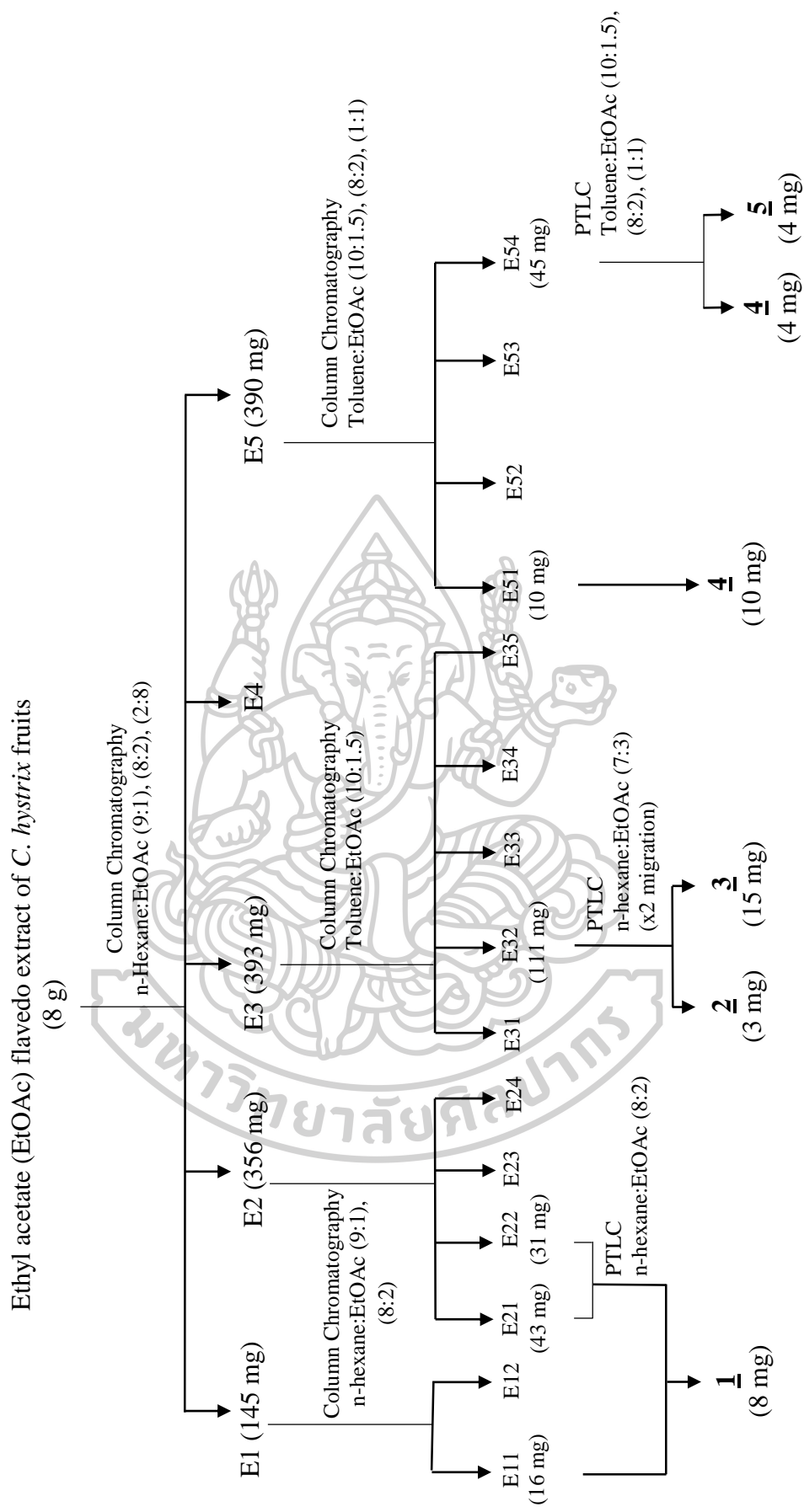


Figure 5. Isolation of active compounds from the flavedo extract of *C. hystrix*

2.4 P-gp function assay

This assay was used to study the effect of extracts, fractions from column chromatography and isolated compounds on P-gp. Firstly, four parts of the *C. hystrix* fruit were used to study on P-gp function. The most active part was chosen to do separation on column chromatography. During the column chromatography all fractions were studied for the effects on P-gp. The fractions that showed P-gp inhibition activity were chosen to isolate active compounds. The isolated compounds were evaluated for their inhibition on P-gp function.

2.4.1 Cell Culture

The Caco-2, a human colonic adenocarcinoma cell line, was cultured in DMEM medium supplemented with 10% heat-inactivated FBS, 1% penicillin (10,000 units/ml)-streptomycin (10 mg/ml), 2 mM L-glutamine, 1% non-essential amino acids at 37°C in a humidified atmosphere of 5% CO₂.

The LLC-PK₁, a porcine kidney epithelial cell line was routinely grown in M199 supplemented with 10% heat-inactivated FBS and 1% Penicillin (10,000 units/ml)-streptomycin (10 mg/ml). The LLC-GA5-COL300, a human P-gp overexpressed-LLC-PK₁ cell line was cultured in M199 supplemented with 10% heat-inactivated FBS, 1% penicillin-streptomycin and 300 ng/ml colchicine, as previously reported (105, 106). Both of the cell lines were maintained in a humidified 5% CO₂ atmosphere at 37°C.

2.4.2 Preparation of extracts, fractions and isolated compounds

On the day of the experiment, the extracts, fractions and isolated compounds were dissolved in methanol and diluted in HBSS to obtain the final methanol concentration not exceeding 1%. The cytotoxicities of the tested extracts, fractions or compounds were evaluated by checking cell morphology under a microscope and analyzed by trypan blue dye exclusion method and neutral red uptake assay.

2.4.3 Uptake study

Caco-2 cells were seeded onto 24-well plate at a cell density of 80,000 cells/cm². Caco-2 cells cultured for 21 days were used for the experiment. LLC-PK₁ (120,000 cells/cm²) and LLC-GA5-COL300 (360,000 cells/cm²) were seeded onto 24-well plate. Both cell lines were grown for 3 days for the study. The medium was changed every other day for all cell lines. For LLC-GA5-COL300, a fresh and colchicine free medium was replaced 6 hr before the experiment.

Calcein-AM uptake assay

On the day of the experiment, cells were washed with HBSS and then preincubated in HBSS with or without the test compounds (80 µg/ml extracts, 30 µg/ml fractions, or 10-200 µM isolated compounds) for 30 min. To start the reaction, a final concentration of 1 µM calcein-AM was added and then incubated at 37°C for 30 min. After the incubation period, the uptake solutions were removed and the cells were washed carefully with an ice-cold HBSS. Following this, the cells were lysed with 0.1% Triton X-100 and measured the amount of calcein and protein concentration. HBSS containing 1% methanol was used as a vehicle control. One hundred µM verapamil was used as the positive control (109).

The accumulated calcein in the cells was directly measured on a microplate reader at an excitation and emission wavelength of 485 nm and 535 nm, respectively. The protein concentration was measured by Qubit[®] fluorometer. The amount of calcein retained in the cells was normalized by the protein concentration. The data were presented as % of control.

$$\% \text{ of control} = \frac{\text{Normalized fluorescence intensity of treated cells}}{\text{Normalized fluorescence intensity of vehicle control}} \times 100$$

Doxorubicin uptake assay

The medium was removed and washed the cells with HBSS. A final concentration of 10 µM Doxorubicin in HBSS was coincubated with various concentrations of the test compounds (2-200 µM cyclosporine, 1-200 µM 6',7'-dihydroxybergamottin, or 2-200 µM oxypeucedanin). The cells were incubated for 2

hr at 37°C. After the incubation period, the uptake solution was discarded and the cells were washed with ice-cold HBSS and were lysed by 0.1% Triton X-100.

The amount of cellular doxorubicin was directly measured on a microplate reader at an excitation and emission wavelength of 485 and 595 nm, respectively. The data were presented as IC₅₀ by plotting the relative fluorescence unit and log concentrations of the test compounds.

2.4.4 Transport study

LLC-PK₁ and LLC-GA5-COL300 was seeded onto polycarbonate insert of Transwell® cluster at a density of 300,000 cells/cm² and 800,000 cells/cm² and grown for 4 days in a humidified 5% CO₂ atmosphere at 37°C. The medium was changed on every other day. A fresh and colchicine free medium was replaced 6 hr before the experiment.

Transport study of doxorubicin

The culture medium was removed from both sides. Cells were preincubated in HBSS for 30 min in the absence or presence of test compounds. To start the experiments, a final concentration of 10 µM doxorubicin in HBSS was added to the donor side and HBSS was added to the receiver side. Then the cells were incubated at 37°C. The donor side is apical side for apical to basolateral (a-b) experiment and the donor side is basolateral side for basolateral to apical (b-a) experiment.

Samples were withdrawn from the receiver side at 4 designated time points (60, 75, 90, 100 min for a-b and 15, 30, 45, 60 for b-a). The amount of doxorubicin was analyzed by reading fluorescence at an excitation and emission wavelength of 485 nm and 595 nm, respectively. The effective permeability coefficient (P_{app} , cm/s) is calculated according to the equation:

$$P_{app} \text{ (cm/s)} = \frac{dQ/dt}{A \times C_0 \times 60}$$

Where dQ/dt = the rate of drug passage into the receiver side, A is the surface area of Transwell® inserts (cm^2), and C_0 is the initial concentration of doxorubicin in the donor side.

An efflux ratio is calculated from the apparent permeability coefficients as follows:

$$\text{Efflux ratio} = \frac{P_{app, b-a}}{P_{app, a-b}}$$

Where, $P_{app, b-a}$ = effective permeability coefficient from basolateral to apical side,
 $P_{app, a-b}$ = effective permeability coefficient from apical to basolateral side.

Transport study of dihydroxybergamottin and oxypeucedanin

Cells were preincubated in HBSS for 30 min. To start the experiment, dihydroxybergamottin (20 μM) or oxypeucedanin (20 μM) in HBSS were added to the donor side and HBSS was added into the receiver side. Then the cells were incubated at 37°C.

Samples were withdrawn from the receiver side at 3 designated time points (30, 45, 60 min for a-b and 15, 25, 35 min for b-a). The compounds were quantified by HPLC as described in 2.3.

The effective permeability coefficient (P_{app} , cm/s) and efflux ratios are calculated according to the above equation.

2.5 Western blotting

The LLC-PK₁ (50,000 cells/ cm^2) and LLC-GA5-COL300 (160,000 cells/ cm^2) were seeded onto cell culture dish. The LLC-PK₁ used for the study was grown for 4 days. The LLC-GA5-COL300 cell lines were grown for 72 hr and then treated with the test compounds (100 μM dihydroxybergamottin and oxypeucedanin) for 24 hr.

2.5.1 Cell lysis and sample preparation

Cells were placed on ice and washed with ice-cold PBS. Then the washing solution was aspirated. Ice-cold PBS is added to harvest the cells with a scraper. The cell suspension was transferred to the microcentrifuge tube and centrifuged at 2,000 rpm for 5 min at 4°C. The supernatant was discarded and the cell pellet was homogenized with hot 1% SDS lysis buffer (50 mM Tris HCl; pH 7.4, 1% SDS and 1 mM PMSF). The cell lysate was centrifuged at 10,000 rpm for 5 min at 4°C and the supernatant was transferred to a new tube. The protein concentration of the supernatant was measured by Pierce BCA protein assay kit to determine the amount of protein to load onto the gel. Then the supernatant was mixed with 4x Laemmli sample loading buffer.

2.5.2 Running the gel

Protein samples (50 µg) along with molecular weight marker were loaded onto SDS-polyacrylamide gel consisting of 10% resolving gel and 4% stacking gel. The proteins were separated by electrophoresis using Tris-glycine running buffer (25 mM Tris base, 192 mM glycine and 0.1 % w/v SDS) at constant 60 volt (current 11-26 mA) for 1-2 hr. The electrophoresis was stopped when the marker band reach the bottom of the gel.

2.5.3 Protein blotting

The polyvinylidene difluoride (PVDF) membrane was used for protein blotting. The membrane was activated with methanol for 1 min and rinsed with transfer buffer. The protein from the gel was transferred to PVDF membrane by utilizing wet transfer buffer (25 mM Tris base, 192 mM glycine and 0.05 % v/v SDS) at constant 48 volt (current 92-115 mA) for 4 hr on ice.

2.5.4 Antibody staining and Detection

Membrane was blocked in 5% skim milk in TBST for overnight at 4°C. After blocking, the membrane was stained with mouse anti-human P-gp monoclonal antibody (1:2,000) and mouse monoclonal anti-actin (1:2,000) separately for overnight at 4°C. Then the membrane was washed three times with Tris-buffered saline with 0.1% Tween (TBST). The membrane was incubated with goat anti-mouse IgG secondary antibody (1:2,000) for 3 hr at room temperature. Then the membrane was washed three times by using TBST. Mouse monoclonal anti-actin (1:2,000) was used as a loading control.

The target protein bands were detected by developing the membrane with an enhanced chemiluminescence (ECL) reagents for 5 min in the dark. The protein intensity was calculated by a gel documentation system.

Data analysis

All data are presented as the mean \pm SEM of n-replicate of the separate experiments or otherwise stated. A p-value ≤ 0.05 was considered statistically significant. Kruskal-Wallis and Dunns tests were performed for all tests (GraphPad Software Inc, San Diego, CA).

Chapter 3

Results and discussions

1. Effects of *C. hystrix* fruit extracts on P-gp function

1.1 Extraction of *C. hystrix* fruits

At first, the dried flavedo, albedo, segment membrane and juice of *C. hystrix* fruits were extracted with methanol. The yields of the methanolic extracts from flavedo, albedo, segment membrane and juice extracts were 25 %, 23 %, 40 % and 5 % w/w respectively. Then the extracts were checked by TLC and HPLC.

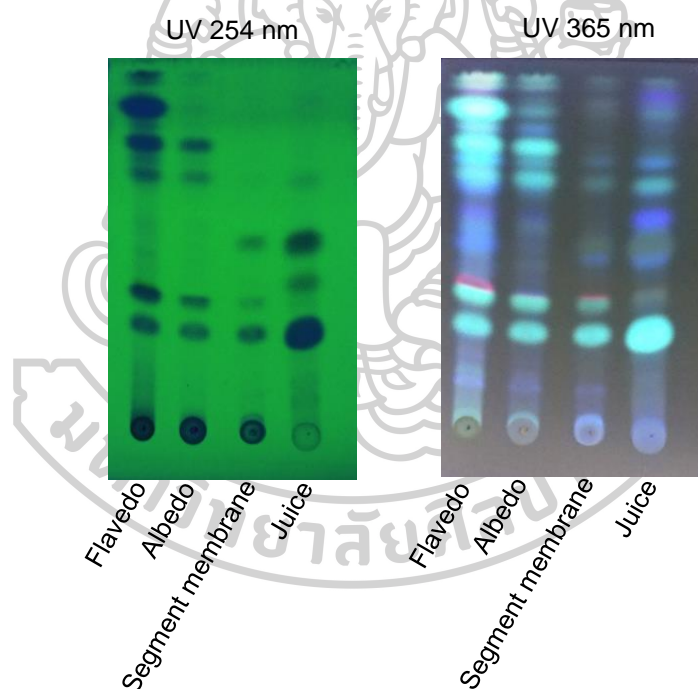


Figure 6. TLC profiles of methanolic extracts obtained from *C. hystrix* fruits
Mobile phase used was toluene:ethyl acetate (10:1.5) x2 migrations followed by
chloroform:methanol (12:1).

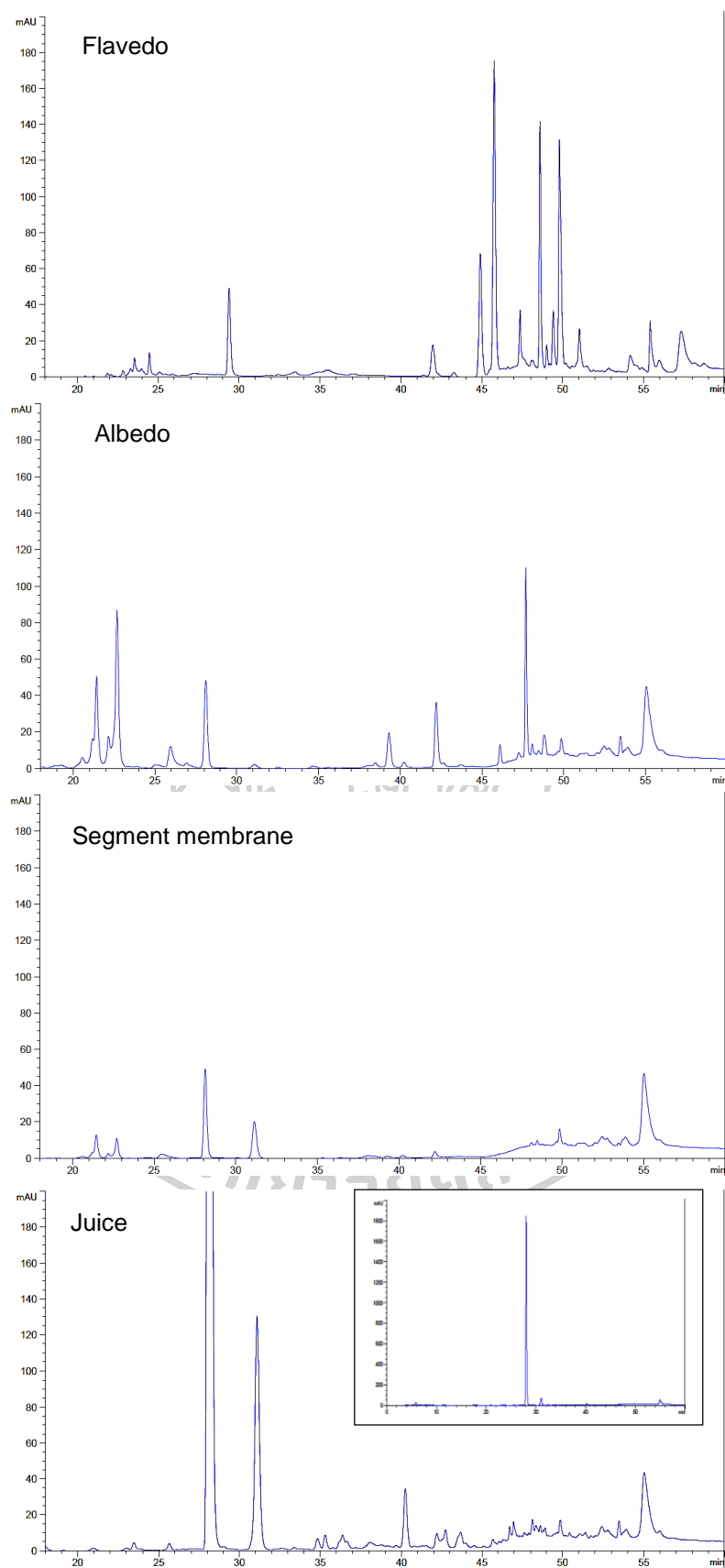


Figure 7. HPLC profiles of methanolic extracts (1 mg/ml) obtained from *C. hystrix* fruits

As seen in figure 6, the phytochemicals of the flavedo, albedo, segment membrane and juice are closely resembled. This was in agreement with HPLC patterns in figure 7. Both TLC and HPLC demonstrate that the flavedo, albedo, segment membrane and juice extracts contain similar chemical compounds but more phytoconstituents were found in the flavedo extract. Phytochemical constituents were further elucidated according to their effects on P-gp function.

1.2 Calcein-AM uptake in Caco-2, LLC-PK₁ and LLC-GA5-COL300

All extracts were evaluated for their effects on P-gp function utilizing calcein-AM uptake assay in *in vitro* cell culture models. The inhibitory effects of *C. hystrix* fruits on P-gp function was investigated by calcein-AM uptake assay in *in vitro* cell culture models including Caco-2, LLC-PK₁ and LLC-GA5-COL300. All concentrations of the extracts, fractions and compounds used in this study were examined by checking cell morphology under a microscope and analyzed by trypan blue dye exclusion method and neutral red uptake assay. The concentrations used in the study did not exhibit toxicity to the all cells.

Fluorescent dye-based uptake assays are increasingly used nowadays for evaluation of the function of transporter because it is feasible, cost effective and applicable to high throughput assays and allow the examination of cellular processes in real-time (107). Acetoxymethyl (AM) esters of calcein is a commonly used P-gp substrate fluorescent dye (108). Calcein-AM is a non-fluorescent substrate of P-gp. It is a lipophilic compound and can diffuse through the cell membrane by passive diffusion. It will be hydrolyzed to fluorescent calcein in the living cells by endogenous cytoplasmic esterases. P-gp located at the cell membrane pumps out the calcein-AM before it is converted to calcein (109).

Caco-2 is widely used for studying absorption process as an *in vitro* model of human small intestinal mucosa (110, 111). It forms polarized monolayers with well-established tight junctions that mimics intestinal epithelial cells. Caco-2 expresses many efflux transporter including P-gp. This cell line is commonly utilized in investigation of potential transporter-mediated herb-drug interactions (112). To confirm the effects of the extracts on human P-gp function, the study was also

performed in comparison between LLC-PK₁ and LLC-GA5-COL300 which is human MDR1 overexpressed LLC-PK₁ (113, 114).

All extracts of *C. hystrix* were primarily screened for their abilities to modulate P-gp function in Caco-2 cells. The calcein-AM uptake in the presence of verapamil (111) in Caco-2 cells was evaluated to validate P-gp function of Caco-2 cells in our laboratory. The results showed that the uptake of calcein-AM was significantly increased to 162 ± 7.33 % of the control in verapamil treated cells, indicating that the function of P-gp in Caco-2 was acceptable for further experiments. The flavedo, albedo, segment membrane and juice extracts noticeably increased calcein accumulation in Caco-2 cells by approximately 1.9, 1.4, 1.2 and 1.6 folds, respectively in relative to the control group. Increasing calcein accumulation in Caco-2 cells indicated their effects on the efflux transporter possibly P-gp. As found, the flavedo extract exhibited the highest activity on calcein accumulation (Figure 8, a).

To confirm their effects on human P-gp function, the uptake assay of calcein-AM were performed in LLC-PK₁ and LLC-GA5-COL300. The accumulation of calcein in LLC-PK₁ (6,971,576 RFU) was about 14 times higher than LLC-GA5-COL300 (502,271 RFU), indicating that P-gp expression in LLC-GA5-COL300 was higher than LLC-PK₁. In the presence of verapamil, the accumulation of calcein was increased in both cell lines. However, the accumulation was significantly enhanced by verapamil in LLC-GA5-COL300 (894 ± 69.5 % of the control) compared with that of LLC-PK₁ (145 ± 5.6 % of the control). The flavedo extract remarkably increased calcein-AM uptake in LLC-GA5-COL300 (1967 ± 159.1 %) compared with that of LLC-PK₁ (176 ± 12.4 %). The effect of the flavedo extract on calcein-AM uptake in LLC-GA5-COL300 substantiated its effect on human P-gp function. However, the other three parts of *C. hystrix* fruits did not show significant differences in the calcein-AM uptake between the two cell lines (Figure 8 b, c). Taken together, the flavedo extract showed the strongest on P-gp inhibition while the albedo, segment membrane and juice extracts had minimal effects on P-gp.

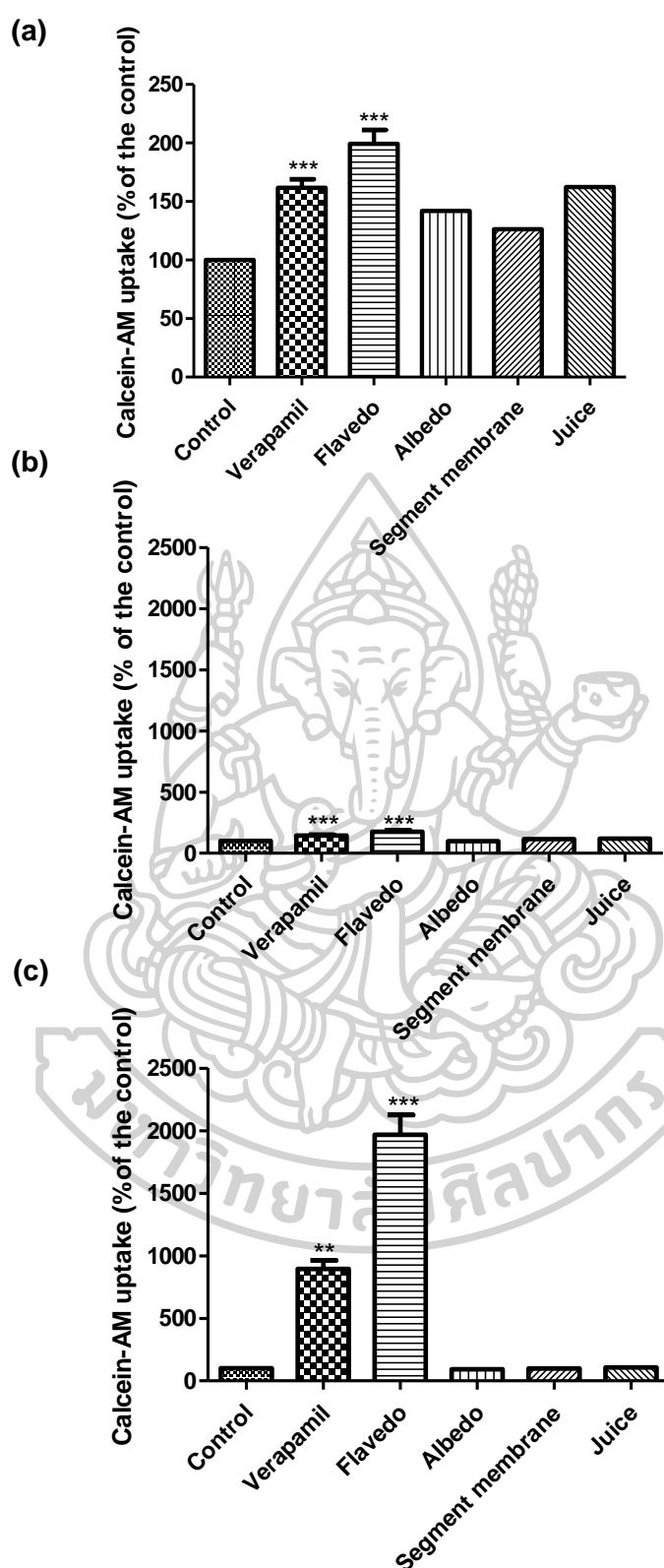


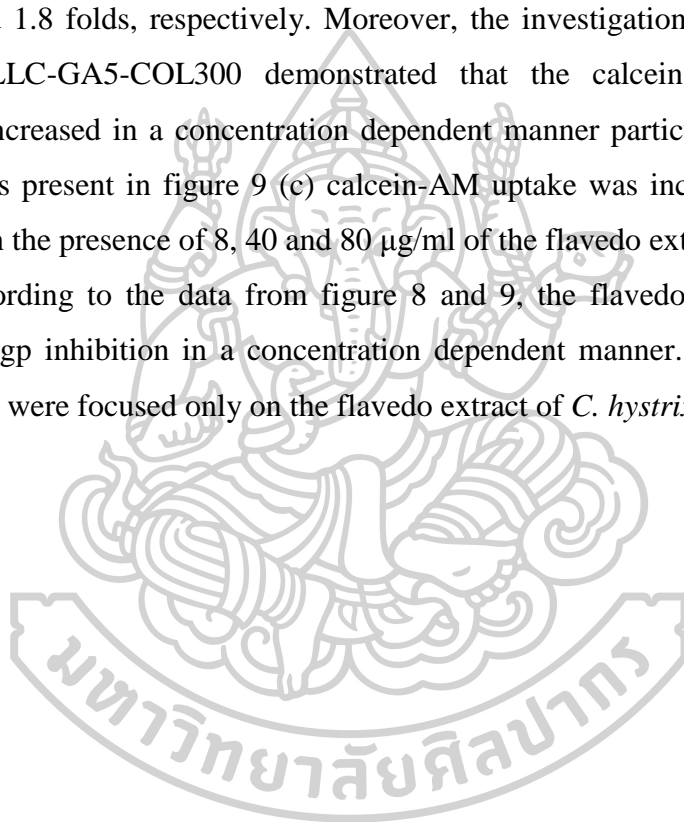
Figure 8. Effects of the *C. hystrix* methanolic extracts (80 µg/ml) on calcein-AM uptake in (a) Caco-2, (b) LLC-PK₁ and (c) LLC-GA5-COL300 (N=5). The data of albedo, segment membrane and juice are presented as the averages from 2 cell passages (**p < 0.01, ***p < 0.001).

2. Effects of the flavedo extract on P-gp function

2.1 Concentration dependent study

To study the concentration dependence of the flavedo extract on calcein-AM uptake, the concentrations of 8, 40 and 80 $\mu\text{g/ml}$ were used. Figure 9 (a) shows the concentration dependent effect on P-gp mediated calcein-AM uptake in Caco-2. In the presence of 8, 40 and 80 $\mu\text{g/ml}$ extract, the accumulation of calcein was increased to 1.2, 1.5 and 1.8 folds, respectively. Moreover, the investigation conducted in LLC-PK₁ and LLC-GA5-COL300 demonstrated that the calcein accumulation was obviously increased in a concentration dependent manner particularly in LLC-GA5-COL300. As present in figure 9 (c) calcein-AM uptake was increased by 2.4, 11.3, 23.8 folds in the presence of 8, 40 and 80 $\mu\text{g/ml}$ of the flavedo extract.

According to the data from figure 8 and 9, the flavedo extract showed the strongest P-gp inhibition in a concentration dependent manner. As a result, further experiments were focused only on the flavedo extract of *C. hystrix* fruits.



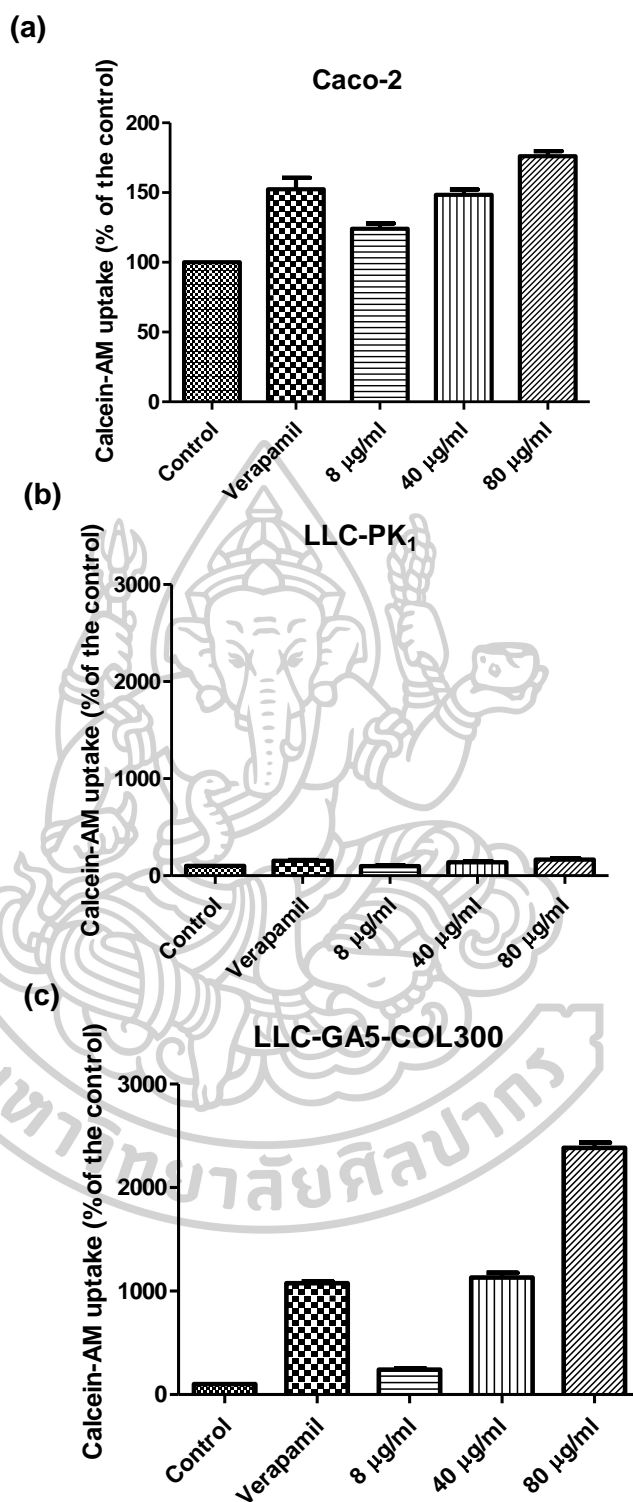


Figure 9. Concentration dependent effects of the flavedo extract on calcein-AM uptake in Caco-2, LLC-PK₁ and LLC-GA5-COL300

(N = 3)

2.2 Fractionation of the flavedo extract and their effects on calcein-AM uptake in Caco-2, LLC-PK₁ and LLC-GA5-COL300

The flavedo extract was selected to isolate and identify the active compounds because it demonstrated a significant effect on P-gp function. At first, the ethyl acetate fraction of the flavedo extract (8 g) was further separated by column chromatography. Five fractions, E1 (145 mg), E2 (356 mg), E3 (393 mg), E4 (432 mg) and E5 (390 mg), were obtained and their TLC chromatograms are shown in figure 10.

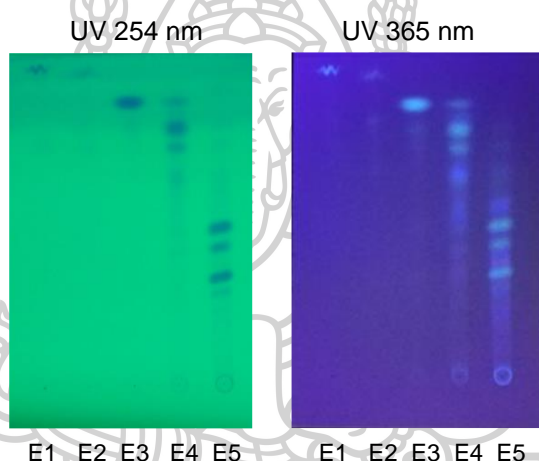


Figure 10. TLC profiles of the fractions obtained from the column chromatography
Mobile phase used was toluene:ethyl acetate (10:1.5) x2 migrations followed by chloroform:methanol (12:1).

All five fractions were then screened for their activities on P-gp. Calcein-AM uptake in Caco-2, LLC-PK₁ and LLC-GA5-COL300 was evaluated. As seen in table 8, the calcein-AM uptake was increased to 147, 173 and 169 % in the presence of fraction E3, E4 and E5. Fractions E1 and E2 showed almost the same calcein accumulation as the control group.

The experiments were further evaluated in LLC-PK₁ and LLC-GA5-COL300. Fractions E3 and E5 demonstrated strong inhibition effects by increasing calcein accumulation to 13.6 and 14.3 folds of the control in LLC-GA5-COL300. Based on

their activities on P-gp function, fractions E3 and E5 were selected for isolation of active compounds. Fraction E4 evidently enhanced calcein accumulation to 8.6 folds of the control, however it contained various compounds according to TLC chromatogram indicating a low probability to isolate the pure compounds from the fraction. Although fraction E1 and E2 showed moderate effects, there were white crystal precipitated out during the column chromatography of fraction E1 which showed one spot on TLC indicating a pure compound named as compound **1**. Similar R_f values of the spots on TLC chromatogram of fractions E1 and E2 convinced compound isolation from these fractions. In summary, isolation of compounds from fractions E1, E2, E3 and E5 were further performed.

Table 8. Effects of the flavedo fractions on calcein-AM uptake in Caco-2, LLC-PK₁ and LLC-GA5-COL300

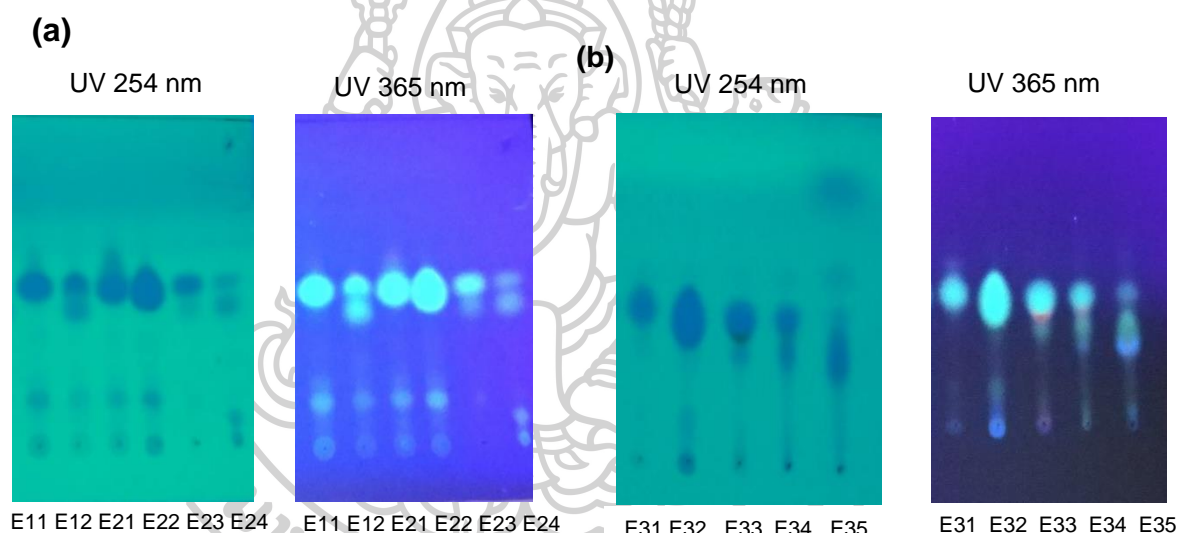
Cell lines (Passage no.)	Calcein-AM uptake (% of the control)					
	Verapamil (100 μ M)	Fraction (30 μ g/ml)				
		E1	E2	E3	E4	E5
Caco-2 (37)	151.3	107.4	96.5	147.7	172.7	169.5
LLC-PK ₁ (37)	141.2	98.4	93.3	128.4	263.3	113.5
LLC-GA5-COL300 (30)	948.8	163.5	291.0	1360.0	865.6	1428.8

Data are presented as the averages of duplicate measurements from one cell passage.

3. Isolation of active compounds from flavedo extract

Fractions E1, E2, E3 and E5 were further isolated by column chromatography for the compounds which were responsible for observed activities. Two sub-fractions E11 (16 mg) and E12 (15 mg) were collected from the separation of fraction E1 (145 mg). Separation of fraction E2 (356 mg) resulted in four sub-fractions, E21 (43 mg), E22 (31 mg), E23 (2 mg) and E24 (2 mg). Fraction E3 (393 mg) was fractionated and

resulted in five sub-fractions, E31 (11 mg), E32 (111 mg), E33 (13 mg), E34 (7 mg) and E35 (15 mg). Separation of fraction E5 (390 mg) provided four sub-fractions, E51 (10 mg), E52 (29 mg), E53 (32 mg) and E54 (45 mg). The sub-fractions with major spots on TLC chromatogram were isolated by PTLC techniques which the conditions used were described in Table 9. As noticed from TLC chromatogram, sub-fraction E51 provided one spot on chromatogram suggesting the pure compound denoted as compound **5**. When comparing the weights of fraction used to isolate compounds and that of sub-fractions obtained, implying there were some compounds retained in the column and could not be eluted by the mobile phase.



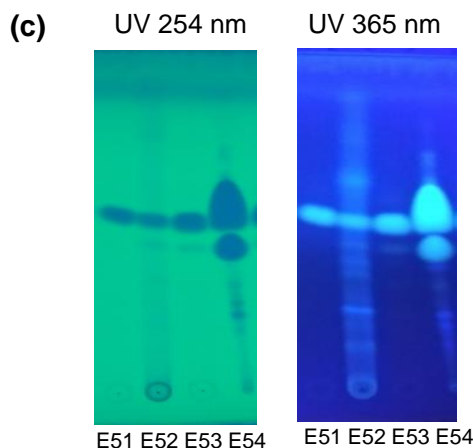


Figure 11. TLC chromatogram of sub-fractions obtained from column chromatography of E1, E2, E3 and E5

Mobile phase used was (a) hexane:ethyl acetate (8:2) (b) toluene:ethyl acetate (10:1.5) (c) toluene: ethyl acetate (10:1.5) x2 migrations followed by chloroform: methanol (12:1).

Table 9. PTLC conditions used to isolate pure compounds

Fractions	Sub-fractions selected for compound isolation	Mobile phase	Isolated pure compound
E1	E11	hexane:ethyl acetate (8:2)	<u>1</u>
E2	E21, E22	hexane:ethyl acetate (8:2)	<u>1</u>
E3	E32	n-hexane:ethyl acetate (7:3) x 2 migrations	<u>2</u> , <u>3</u>
E5	E54	toluene:ethyl acetate (10:1.5) x2 migrations followed by chloroform : methanol (12:1)	<u>4</u> , <u>5</u>

The effects of the pure isolated compounds on P-gp function were screened in Caco-2, LLC-PK₁ and LLC-GA5-COL300. During the preliminary screening study, compound 2 and 3 were mistaken as one compound because of overlapping of spots in TLC chromatogram. However, the oval shape of the spot doubted the presence of one pure compound so that the isolation technique was searched out and the

appropriate system was finally discovered as in Table 9. In Caco-2 experiment, there were 1.2 and 1.5 folds increased in calcein-AM uptake in the presence of compound 2 + 3 and 4. The results were consistent with the findings observed in LLC-PK₁ and LLC-GA5-COL300. In the presence of compound 2 + 3 and 4 the accumulation of calcein was noticeably increased to 9.8 and 7.4 folds in LLC-GA5-COL300 compared to that of LLC-PK₁. Compound 1 and 5 exhibited minimal effects on uptake of calcein-AM. Taken together, compound 2, 3 and 4 suggested the strong inhibition effects on P-gp function. Regardless of their activities, all five pure compounds were identified by chromatographic and spectroscopic analysis.

Table 10. Preliminary screening of the compounds on P-gp function in Caco-2, LLC-PK₁ and LLC-GA5-COL300

Compounds (30 µg/ml)	CAM-uptake (% of the control) in cell line (passage no.)		
	Caco-2 (37, 39)	LLC-PK ₁ (37, 38)	LLC-GA5-COL300 (30, 31)
<u>1</u>	100.1	84.5	161.7
<u>2</u> + <u>3</u>	124.5	133.8	975.0
<u>4</u>	148.9	101.9	735.3
<u>5</u>	107.3	97.3	180.4

Data are presented as the averages from two cell passages.

4. Identification of the active compounds and their activities on P-gp function

4.1 Identification of the isolated pure compounds

Five compounds (1 - 5) were identified by various methods. The R_f values on TLC chromatogram of the isolated pure compound were compared with the available standard. The molecular weights of the compounds were analyzed by LC-MS technique. ¹H-NMR spectral data of the compounds were compared to those of the published data. All five compounds are classified as furanocoumarins. The

information of LC-MS and ^1H -NMR chromatograms of the isolated compounds is shown in appendix 2.

Compound **1** was obtained as white powder. The R_f value was 0.65 when hexane:ethyl acetate (8:2) was used as the mobile phase. The R_f value of compound **1** was comparable with standard bergamottin (Apin Chemicals, Code: 06450b) as shown in figure 12. HPLC analysis showed the peak with retention time at 53.6 min resembled that of standard bergamottin. The MS chromatogram of compound **1** showed a parent $[\text{M}+\text{H}]^+$ ion at m/z 339, indicating the molecular weight of the compound. Taken together, compound **1** was identified as bergamottin. The molecular formula is $\text{C}_{21}\text{H}_{22}\text{O}_4$, with molecular weight of 338 (115-118).

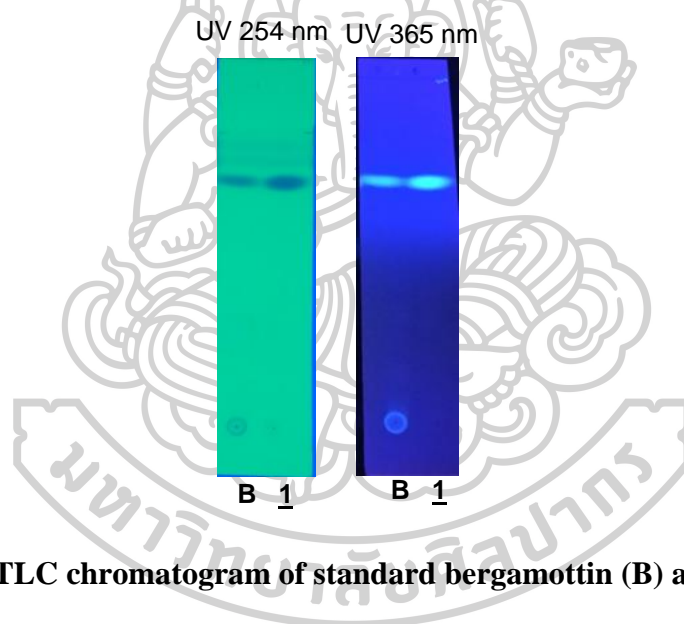


Figure 12. TLC chromatogram of standard bergamottin (B) and compound **1**

The TLC chromatogram of the compound **2** showed R_f value at 0.84 by developing TLC plate in toluene:ethyl acetate (10:1.5) followed by chloroform:methanol (12:1) (Figure 13). ^1H -NMR pattern was as follows; ^1H -NMR (CD_3OD) δ 1.25 (3H, s, $4'\text{CH}_3$), δ 1.27 (3 H, s, $3'\text{CH}_3$), δ 3.31 (3H, s, $1'\text{CH}_3$), δ 5.05 (1H, dd, $1'\text{H}$), δ 5.08 (1H, dd, $2'\text{H}$), δ 6.30 (1H, d, 3H), δ 7.19 (1H, dd, 11H), δ 7.22 (1H, s, 8H), δ 7.81 (1H, s, 12H), δ 8.30 (1H, d, 4H), which was comparable with the pattern of epoxybergamottin (119, 120). The mass spectrum of compound **2** was characterized by a parent $[\text{M}+\text{H}]^+$ ion at m/z 355 which is the molecular weight of epoxybergamottin. In summary, compound **2** is white powder identified as

epoxybergamottin, which molecular formula is $C_{21}H_{22}O_5$, with molecular weight of 354 (115, 117, 121).

Compound **3** is white powder and TLC chromatogram showed R_f value at 0.79 by developing in toluene:ethyl acetate (10:1.5) followed by chloroform: methanol (12:1) (Figure 13). 1H -NMR pattern was comparable with oxypeucedanin reported in the literature (17-19). 1H -NMR pattern was as follows; 1H -NMR (CD_3OD) δ 1.34 (3H, s, 4' CH_3), δ 1.39 (3 H, s, 3' CH_3), δ 3.33 (3H, s, 1' OCH_3), δ 4.45 (1H, dd, 1'H), δ 4.76 (1H, dd, 2'H), δ 6.33 (1H, d, 3H), δ 7.19 (1H, dd, 11H), δ 7.24 (1H, s, 8H), δ 7.82 (1H, d, 12H), δ 8.35 (1H, d, 4H). The chemical ionization MS of compound **3** manifested a parent $[M+H]^+$ ion at m/z 287 related to the molecular weight of oxypeucedanin. According to these results, compound **3** was identified as oxypeucedanin, which molecular formula is $C_{16}H_{14}O_5$, with molecular weight of 286 (115, 122).

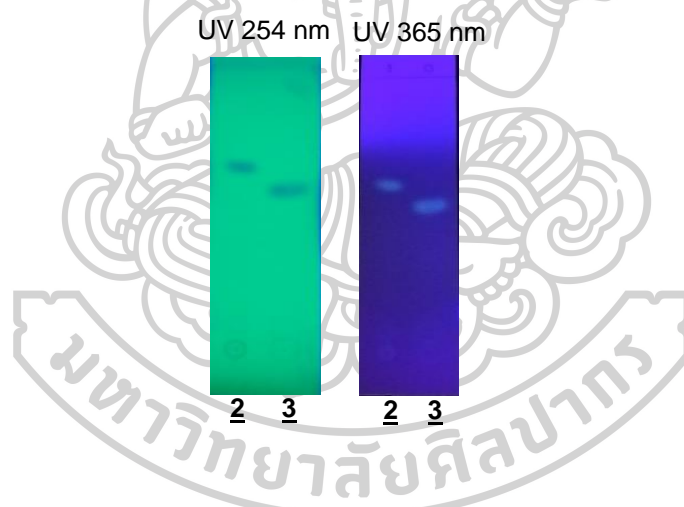


Figure 13. TLC chromatogram of compound **2 and oxypeucedanin **3****

Compound **4** was collected as white powder. TLC chromatogram showed R_f value at 0.28 by developing in toluene:ethyl acetate (10:1.5) followed by chloroform: methanol (12:1). Its R_f was comparable with standard dihydroxybergamottin (Figure 14). HPLC analysis showed the peak with retention time at 43.2 min resembled that of standard dihydroxybergamottin. The chemical ionization MS of compound **4** expressed a parent $[M+H]^+$ ion at m/z 373 which was related to the molecular weight of dihydroxybergamottin. Taken together, compound **4** was identified as

dihydroxybergamottin, which molecular formula is $C_{21}H_{24}O_6$, with molecular weight of 372 (117, 118, 123).

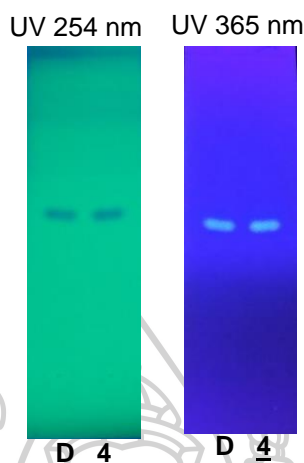


Figure 14. TLC chromatogram of standard dihydroxybergamottin (D) and compound 4

Compound 5 was obtained as white powder. TLC chromatogram showed R_f value at 0.24 by developing in toluene:ethyl acetate (10:1.5) followed by chloroform:methanol (12:1), which was comparable with standard oxypeucedanin hydrate (Figure 14). HPLC analysis showed the peak with retention time at 28.9 min resembled that of standard oxypeucedanin hydrate. The chemical ionization MS of compound 5 demonstrated a parent $[M+H]^+$ ion at m/z 305 which equals to the molecular weight of oxypeucedanin hydrate. Therefore, compound 5 was identified as oxypeucedanin hydrate, which molecular formula is $C_{16}H_{16}O_6$, with molecular weight of 304 (115).

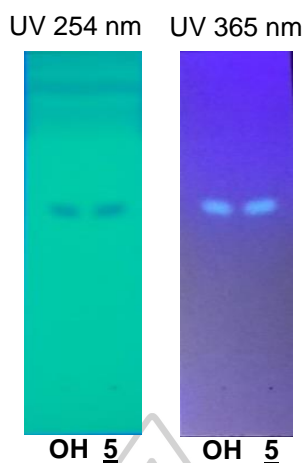


Figure 15. TLC chromatogram of standard oxypeucedanin hydrate (OH) and compound 5

TLC chromatogram in figure 16 depicts five isolated compounds in flavedo extract of *C. hystrix* fruit. As seen in figure 17, HPLC analysis provided the retention time of bergamottin, epoxybergamottin, oxypeucedanin, dihydroxybergamottin and oxypeucedanin hydrate is 53.6, 48.8, 43.4, 42.8 and 28.9 min, respectively. Table 11 presents the content of each furanocoumarin found in the flavedo extract of *C. hystrix* fruit calculated from HPLC analysis. Among all furanocoumarins isolated from this study, oxypeucedanin was the highest and bergamottin was the lowest content found in the flavedo extract.

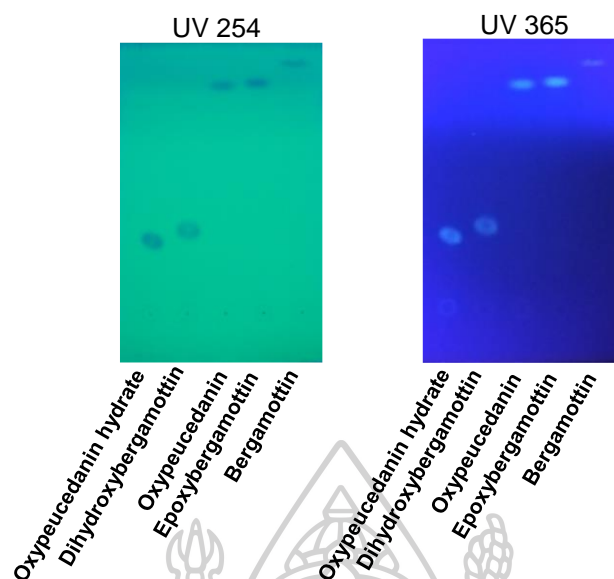


Figure 16. TLC chromatogram of the isolated pure compounds

Mobile phase used was toluene:ethyl acetate (10:1.5) x2 migrations followed by chloroform:methanol (12:1).

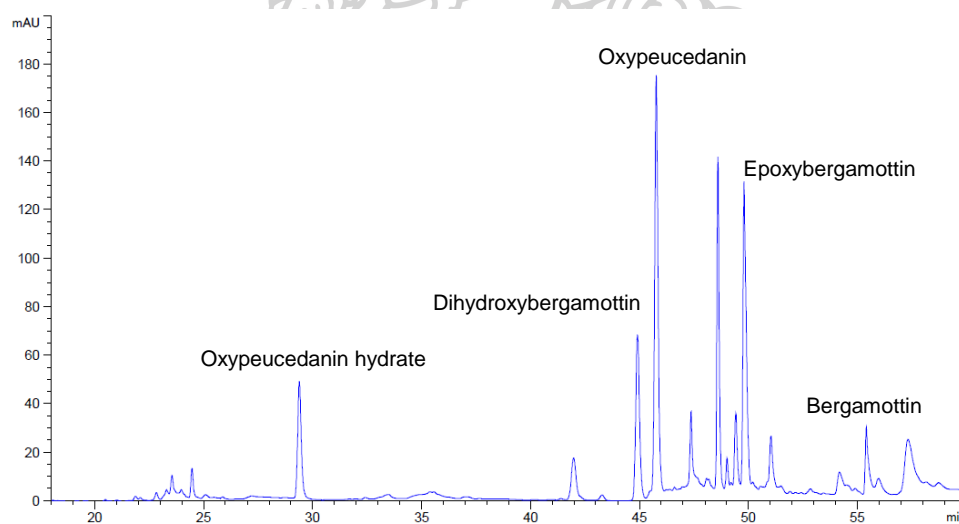
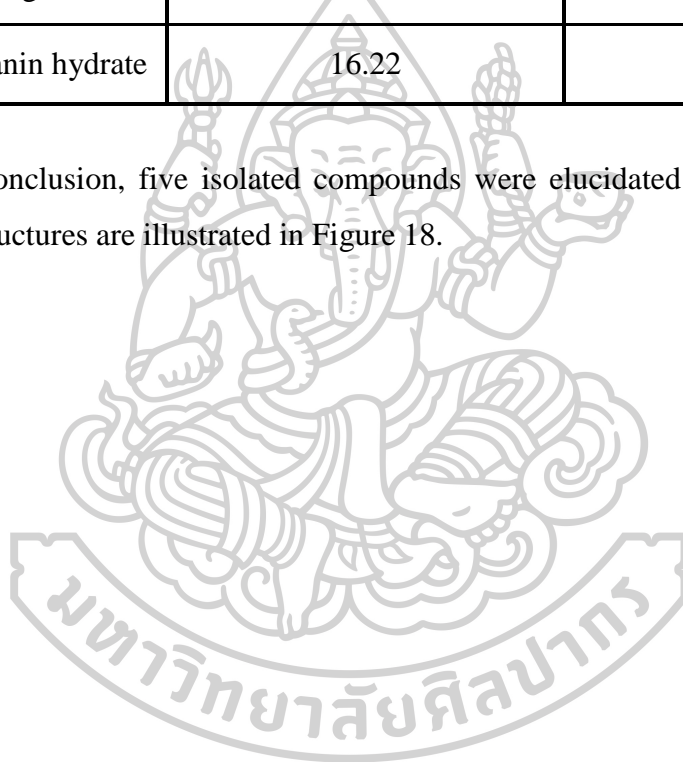


Figure 17. HPLC chromatogram of furanocoumarins found in flavedo extract of *C. hystrix* fruit

Table 11. The content of furanocoumarins found in the flavedo of *C. hystrix* fruit

Compounds	Content in flavedo extract (µg/mg)	Content in dried flavedo (µg/mg)
Bergamottin	8.9	2.2
Epoxybergamottin	47.58	11.6
Oxypeucedanin	48.26	11.8
Dihydroxybergamottin	23.68	5.8
Oxypeucedanin hydrate	16.22	4.0

In conclusion, five isolated compounds were elucidated as furanocoumarins and their structures are illustrated in Figure 18.



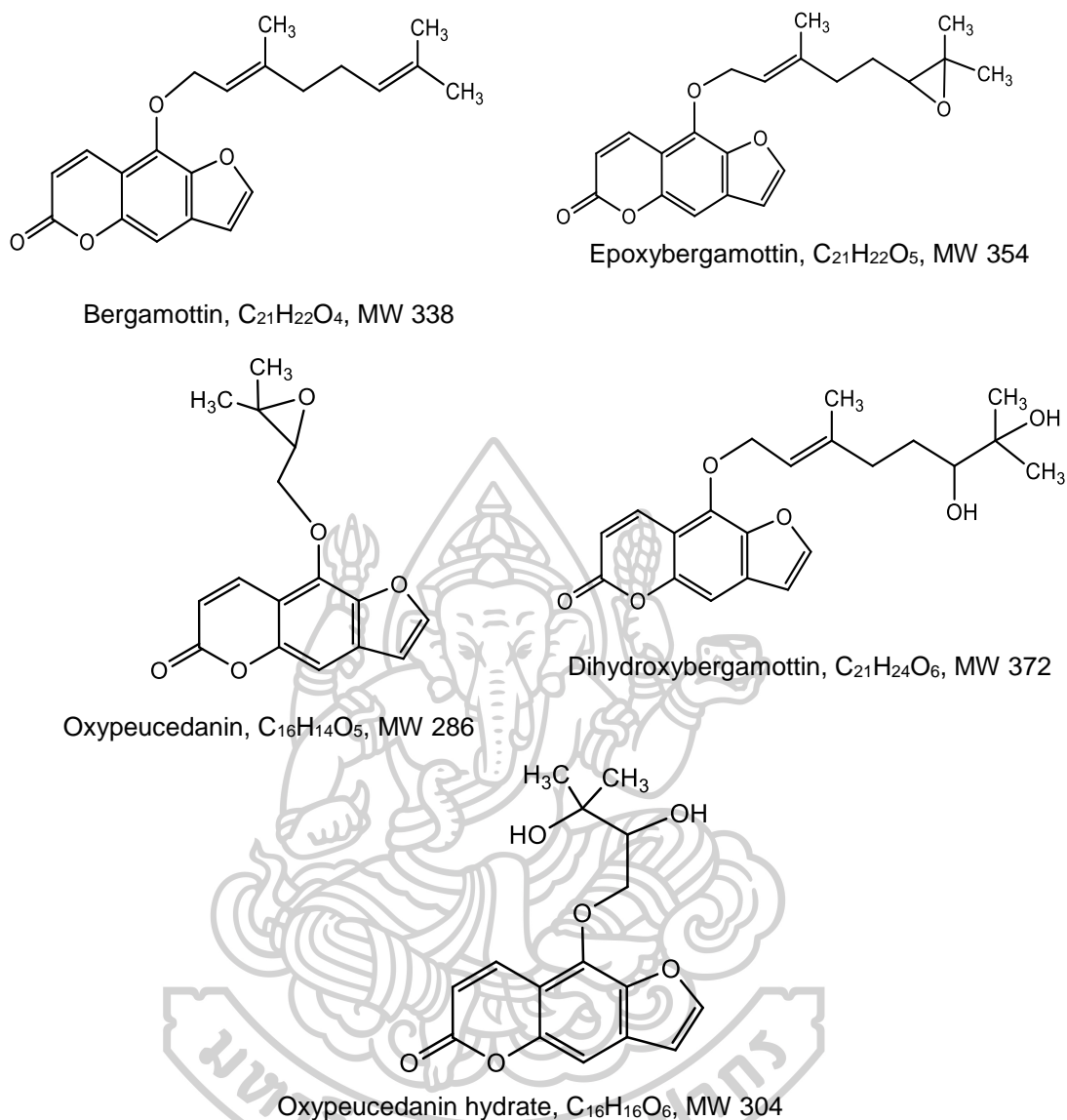


Figure 18. Structures of isolated furanocoumarins from *C. hystrix flavedo*

4.2 Effects of the isolated furanocoumarins on P-gp function

The effect of five furanocoumarins on P-gp function was performed by comparing calcein-AM uptake in LLC-PK₁ and LLC-GA5-COL300. No statistically significant increase in calcein-AM uptake was observed in LLC-PK₁ in the presence of the test furanocoumarins. However, the accumulation of calcein in LLC-GA5-COL300 was significantly enhanced in the presence of epoxybergamottin (16.7 folds), dihydroxybergamottin (7.3 folds) and oxypeucedanin (4.5 folds) compared to that of the control (Figure 19) suggesting that these compounds could inhibit P-gp function.

As found, bergamottin weakly increased the uptake of calcein-AM and oxypeucedanin hydrate showed the weakest effect on P-gp function. Epoxybergamottin, dihydroxybergamottin and oxypeucedanin showed statistically significant effects on P-gp inhibition.

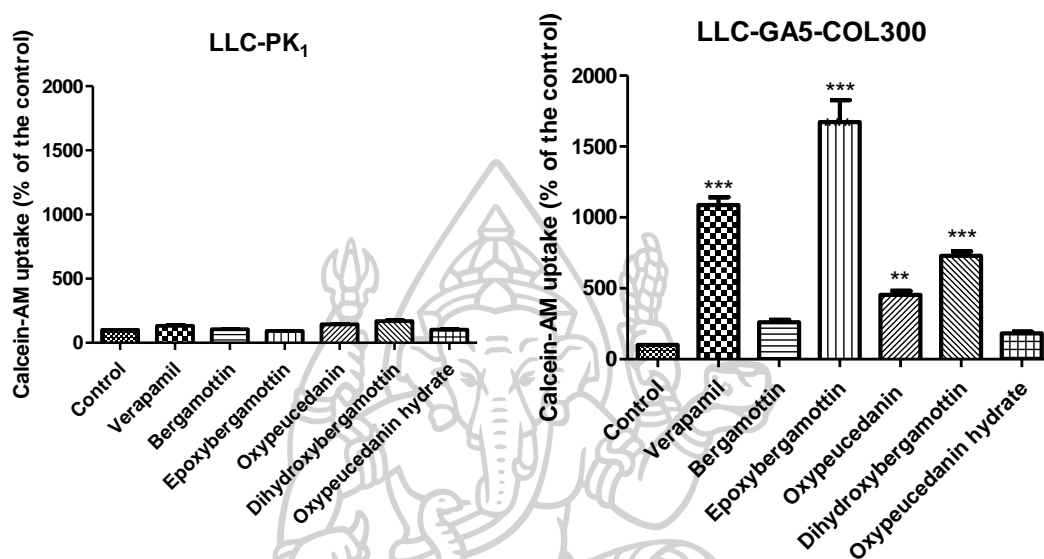


Figure 19. Effects of furanocoumarins (100 µM) on calcein-AM uptake in LLC-PK₁ and LLC-GA5-COL300

LLC-PK₁ (N=2) and LLC-GA5-COL300 (N ≥ 3, ***p < 0.001, **p < 0.01)

Hence, concentration dependent effects of the epoxybergamottin, dihydroxybergamottin and oxypeucedanin on P-gp inhibition were further investigated in LLC-GA5-COL300. The concentrations of each furanocoumarin were varied from 10 to 200 µM. As noticed in table 12, epoxybergamottin increased calcein-AM uptake about 2.5-25 folds. Approximately 2-28 folds increased in the accumulation of calcein were observed in the presence of dihydroxybergamottin. Oxypeucedanin also enhanced calcein accumulation by approximately 2-20 folds.

Table 12. Concentration dependent effects of epoxybergamottin, dihydroxybergamottin and oxypeucedanin on calcein-AM uptake in LLC-GA5-COL300
(N ≥ 3)

Compounds	Calcein-AM uptake (% of the control)				
	Concentration (μM)				
	10	25	50	100	200
Epoxybergamottin	250.9 ± 16.8	903.6 ± 28.1	1404.3 ± 40.5	1672.0 ± 155.8	2445.6 ± 40.7
Dihydroxybergamottin	219.0 ± 35.0	248.1 ± 20.0	455.3 ± 11.3	729.6 ± 32.0	2194.2 ± 272.6
Oxypeucedanin	186.0 ± 44.0	214.7 ± 29.1	260.6 ± 25.6	453.5 ± 29.2	1030.8 ± 126.4

Furanocoumarins derived from citrus fruits and vegetables can act as anti-coagulant, antiviral, antibacterial, antioxidant, anti-inflammatory, immunomodulator, apoptotic and anticancer agents (124). Moreover, furanocoumarins have been reported as efflux transporter P-gp inhibitors *in vitro* and in animal studies (125). Dihydroxybergamottin was reported to significantly increase vinblastine accumulation in Caco-2 and LLC-GA5-COL300 cells suggesting P-gp inhibition. Bergamottin also exhibited significant increase in accumulation of vinblastine in Caco-2 but showed less potency than dihydroxybergamottin (126). Dihydroxybergamottin was also shown to potentiate the vinblastine and saquinavir uptake indicating interaction with P-gp (84). In the present study, dihydroxybergamottin inhibited P-gp and its potency was higher than bergamottin, which are in agreement with the previous studies.

Castro *et al.* studied the effect of the components of grapefruit juice on P-gp mediated talinolol transport in Caco-2. They reported that epoxybergamottin was the most potent inhibitor of P-gp, followed by dihydroxybergamottin (127). On the other hand, bergamottin did not show any inhibition on P-gp mediated talinolol in Caco-2 (127). This is in accordance with the present study that shows epoxybergamottin with the highest activity on P-gp inhibition, followed by dihydroxybergamottin. Bergamottin showed the moderate inhibition on P-gp activity. Dong *et al.* reported that oxypeucedanin significantly inhibited P-gp function in MDCK-MDR1 cells but did not demonstrate dose dependence (128). In contrast to this study, oxypeucedanin displayed P-gp inhibition in concentration dependent manner. The present study used LLC-GA5-COL300 while the Dong *et al.* study utilized MDCK-MDR1. The difference in the cell culture model used may lead to different results.

Collectively, the data suggested that all five furanocoumarins could inhibit P-gp function. The order of inhibitory potency was epoxybergamottin, dihydroxybergamottin, oxypeucedanin, bergamottin and oxypeucedanin hydrate. Epoxybergamottin, dihydroxybergamottin and oxypeucedanin significantly enhanced calcein-AM uptake in the concentration dependent manner, indicating that these three furanocoumarins strongly inhibited P-gp efflux function.

5. Effects of dihydroxybergamottin and oxypeucedanin on P-gp function and expression

Dihydroxybergamottin and oxypeucedanin were selected to perform the studies on P-gp function and expression. Although epoxybergamottin exhibited strong inhibition effect on P-gp, the limited content of the compound made it not available for extensive study.

5.1 Evaluation of dihydroxybergamottin and oxypeucedanin as P-gp substrate

To identify the roles of dihydroxybergamottin and oxypeucedanin as substrates of P-gp, bidirectional transport study suggested by USFDA regulatory agencies (45) was used. The study was performed in LLC-GA5-COL300 and parental LLC-PK₁. When using transfected cell lines, the efflux ratios of the transfected cell line to the parental cell line were reported. The compound is classified as P-gp substrate when its corrected net flux ratio is equal to or higher than 2.

As seen in table 13, the corrected net flux ratio of dihydroxybergamotin which was correlated to the ratio observed in LLC-GA5-COL300 relative to the ratio observed in respective LLC-PK₁ was 1.5 ± 0.2 . The corrected net flux ratio of dihydroxybergamottin determined was apparently lower than the cut off value indicated by the USFDA. On the other hand, the corrected net flux value for oxypeucedanin obtained from comparing the efflux ratio of LLC-GA5-COL300 and that of LLC-PK₁ was 3.1 ± 0.2 which clearly fulfilled the USFDA criteria, indicating that oxypeucedanin was likely to be P-gp substrate.

According to the FDA guidance, if the efflux ratio of the test compound is decreased to greater than 50% of the efflux ratio in the absence of inhibitor or to a unity by known P-gp inhibitor, it is proven to be P-gp substrate (45). To confirm that the compounds were substrates of P-gp, the efflux was evaluated in the presence and absence of a P-gp inhibitor, cyclosporine. In the presence of cyclosporine, the efflux ratio of dihydroxybergamottin was reduced from 2.1 ± 0.2 to 1 ± 0.2 . While the basolateral to apical transport of oxypeucedanin was significantly decreased in the presence of cyclosporine (figure 20). The efflux ratio of oxypeucedanin reduced from

3.7 ± 0.2 to 1.6 ± 0.03 in the presence of cyclosporine. The reduction of the efflux ratio of oxypeucedanin seen in the presence of cyclosporine was greater than 50 % which was in accordance with the guidance.

According to the data from the corrected efflux ratio and inhibitor effects, oxypeucedanin is probably substrate of P-gp while dihydroxybergamottin was unlikely to be substrate of P-gp.

Table 13. Apparent permeability coefficients and efflux ratio of dihydroxybergamottin and oxypeucedanin in bidirectional transport study (N=3)

Compounds	$P_{app, a-b}$ (10^{-5} cm/s)	$P_{app, b-a}$ (10^{-5} cm/s)	Efflux ratio	Net flux ratio (corrected)
Dihydroxybergamottin	3.7 ± 0.8	7.5 ± 1.1	2.1 ± 0.2	1.5 ± 0.2
Oxypeucedanin	5.8 ± 2.6	20.3 ± 8.2	3.7 ± 0.2	3.1 ± 0.2

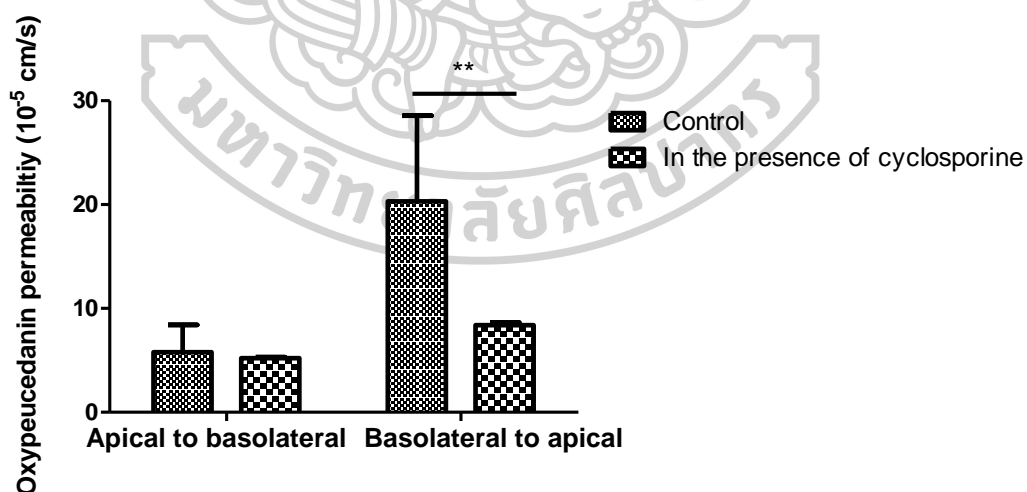


Figure 20. Effect of cyclosporine (10 μ M) on oxypeucedanin transport in LLC-GA5-COL300

(N=3, **p < 0.01)

5.2 Evaluation of dihydroxybergamottin and oxypeucedanin as P-gp inhibitor

The effect of dihydroxybergamottin and oxypeucedanin on P-gp inhibition was studied by utilizing doxorubicin uptake and transport. Doxorubicin is a widely used chemotherapeutic agent which is a selective P-gp substrate and useful in studying P-gp functionality *in vitro* (70, 129). This study was performed in LLC-GA5-COL300, which is overexpressed human P-gp cell line. Cyclosporine was used as a positive control (130).

5.2.1 Doxorubicin uptake assay

This study exhibited that the increased concentration of cyclosporine resulted in the increase in fluorescence signal of intracellular doxorubicin caused by the inhibition of P-gp pump. Similarly, doxorubicin uptake in LLC-GA5-COL300 was enhanced when the concentrations of dihydroxybergamottin and oxypeucedanin were increased (Figure 21). IC_{50} values for P-gp activity, which correspond to EC_{50} values for increase of doxorubicin accumulation, were obtained from the plot of doxorubicin accumulation and compound concentrations. Cyclosporine was shown to be the most potent with IC_{50} of $2.4 \pm 0.1 \mu M$ and this value is in accordance with the published IC_{50} (131). From the study, dihydroxybergamottin is about 17 times less potent than cyclosporine. Between two furanocoumarins tested in this assay, oxypeucedanin is less potent than dihydroxybergamottin.

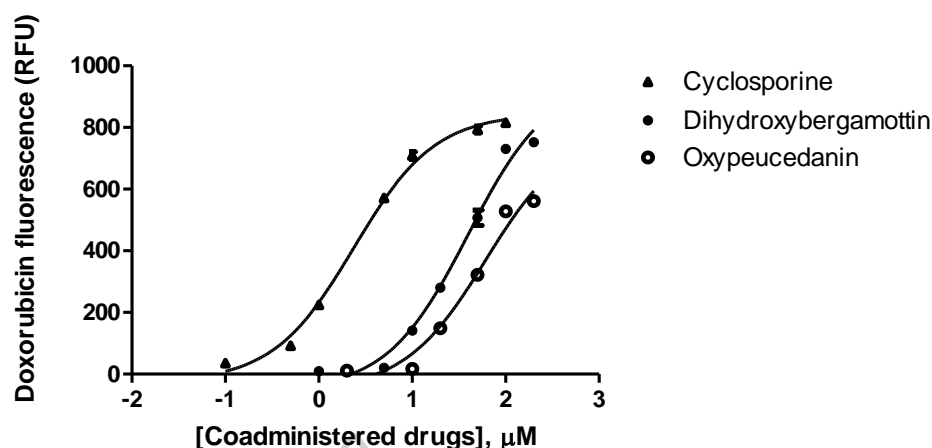


Figure 21. Effects of dihydroxybergamottin and oxypeucedanin on intracellular accumulation of doxorubicin in LLC-GA5-COL300 (N = 3)

5.2.2 Doxorubicin transport assay

To validate the function of P-gp, the transport of doxorubicin in LLC-GA5-COL300 compared with that of LLC-PK₁ was performed. The average permeability coefficients of doxorubicin performed in LLC-GA5-COL300 were 1.1×10^{-5} cm/s from apical to basolateral and 4.6×10^{-5} cm/s from basolateral to apical (n=2), respectively. Transepithelial transport of doxorubicin across LLC-GA5-COL300 showed a marked asymmetry with average net efflux value of 4.2. In LLC-PK₁, $P_{app, a-b}$ for doxorubicin transport was 3.3×10^{-5} cm/s and $P_{app, b-a}$ was 3.2×10^{-5} cm/s, giving an efflux ratio of close to unity. Increased an efflux ratio of doxorubicin in LLC-GA5-COL300 compared to that of LLC-PK₁ demonstrated that P-gp function in LLC-GA5-COL300 was acceptable.

Unidirectional (basolateral to apical) transport studies recommended by EMA (46) and FDA (45) regulatory guidelines were used in the experiment. The effects of various concentrations of dihydroxybergamottin and oxypeucedanin on P-gp function were investigated by measuring basolateral to apical transport of doxorubicin across LLC-GA5-COL300. The percentage of the control transport activity in the presence of each furanocoumarin was calculated by the equation as follows;

$$\% \text{ control activity} = \frac{(P_{\text{app (+ test compound)}} - P_{\text{app (passive)}})}{(P_{\text{app (vehicle control)}} - P_{\text{app (passive)}})} \times 100$$

Where,

$P_{\text{app (+test compound)}}$ is the P_{app} of doxorubicin in LLC-GA5-COL300 in the presence of test compound.

$P_{\text{app (vehicle control)}}$ is the P_{app} of doxorubicin in LLC-GA5-COL300 in the absence of test compound.

$P_{\text{app (passive)}}$ is the P_{app} of doxorubicin in the LLC-PK₁ in the absence of test compound.

The IC₅₀ of the compounds were calculated from the concentration which produces 50% inhibition of vehicle control transport activity. As seen in table 14, doxorubicin transport in the secretory direction (basolateral to apical) in LLC-GA5-COL300 was reduced in the presence of dihydroxybergamottin and oxypeucedanin. The P-gp inhibition effects was concentration dependent. The IC₅₀ values of dihydroxybergamottin and oxypeucedanin are shown in table 15. As seen, the IC₅₀ values of dihydroxybergamottin and oxypeucedanin discovered from uptake study of doxorubicin are comparable with those of transport study. Dihydroxybergamottin is a stronger P-gp inhibitor than oxypeucedanin.

USFDA draft guidance (45) states that if the efflux ratio of a known P-gp substrate is decreased with the increasing concentration of the test compound in unidirectional transport assay, they will probably be inhibitor of P-gp. The present study was in agreement with the guidance that both dihydroxybergamottin and oxypeucedanin apparently reduced the efflux ratio of the P-gp substrate doxorubicin. As mentioned in the guidance, the compound has the potential to inhibit P-gp *in vivo* when administered orally where the $[I]_2 / IC_{50} \geq 10$, where $[I]_2$ = dose of inhibitor / 250 ml. From the estimation, dihydroxybergamottin has the potential to inhibit P-gp *in vivo* at the dose of ≥ 37.2 mg and oxypeucedanin does at the dose of ≥ 35.8 mg.

Table 14. P_{app} , $b-a$ values of doxorubicin and the percentage of the control transport activity in the absence and presence of dihydroxybergamottin and oxypeucedanin performed in LLC-GA5-COL300 (N = 3)

Concentration of furanocoumarins (μM)	$P_{app, b-a}$ (10^{-5} cm/s)	% of the control activity
Dihydroxybergamottin		
0	6.2 ± 0.15	100
5	5.9 ± 0.10	94 ± 3.0
25	4.7 ± 0.07	68 ± 2.0
50	3.6 ± 0.03	45 ± 2.0
100	2.6 ± 0.10	21 ± 0.7
200	1.9 ± 0.01	6 ± 1.5
Oxypeucedanin		
0	6.2 ± 0.15	100
5	6.3 ± 0.01	103 ± 2.6
25	4.8 ± 0.06	70 ± 1.5
50	3.8 ± 0.05	49 ± 1.5
100	2.9 ± 0.15	30 ± 5.0
200	2.0 ± 0.03	8 ± 1.9

Table 15. The IC₅₀ values of the dihydroxybergamottin and oxypeucedanin calculated from doxorubicin uptake and transport studies

(N = 3)

Compounds	IC ₅₀ (μM)	
	Uptake study	Transport study
Dihydroxybergamottin	39.8 ± 0.8	41.5 ± 2.1
Oxypeucedanin	60.3 ± 1.0	50.7 ± 5.1

5.2.3 Inhibition mechanisms

The inhibition mechanism of dihydroxybergamottin and oxypeucedanin on P-gp activity was investigated by comparing the uptake of calcein-AM in the presence of a furanocoumarin under various incubation conditions. The study was conducted in LLC-GA5-COL300 under three incubation conditions, including 1) only preincubation, 2) only coincubation and 3) preincubation and coincubation. As seen in figure 22, the preincubation condition shows the lowest effect on calcein accumulation. Dihydroxybergamottin and oxypeucedanin increased calcein-AM uptake by 1.3 folds and 1.4 folds of the control in preincubation condition. The accumulation of calcein increased to 4.7 folds and 3.1 folds of the control when dihydroxybergamottin and oxypeucedanin were coincubated with P-gp substrate calcein-AM in the experiment. Differences in the calcein-AM uptake can be found between preincubation and coincubation conditions, suggesting that inhibition of P-gp can be reversible after removing the compounds. The similar pattern was seen with verapamil which is a reversible P-gp inhibitor (132).

On the other hand, irreversible inhibitors were reported to exhibit no difference between preincubation and coincubation conditions indicating P-gp function is permanently inhibited even after removing the inhibitors e.g. N-ethylmaleimide, PSC 833 (132, 133). These results suggested that

dihydroxybergamottin and oxypeucedanin are reversible P-gp inhibitors. Interestingly, the highest calcein-AM uptake was noticed when both preincubation and coincubation were used in the study for all compounds tested.

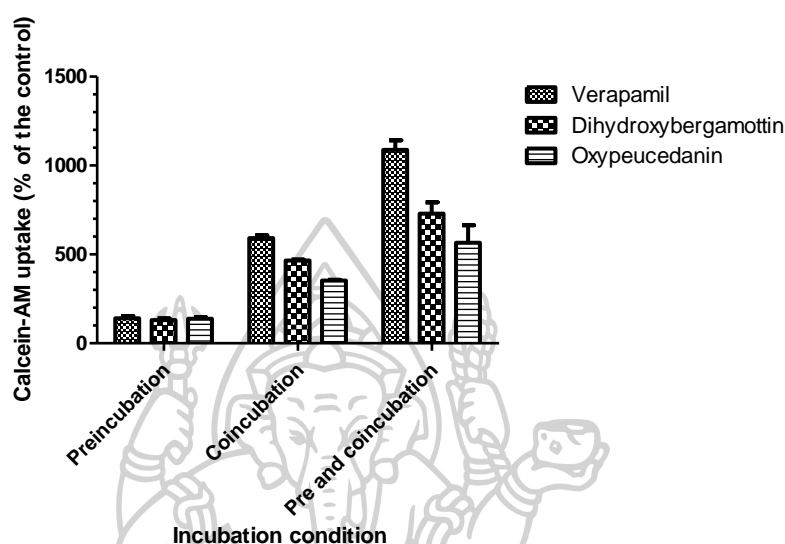


Figure 22. Effect of incubation conditions on calcein-AM uptake in LLC-GA5-COL300 in the presence of dihydroxybergamottin and oxypeucedanin (N = 3), Verapamil was used as the positive control

5.3 Effects of dihydroxybergamottin and oxypeucedanin on P-gp expression

The regulations of dihydroxybergamottin and oxypeucedanin on P-gp protein expression in LLC-GA5-COL300 were explored by utilizing western blot. The expression of human P-gp in LLC-GA5-COL300 was validated by comparing with that of LLC-PK₁. P-gp was highly expressed in the LLC-GA5-COL300 cell line but undetectable in the parental LLC-PK₁ cell line under the same condition, indicating that LLC-GA5-COL300 expressed human MDR1 protein as stated (Figure 23). Consequently, LLC-GA5-COL300 was used to investigate the effect of dihydroxybergamottin and oxypeucedanin on P-gp protein expression. Verapamil was used as a positive control in the study. As seen, 100 μ M verapamil noticeably suppressed the P-gp protein expression of the LLC-GA5-COL300 cells (Figure 24).

Dihydroxybergamottin at 25 μM and 50 μM did not significantly modulate the P-gp expression level, although inhibition on P-gp expression appeared to be approximately 20% at 50 μM dihydroxybergamottin. At 100 μM , dihydroxybergamottin significantly reduced the P-gp expression level to about 40 % (Figure 24). P-gp protein expression decreased when the concentrations of dihydroxybergamottin were increased, suggesting that dihydroxybergamottin could concentration dependently down-regulate P-gp expression in LLC-GA5-COL300.

Oxypeucedanin suppressed P-gp protein expression to about 72 % and 63 % of the control at 25 μM and 50 μM , respectively. In particular, P-gp protein expression level in the presence of 100 μM oxypeucedanin significantly decreased to 57 % compared with that in the control (Figure 24). As seen, oxypeucedanin reduced P-gp expression in a concentration dependent manner. The inhibitory action of oxypeucedanin on P-gp protein expression was slightly stronger than dihydroxybergamottin. In agreement with the present study, oxypeucedanin was also reported to inhibit P-gp protein expression in MDCK-MDR1 cell line (128). The results from this study demonstrated that dihydroxybergamottin and oxypeucedanin could down-regulate P-gp protein expression.

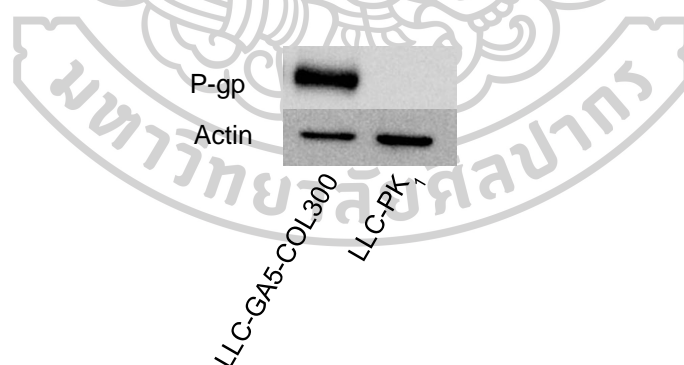


Figure 23. MDR1 expression in LLC-PK₁ and LLC-GA5-COL300

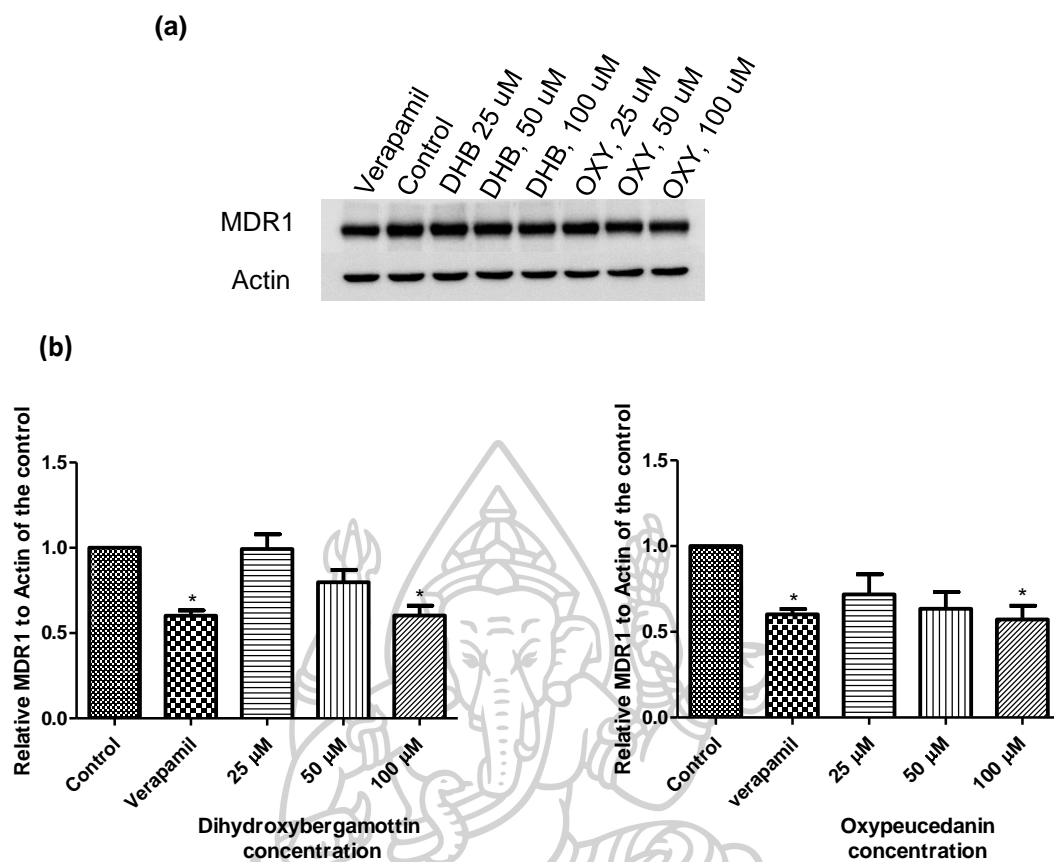


Figure 24. Effects of dihydroxybergamottin and oxypeucedanin on P-gp protein expression in LLC-GA5-COL300

(a) Representative P-gp expression by western blot on LLC-GA5-COL300 treated with various concentrations of dihydroxybergamottin (DHB) and oxypeucedanin (OXY). (b) Quantitative data of P-gp expression (N=3, *p < 0.05)

Chapter 4

Conclusion

A drug can be administered by various routes of administration. Among them the oral route of administration is the most common and acceptable route of administration. However, oral route represents the greatest number of barriers of drugs to be absorbed into systemic circulation. Recently, P-gp has been reported to modify the bioavailability of many orally administered drugs through its ability to efflux substrates back into the intestinal lumen (33).

Food can interact with orally administered drugs and can modify the pharmacokinetic and/or pharmacodynamics profile of drugs, some of which may be clinically significant. Among all food, fruits have a high potential for interacting with drugs since they are widely available and frequently consumed, either as whole fruits, meal condiments, fruit juices, flavored processed drinks or preserved snacks (134). *C. hystrix* fruit is commonly found in Thailand and Myanmar. It has been reported that this fruit inhibited intestinal CYP3A4 and CYP2C9 (102). However, there is no information about the role of *C. hystrix* on P-gp activity. Since the substrates, inhibitors, and inducers of CYP enzymes and P-gp overlapped (103, 104), the effect of *C. hystrix* fruit on the efflux transporter P-gp challenged the study. Therefore, this study was conducted to investigate the possibility of P-gp mediated drug interactions of *C. hystrix*.

The *C. hystrix* fruits were separated into flavedo, albedo, segment membrane and juice. TLC and HPLC analysis of the methanolic extracts revealed that the flavedo consists of more phytochemical constituents than albedo, segment membrane and juice. The study of these extracts on P-gp function demonstrated the highest inhibition of flavedo extract on human P-gp in a concentration dependent manner.

The flavedo extract was further separated by column chromatography and PTLC techniques. The active compounds were isolated based on their inhibition activities on human P-gp function. As found, five furanocoumarins were elucidated, namely, bergamottin, epoxybergamottin, oxypeucedanin, dihydroxybergamottin, and

oxypeucedanin hydrate. According to the result from HPLC analysis, oxypeucedanin was the highest and bergamottin was the lowest content found in the flavedo extract.

The effects of all five furanocoumarins on P-gp function were performed by comparing calcein-AM uptake between LLC-PK₁ and LLC-GA5-COL300. Epoxybergamottin, dihydroxybergamottin and oxypeucedanin showed statistically significant effects on P-gp inhibition while bergamottin exhibited moderate, and oxypeucedanin hydrate demonstrated the lowest effect on P-gp function. The highest to lowest order of inhibitory potency was epoxybergamottin, dihydroxybergamottin, oxypeucedanin, bergamottin and oxypeucedanin hydrate. Moreover, epoxybergamottin, dihydroxybergamottin and oxypeucedanin exhibited concentration dependent on P-gp inhibition.

Two furanocoumarins, dihydroxybergamottin and oxypeucedanin, were selected for investigation their roles on human P-gp inhibition. The effects on P-gp function and protein expression were further elucidated. Firstly, evaluation of dihydroxybergamottin and oxypeucedanin as substrates for P-gp was performed. The results showed that dihydroxybergamottin is not likely to be P-gp substrate but oxypeucedanin could potentially be substrate of P-gp. Secondly, determination of dihydroxybergamottin and oxypeucedanin as P-gp inhibitors was conducted. The results exhibited that both dihydroxybergamottin and oxypeucedanin acted as P-gp inhibitors. The IC₅₀ values of dihydroxybergamottin were $39.8 \pm 0.8 \mu\text{M}$ and $41.5 \pm 2.1 \mu\text{M}$ from uptake and transport studies, respectively. The IC₅₀ values of oxypeucedanin from uptake and transport studies were respectively $60.3 \pm 1.0 \mu\text{M}$ and $50.7 \pm 5.1 \mu\text{M}$. Moreover, the inhibition mechanism of both dihydroxybergamottin and oxypeucedanin appeared to be reversible. Thirdly, investigation of dihydroxybergamottin and oxypeucedanin P-gp protein expression was done using western blotting. The results demonstrated that both dihydroxybergamottin and oxypeucedanin could down-regulate the protein expression of P-gp in a concentration dependent manner. As noticed, oxypeucedanin seemed to be a little stronger inhibitor than dihydroxybergamottin.

Taken together, *C. hystrix* fruit contains furanocoumarins that have the ability to inhibit P-gp function and protein expression. These results imply the possibility of P-gp mediated drug interaction of the fruit and the furanocoumarin, when taken with

P-gp substrate drugs. However, a number of researchers have recently applied the P-gp inhibition effect of compounds as oral bioavailability enhancer. As found from this study, dihydroxybergamottin and oxypeucedanin have the potential to be bioavailability enhancers. Consequently, the *in vivo* study should be considered to confirm their effects.



REFERENCES

1. Buxton ILO, Benet LZ. Pharmacokinetics: The Dynamics of Drug Absorption, Distribution, Metabolism, and Elimination. 12th ed. Brunton LL, Chabner BA, Knollmann BC, editors. United States: The McGraw-Hill; 2011.
2. Giacomini KM, Sugiyama Y. Membrane Transporters and Drug Response. 12th ed. Brunton LL, Chabner BA, Knollmann BC, editors. United States: The McGraw-Hill; 2011.
3. Yu J, Zhou P, Asenso J, Yang XD, Wang C, Wei W. Advances in plant-based inhibitors of P-glycoprotein. *Journal of enzyme inhibition and medicinal chemistry*. 2016;31(6):867-81.
4. Zakeri-Milani P, Valizadeh H. Intestinal transporters: enhanced absorption through P-glycoprotein-related drug interactions. *Expert opinion on drug metabolism & toxicology*. 2014;10(6):859-71.
5. Amin ML. P-glycoprotein Inhibition for Optimal Drug Delivery. *Drug Target Insights*. 2013;7:27-34.
6. Rodríguez-Fragoso L, Reyes-Esparz J. Fruit/Vegetable-Drug Interactions: Effects on Drug Metabolizing Enzymes and Drug Transporters. 2013.
7. Lombard J. Once upon a time the cell membranes: 175 years of cell boundary research. *Biology Direct*. 2014;9(32):1-35.
8. Anderson JM. Molecular Structure of Tight Junctions and Their Role in Epithelial Transport. *Physiology*. 2001;16(3):126-30.
9. Keogh J, Hagenbuch B, Rynn C, Stiger B, Nicholls G. RSC Drug Discovery Series No. 54: Drug Transporters: Volume 1: Role and Importance in ADME and Drug Development. United Kingdom: The Royal Society of Chemistry; 2016.
10. Aloui L, Kossentini M, Geffroy-Rodier C, Guillard J, Zouari S. Phytochemical Investigation, Isolation and Characterization of Coumarins from Aerial Parts and Roots of Tunisian *Pituranthus chloranthus* (Apiaceae). *Pharmacognosy Communications*. 2015;5(4):237-43.
11. Artursson P, Karlsson J, Ocklind G, Schipper N. Studying transport processes in absorptive epithelia. Shaw AJ, editor. New York: Oxford University Press; 1996.
12. Brennan MB. Drug Discovery: Filtering out failures early in the game. *Chemical & Engineering News Archive*. 2000;78(23):63-73.
13. Panawala L. Difference between endocytosis and exocytosis. *PEDIAA*. 2017.
14. Zakeri-Milani P, Valizadeh H. Intestinal transporters: enhanced absorption through P-glycoprotein-related drug interactions. *Expert opinion on drug metabolism & toxicology*. 2014;10(6):859-71.
15. König J, Müller F, Fromm MF. Transporters and drug-drug interactions: important determinants of drug disposition and effects. *Pharmacological reviews*. 2013;65(3):944-66.
16. Liang Y, Li S, Chen L. The physiological role of drug transporters. *Protein & cell*. 2015;6(5):334-50.
17. Zhang Y, Zhang Y, Sun K, Meng Z, Chen L. The SLC transporter in nutrient and metabolic sensing, regulation, and drug development. *Journal of molecular cell biology*. 2019;11(1):1-13.

18. Jaramillo A, Saig F, Cloos J, Jansen G, Peters G. How to overcome ATP-binding cassette drug efflux transporter-mediated drug resistance? *Cancer Drug Resistance*. 2018;1:6-29.
19. Montanari F, Ecker GF. Prediction of drug-ABC-transporter interaction--Recent advances and future challenges. *Adv Drug Deliv Rev*. 2015;86:17-26.
20. Silva R, Vilas-Boas V, Carmo H, Dinis-Oliveira RJ, Carvalho F, de Lourdes Bastos M, et al. Modulation of P-glycoprotein efflux pump: induction and activation as a therapeutic strategy. *Pharmacol Ther*. 2015;149:1-123.
21. Chen Z, Shi T, Zhang L, Zhu P, Deng M, Huang C, et al. Mammalian drug efflux transporters of the ATP binding cassette (ABC) family in multidrug resistance: A review of the past decade. *Cancer Letters*. 2016;370(1):153-64.
22. Li W, Zhang H, Assaraf YG, Zhao K, Xu X, Xie J, et al. Overcoming ABC transporter-mediated multidrug resistance: Molecular mechanisms and novel therapeutic drug strategies. *Drug resistance updates : reviews and commentaries in antimicrobial and anticancer chemotherapy*. 2016;27:14-29.
23. Kim Y, Chen J. Molecular structure of human P-glycoprotein in the ATP-bound, outward-facing conformation. *Science (New York, NY)*. 2018;359(6378):915-9.
24. Hoosain FG, Choonara YE, Tomar LK, Kumar P, Tyagi C, du Toit LC, et al. Bypassing P-Glycoprotein Drug Efflux Mechanisms: Possible Applications in Pharmacoresistant Schizophrenia Therapy. *Biomed Res Int*. 2015;2015:484963-.
25. Sharom FJ. Complex Interplay between the P-Glycoprotein Multidrug Efflux Pump and the Membrane: Its Role in Modulating Protein Function. *Front Oncol*. 2014;4:41-.
26. Ferreira RJ, Ferreira MJ, dos Santos DJ. Molecular docking characterizes substrate-binding sites and efflux modulation mechanisms within P-glycoprotein. *Journal of chemical information and modeling*. 2013;53(7):1747-60.
27. Seelig A. A general pattern for substrate recognition by P-glycoprotein. *European Journal of Biochemistry*. 2017;251(1-2):252-61.
28. Fortuna A, Alves G, Falcão A. In vitro and In vivo Relevance of the P-glycoprotein Probe Substrates in Drug Discovery and Development: Focus on Rhodamine 123, Digoxin and Talinolol. *Journal of Bioequivalence & Bioavailability*. 2011;01.
29. Juliano RL, Ling V. A surface glycoprotein modulating drug permeability in Chinese hamster ovary cell mutants. *Biochimica et biophysica acta*. 1976;455(1):152-62.
30. Abdallah HM, Al-Abd AM, El-Dine RS, El-Halawany AM. P-glycoprotein inhibitors of natural origin as potential tumor chemo-sensitizers: A review. *Journal of advanced research*. 2015;6(1):45-62.
31. Sharom FJ. ABC multidrug transporters: structure, function and role in chemoresistance. *Pharmacogenomics*. 2008;9(1):105-27.
32. Hamed AR, Abdel-Azim NS, Shams KA, Hammouda FM. Targeting multidrug resistance in cancer by natural chemosensitizers. *Bulletin of the National Research Centre*. 2019;43(1):8.
33. Anwar-Mohamed A, El-Kadi A. P-glycoprotein effects on drugs

- pharmacokinetics and drug-drug-interactions and their clinical implications. The Libyan Journal of Pharmacy and Clinical Pharmacology LJPCP. 2012.
34. Srivalli KMR, Lakshmi PK. Overview of P-glycoprotein inhibitors: a rational outlook Brazilian Journal of Pharmaceutical Sciences. 2012;48(3):353-67.
 35. Srivalli KMR, Lakshmi PK. Overview of P-glycoprotein inhibitors: A rational outlook. Brazilian Journal of Pharmaceutical Sciences. 2012;48:353-67.
 36. Elmeliegy M, Vourvahis M, Guo C, Wang DD. Effect of P-glycoprotein (P-gp) Inducers on Exposure of P-gp Substrates: Review of Clinical Drug-Drug Interaction Studies. Clinical pharmacokinetics. 2020.
 37. Xie F, Ding X, Zhang Q-Y. An update on the role of intestinal cytochrome P450 enzymes in drug disposition. Acta Pharm Sin B. 2016;6(5):374-83.
 38. Lassoued MA, Sfar S, Bouraoui A, Khemiss F. Absorption enhancement studies of clopidogrel hydrogen sulphate in rat everted gut sacs. The Journal of pharmacy and pharmacology. 2012;64(4):541-52.
 39. Lund M, Petersen TS, Dalhoff KP. Clinical Implications of P-Glycoprotein Modulation in Drug-Drug Interactions. Drugs. 2017;77(8):859-83.
 40. Meerum Terwogt JM, Malingré MM, Beijnen JH, ten Bokkel Huinink WW, Rosing H, Koopman FJ, et al. Coadministration of Oral Cyclosporin A Enables Oral Therapy with Paclitaxel. Clinical Cancer Research. 1999;5(11):3379.
 41. Hoosain FG, Choonara YE, Tomar LK, Kumar P, Tyagi C, du Toit LC, et al. Bypassing P-Glycoprotein Drug Efflux Mechanisms: Possible Applications in Pharmacoresistant Schizophrenia Therapy. Biomed Res Int. 2015;2015:484963.
 42. UCSF-FDA. Transporter database index San Francisco: University of California; 2020 [
 43. Cascorbi I. Drug interactions--principles, examples and clinical consequences. Dtsch Arztebl Int. 2012;109(33-34):546-56.
 44. Bushra R, Aslam N, Khan AY. Food-drug interactions. Oman Med J. 2011;26(2):77-83.
 45. FDA. Draft guidance for Industry: Drug Interaction Studies - Study Design, Data Analysis, and Implications for Dosing and Labeling Recommendations. 2012.
 46. EMA. Guideline on the Investigation of Drug Interactions. United Kingdom: European Medicines Agency; 2012.
 47. Yu J, Zhou Z, Tay-Sontheimer J, Levy RH, Ragueneau-Majlessi I. Risk of Clinically Relevant Pharmacokinetic-Based Drug-Drug Interactions with Drugs Approved by the U.S. Food and Drug Administration Between 2013 and 2016. Drug metabolism and disposition: the biological fate of chemicals. 2018;46(6):835-45.
 48. Palleria C, Di Paolo A, Giofrè C, Caglioti C, Leuzzi G, Siniscalchi A, et al. Pharmacokinetic drug-drug interaction and their implication in clinical management. J Res Med Sci. 2013;18(7):601-10.
 49. Bhosle VK, Altit G, Autmizguine J, Chemtob S. 18 - Basic Pharmacologic Principles. In: Polin RA, Abman SH, Rowitch DH, Benitz WE, Fox WW, editors. Fetal and Neonatal Physiology (Fifth Edition): Elsevier; 2017. p. 187-201.e3.

50. Sultatos L. First-Pass Effect. In: Enna SJ, Bylund DB, editors. *xPharm: The Comprehensive Pharmacology Reference*. New York: Elsevier; 2007. p. 1-2.
51. Pharmaceuticals and Medical Devices Agency of Japan P. Drug Interaction Guideline for Drug Development and Labeling Recommendations. In: (PMDA) PaMDAoJ, editor. Japan: Pharmaceuticals and Medical Devices Agency of Japan (PMDA) 2017.
52. Zha W. Transporter-mediated natural product–drug interactions for the treatment of cardiovascular diseases. *Journal of Food and Drug Analysis*. 2017;26.
53. Food and Drug Administration F. In Vitro Metabolism- and Transporter-Mediated Drug-Drug Interaction Studies Guidance for Industry. 2017.
54. Palleria C, Di Paolo A, Giofrè C, Caglioti C, Leuzzi G, Siniscalchi A, et al. Pharmacokinetic drug-drug interaction and their implication in clinical management. *J Res Med Sci*. 2013;18(7):601-10.
55. Jouan E, Le Vée M, Mayati A, Denizot C, Parmentier Y, Fardel O. Evaluation of P-Glycoprotein Inhibitory Potential Using a Rhodamine 123 Accumulation Assay. *Pharmaceutics*. 2016;8(2).
56. WHO. The World Traditional Medicines Situation, in *Traditional medicines: Global Situation, Issues and Challenges*. 3rd Edition ed. Geneva 2011.
57. Fasinu PS, Bouic PJ, Rosenkranz B. An overview of the evidence and mechanisms of herb-drug interactions. *Frontiers in pharmacology*. 2012;3:69-.
58. Brazier NC, Levine MA. Drug-herb interaction among commonly used conventional medicines: a compendium for health care professionals. *American journal of therapeutics*. 2003;10(3):163-9.
59. Kennedy DA, Seely D. Clinically based evidence of drug-herb interactions: a systematic review. *Expert opinion on drug safety*. 2010;9(1):79-124.
60. Tarirai C, Viljoen AM, Hamman JH. Herb-drug pharmacokinetic interactions reviewed. *Expert opinion on drug metabolism & toxicology*. 2010;6(12):1515-38.
61. Chieli E, Romiti N, Rodeiro I, Garrido G. In vitro effects of *Mangifera indica* and polyphenols derived on ABCB1/P-glycoprotein activity. *Food and Chemical Toxicology*. 2009;47(11):2703-10.
62. Liang Y, Zhou Y, Zhang J, Liu Y, Guan T, Wang Y, et al. In vitro to in vivo evidence of the inhibitor characteristics of *Schisandra* lignans toward P-glycoprotein. *Phytomedicine : international journal of phytotherapy and phytopharmacology*. 2013;20(11):1030-8.
63. Oga EF, Sekine S, Shitara Y, Horie T. P-glycoprotein mediated efflux in Caco-2 cell monolayers: The influence of herbals on digoxin transport. *Journal of ethnopharmacology*. 2012;144(3):612-7.
64. Singh R, Rachumallu R, Bhateria M, Panduri J, Bhatta RS. In vitro effects of standardized extract of *Bacopa monniera* and its five individual active constituents on human P-glycoprotein activity. *Xenobiotica; the fate of foreign compounds in biological systems*. 2015;45(8):741-9.
65. Konishi T, Satsu H, Hatsugai Y, Aizawa K, Inakuma T, Nagata S, et al. Inhibitory effect of a bitter melon extract on the P-glycoprotein activity in intestinal Caco-2 cells. *British journal of pharmacology*. 2004;143(3):379-87.
66. Choi RJ, Ngoc TM, Bae K, Cho HJ, Kim DD, Chun J, et al. Anti-

- inflammatory properties of anthraquinones and their relationship with the regulation of P-glycoprotein function and expression. *Eur J Pharm Sci.* 2013;48(1-2):272-81.
67. Nabekura T, Yamaki T, Hiroi T, Ueno K, Kitagawa S. Inhibition of anticancer drug efflux transporter P-glycoprotein by rosemary phytochemicals. *Pharmacological research.* 2010;61(3):259-63.
 68. Wongwanakul R, Vardhanabhuti N, Siripong P, Jianmongkol S. Effects of rhinacanthin-C on function and expression of drug efflux transporters in Caco-2 cells. *Fitoterapia.* 2013;89:80-5.
 69. Kim RB. Transporters and xenobiotic disposition. *Toxicology.* 2002;181-182:291-7.
 70. Kim TH, Shin S, Yoo SD, Shin BS. Effects of Phytochemical P-Glycoprotein Modulators on the Pharmacokinetics and Tissue Distribution of Doxorubicin in Mice. *Molecules.* 2018;23(2).
 71. Li Y, Revalde J, Paxton JW. The effects of dietary and herbal phytochemicals on drug transporters. *Adv Drug Deliv Rev.* 2017;116:45-62.
 72. Knop J, Misaka S, Singer K, Hoier E, Müller F, Glaeser H, et al. Inhibitory Effects of Green Tea and (–)-Epigallocatechin Gallate on Transport by OATP1B1, OATP1B3, OCT1, OCT2, MATE1, MATE2-K and P-Glycoprotein. *PloS one.* 2015;10(10):e0139370.
 73. Bailey DG, Spence JD, Edgar B, Bayliff CD, Arnold JM. Ethanol enhances the hemodynamic effects of felodipine. *Clinical and investigative medicine Medecine clinique et experimentale.* 1989;12(6):357-62.
 74. Dahan A, Amidon GL. Grapefruit juice and its constituents augment colchicine intestinal absorption: potential hazardous interaction and the role of p-glycoprotein. *Pharmaceutical research.* 2009;26(4):883-92.
 75. Spahn-Langguth H, Langguth P. Grapefruit juice enhances intestinal absorption of the P-glycoprotein substrate talinolol. *Eur J Pharm Sci.* 2001;12(4):361-7.
 76. Guo Y, Ding Y, Zhang T, An H. Sinapine reverses multi-drug resistance in MCF-7/dox cancer cells by downregulating FGFR4/FRS2alpha-ERK1/2 pathway-mediated NF-kappaB activation. *Phytomedicine : international journal of phytotherapy and phytopharmacology.* 2016;23(3):267-73.
 77. Liu Z, Duan ZJ, Chang JY, Zhang ZF, Chu R, Li YL, et al. Sinomenine sensitizes multidrug-resistant colon cancer cells (Caco-2) to doxorubicin by downregulation of MDR-1 expression. *PloS one.* 2014;9(6):e98560.
 78. Wang L, Wang C, Peng J, Liu Q, Meng Q, Sun H, et al. Dioscin enhances methotrexate absorption by down-regulating MDR1 in vitro and in vivo. *Toxicology and applied pharmacology.* 2014;277(2):146-54.
 79. Zhang J, Lu M, Zhou F, Sun H, Hao G, Wu X, et al. Key role of nuclear factor-κB in the cellular pharmacokinetics of adriamycin in MCF-7/Adr cells: the potential mechanism for synergy with 20(S)-ginsenoside Rh2. *Drug metabolism and disposition: the biological fate of chemicals.* 2012;40(10):1900-8.
 80. Izzo AA. Herb-drug interactions: an overview of the clinical evidence. *Fundamental & clinical pharmacology.* 2005;19(1):1-16.
 81. Ötles S, Senturk A. Food and drug interactions: a general review. *Acta*

- scientiarum polonorum *Technologia alimentaria*. 2014;13(1):89-102.
82. Chen M, Zhou SY, Fabriaga E, Zhang PH, Zhou Q. Food-drug interactions precipitated by fruit juices other than grapefruit juice: An update review. *J Food Drug Anal*. 2018;26(2s):S61-s71.
 83. Lim SL, Tan TM-C, Lim L-Y. Effects of Citrus Fruit Juices on P-glycoprotein-mediated Transport in L-MDR1 Cells and CYP3A4-mediated Metabolism in Human Intestinal Microsomes. *Tree and Forestry Science and Biotechnology*. 2008;2(1):102-11.
 84. Honda Y, Ushigome F, Koyabu N, Morimoto S, Shoyama Y, Uchiumi T, et al. Effects of grapefruit juice and orange juice components on P-glycoprotein- and MRP2-mediated drug efflux. *British journal of pharmacology*. 2004;143(7):856-64.
 85. El-Readi MZ, Hamdan D, Farrag N, El-Shazly A, Wink M. Inhibition of P-glycoprotein activity by limonin and other secondary metabolites from Citrus species in human colon and leukaemia cell lines. *European journal of pharmacology*. 2010;626(2-3):139-45.
 86. Ma W, Feng S, Yao X, Yuan Z, Liu L, Xie Y. Nobiletin enhances the efficacy of chemotherapeutic agents in ABCB1 overexpression cancer cells. *Scientific reports*. 2015;5:18789.
 87. Dong W, Liao ZG, Zhao GW, Guan XJ, Zhang J, Liang XL, et al. Reversal Effect of Oxypeucedanin on P-glycoprotein-mediated Drug Transport. *Molecules*. 2018;23(8).
 88. Liang X-l, Tang T, Zhao GW, Dong W, Guan X-j, Liao Z-g, et al. Mechanism underlying bergapten-mediated regulation of vincristine transport in MDCK-MDR1 cells 2018.
 89. Won CS, Oberlies NH, Paine MF. Mechanisms underlying food-drug interactions: inhibition of intestinal metabolism and transport. *Pharmacol Ther*. 2012;136(2):186-201.
 90. Di Marco MP, Edwards DJ, Wainer IW, Ducharme MP. The effect of grapefruit juice and seville orange juice on the pharmacokinetics of dextromethorphan: the role of gut CYP3A and P-glycoprotein. *Life sciences*. 2002;71(10):1149-60.
 91. Wongpornchai S. *Handbook of Herbs and spices*. second ed. Cambridge: Woodhead Publishing; 2012.
 92. DeFilipps RA, Krupnick GA. The medicinal plants of Myanmar. *PhytoKeys*. 2018(102):1-341.
 93. Ali M, Akhter R, Narjish SN, Shahriar M, Bhuiyan MA. Studies of preliminary phytochemical screening, membrane stabilizing activity, thrombolytic activity and in-vitro antioxidant activity of leaf extract of citrus hystrix. *International Journal of Pharmaceutical Sciences and Research*. 2015;6(6):2367-74.
 94. Abirami A, Nagarani G, Siddhuraju P. The medicinal and nutritional role of underutilized citrus fruit- citrus hystrix (Kaffir Lime): a review. *Drug INvention Today*. 2014;6(1):1-5.
 95. Abirami A, Nagarani G, Siddhuraju P. In vitro antioxidant, anti-diabetic, cholinesterase and tyrosinase inhibitory potential of fresh juice from Citrus hystrix and C. maxima fruits. *Food Science and Human Wellness*.

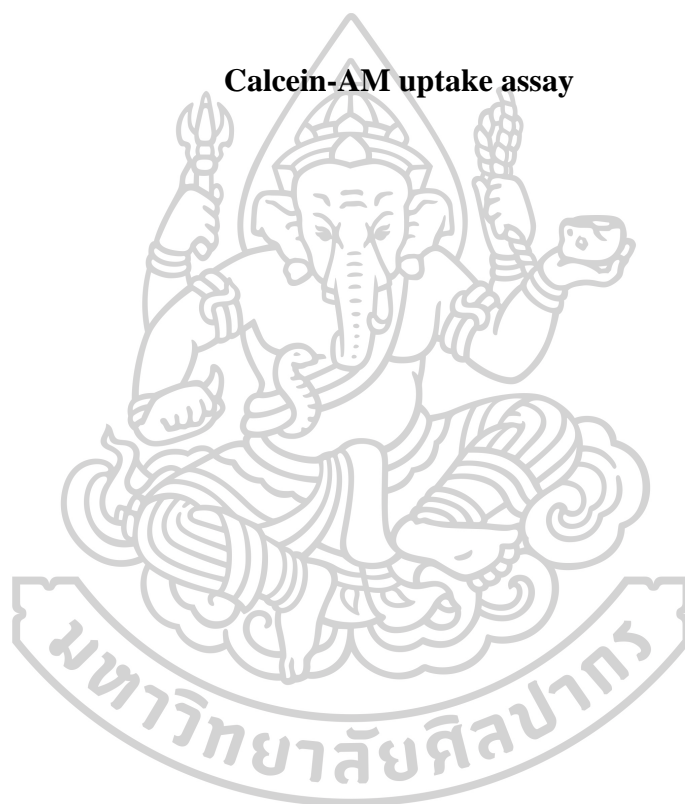
- 2014;3(1):16-25.
96. Dugrand A, Olry A, Duval T, Hehn A, Froelicher Y, Bourgaud F. Coumarin and furanocoumarin quantitation in citrus peel via ultraperformance liquid chromatography coupled with mass spectrometry (UPLC-MS). *J Agric Food Chem.* 2013;61(45):10677-84.
 97. Seeka C, Sutthivaiyakit P, Youkwan J, Hertkorn N, Harir M, Schmitt-Kopplin P, et al. Prenylfuranocoumarin-HMGA-flavonol glucoside conjugates and other constituents of the fruit peels of *Citrus hystrix* and their anticholinesterase activity. *Phytochemistry.* 2016;127:38-49.
 98. Rafiq S, Kaul R, Sofi SA, Bashir N, Nazir F, Ahmad Nayik G. Citrus peel as a source of functional ingredient: A review. *Journal of the Saudi Society of Agricultural Sciences.* 2018;17(4):351-8.
 99. Abirami A, Nagarani G, Siddhuraju P. Measurement of functional properties and health promoting aspects-glucose retardation index of peel, pulp and peel fiber from *Citrus hystrix* and *Citrus maxima*. *Bioactive Carbohydrates and Dietary Fibre.* 2014;4(1):16-26.
 100. Putri H, Nagadi S, Larasati YA, Wulandari N, Hermawan A. Cardioprotective and hepatoprotective effects of *Citrus hystrix* peels extract on rats model. *Asian Pacific Journal of Tropical Biomedicine.* 2013;3(5):371-5.
 101. Fardel O, Le Vee M, Jouan E, Denizot C, Parmentier Y. Nature and uses of fluorescent dyes for drug transporter studies. *Expert opinion on drug metabolism & toxicology.* 2015;11(8):1233-51.
 102. Kimura Y, Ito H, Hatano T. Effects of mace and nutmeg on human cytochrome P450 3A4 and 2C9 activity. *Biological & pharmaceutical bulletin.* 2010;33(12):1977-82.
 103. Christians U, Schmitz V, Haschke M. Functional interactions between P-glycoprotein and CYP3A in drug metabolism. *Expert opinion on drug metabolism & toxicology.* 2005;1(4):641-54.
 104. Wachter VJ, Wu CY, Benet LZ. Overlapping substrate specificities and tissue distribution of cytochrome P450 3A and P-glycoprotein: implications for drug delivery and activity in cancer chemotherapy. *Molecular carcinogenesis.* 1995;13(3):129-34.
 105. Tanigawara Y, Okamura N, Hirai M, Yasuhara M, Ueda K, Kioka N, et al. Transport of digoxin by human P-glycoprotein expressed in a porcine kidney epithelial cell line (LLC-PK1). *The Journal of pharmacology and experimental therapeutics.* 1992;263(2):840-5.
 106. Ueda K, Okamuraj N, Hirai M, Tanigawara Y, Saeki T, Kioka N, et al. Human P-glycoprotein Transports Cortisol, Aldosterone, and Dexamethasone, but Not Progesterone. *The Journal of biological chemistry.* 1992;267(34):24248-52.
 107. Sharom F, Siarheyeva A. Functional assays for identification of compounds that interact with P-gp. 2008. p. 261-90.
 108. Holló Z, Homolya L, Davis CW, Sarkadi B. Calcein accumulation as a fluorometric functional assay of the multidrug transporter. *Biochimica et Biophysica Acta (BBA) - Biomembranes.* 1994;1191(2):384-8.
 109. Di L, Kerns EH. Chapter 9 - Transporters. In: Di L, Kerns EH, editors. *Drug-Like Properties (Second Edition)*. Boston: Academic Press; 2016. p. 113-40.
 110. Matsumoto T, Kaifuchi N, Mizuhara Y, Warabi E, Watanabe J. Use of a Caco-

- 2 permeability assay to evaluate the effects of several Kampo medicines on the drug transporter P-glycoprotein. *Journal of natural medicines*. 2018;72(4):897-904.
111. Tsuruo T, Iida H, Tsukagoshi S, Sakurai Y. Increased accumulation of vincristine and adriamycin in drug-resistant P388 tumor cells following incubation with calcium antagonists and calmodulin inhibitors. *Cancer research*. 1982;42(11):4730-3.
 112. Awortwe C, Fasinu PS, Rosenkranz B. Application of Caco-2 cell line in herb-drug interaction studies: current approaches and challenges. *Journal of pharmacy & pharmaceutical sciences : a publication of the Canadian Society for Pharmaceutical Sciences, Societe canadienne des sciences pharmaceutiques*. 2014;17(1):1-19.
 113. Yamamoto C, Murakami H, Koyabu N, Takanaga H, Matsuo H, Uchiumi T, et al. Contribution of P-glycoprotein to efflux of ramosetron, a 5-HT₃ receptor antagonist, across the blood-brain barrier. *The Journal of pharmacy and pharmacology*. 2002;54:1055-63.
 114. Brouwer KL, Keppler D, Hoffmaster KA, Bow DA, Cheng Y, Lai Y, et al. In vitro methods to support transporter evaluation in drug discovery and development. *Clinical pharmacology and therapeutics*. 2013;94(1):95-112.
 115. Frérot E, Decorzant E. Quantification of Total Furocoumarins in Citrus Oils by HPLC Coupled with UV, Fluorescence, and Mass Detection. *Journal of Agricultural and Food Chemistry*. 2004;52(23):6879-86.
 116. Murakami A, Gao G, Kim OK, Omura M, Yano M, Ito C, et al. Identification of Coumarins from the Fruit of *Citrus hystrix* DC as Inhibitors of Nitric Oxide Generation in Mouse Macrophage RAW 264.7 Cells. *Journal of Agricultural and Food Chemistry*. 1999;47(1):333-9.
 117. Manthey JA, Buslig BS. Distribution of Furanocoumarins in Grapefruit Juice Fractions. *Journal of Agricultural and Food Chemistry*. 2005;53(13):5158-63.
 118. John A M, Kyung M. The isolation of minor-occurring furanocoumarins in grapefruit and analysis of their inhibition of CYP3A4 and P-glycoprotein transport of talinolol from Caco-2 cells *Proc Fla State Hort Soc*. 2006;119:361-6.
 119. Wangensteen H, Molden E, Christensen H, E Malterud K. Identification of epoxybergamottin as a CYP3A4 inhibitor in grapefruit peel. *European journal of clinical pharmacology*. 2003;58:663-8.
 120. P Siskos E, E Mazomenos B, Konstantopoulou M. Isolation and Identification of Insecticidal Components from *Citrus aurantium* Fruit Peel Extract. *Journal of agricultural and food chemistry*. 2008;56:5577-81.
 121. John A. Manthey, Ka-Fu Yung. The isolation of minor-occurring furanocoumarins in grapefruit and analysis of their inhibition of CYP3A4 and P-glycoprotein transport of talinolol from Caco-2 cells *Proc Fla State Hort Soc*. 2006;119:361-6.
 122. Hwang Y-H, Yang HJ, Ma JY. Simultaneous Determination of Three Furanocoumarins by UPLC/MS/MS: Application to Pharmacokinetic Study of *Angelica dahurica* Radix after Oral Administration to Normal and Experimental Colitis-Induced Rats. *Molecules* (Basel, Switzerland). 2017;22(3):416.

123. Edwards DJ, Bellevue FH, 3rd, Woster PM. Identification of 6',7'-dihydroxybergamottin, a cytochrome P450 inhibitor, in grapefruit juice. *Drug metabolism and disposition: the biological fate of chemicals*. 1996;24(12):1287-90.
124. Mirzaei SA, Gholamian Dehkordi N, Ghamghami M, Amiri AH, Dalir Abdolahinia E, Elahian F. ABC-transporter blockage mediated by xanthotoxin and bergapten is the major pathway for chemosensitization of multidrug-resistant cancer cells. *Toxicology and applied pharmacology*. 2017;337:22-9.
125. Paine MF, Widmer WW, Pusek SN, Beavers KL, Criss AB, Snyder J, et al. Further characterization of a furanocoumarin-free grapefruit juice on drug disposition: studies with cyclosporine. *The American journal of clinical nutrition*. 2008;87(4):863-71.
126. Ohnishi A, Matsuo H, Yamada S, Takanaga H, Morimoto S, Shoyama Y, et al. Effect of furanocoumarin derivatives in grapefruit juice on the uptake of vinblastine by Caco-2 cells and on the activity of cytochrome P450 3A4. *British journal of pharmacology*. 2000;130:1369-77.
127. De Castro W, Mertens-Talcott S, Derendorf H, Butterweck V. Grapefruit juice-drug interactions: Grapefruit juice and its components inhibit P-glycoprotein (ABCB1) mediated transport of talinolol in Caco-2 cells. *Journal of pharmaceutical sciences*. 2007;96:2808-17.
128. Dong W, Liao Z-G, Zhao G-W, Guan X-J, Zhang J, Liang X-L, et al. Reversal Effect of Oxypeucedanin on P-glycoprotein-mediated Drug Transport. *Molecules*. 2018;23(8):1841.
129. van der Sandt IC, Blom-Roosemalen MC, de Boer AG, Breimer DD. Specificity of doxorubicin versus rhodamine-123 in assessing P-glycoprotein functionality in the LLC-PK1, LLC-PK1:MDR1 and Caco-2 cell lines. *Eur J Pharm Sci*. 2000;11(3):207-14.
130. Liow JS, Lu S, McCarron JA, Hong J, Musachio JL, Pike VW, et al. Effect of a P-glycoprotein inhibitor, Cyclosporin A, on the disposition in rodent brain and blood of the 5-HT_{1A} receptor radioligand, [¹¹C](R)-(-)-RWAY. *Synapse (New York, NY)*. 2007;61(2):96-105.
131. biosciences I. Human P-Glycoprotein / MDR1 Drug Interaction Assay.
132. Netsomboon K, Laffleur F, Suchaoin W, Bernkop-Schnürch A. Novel in vitro transport method for screening the reversibility of P-glycoprotein inhibitors. *Eur J Pharm Biopharm*. 2016;100:9-14.
133. Jetté L, Murphy GF, Béliveau R. Drug binding to P-glycoprotein is inhibited in normal tissues following SDZ-PSC 833 treatment. *International journal of cancer*. 1998;76(5):729-37.
134. LAM LS. Modulation of drug transport by citrus fruit juices. 2007.

Appendix 1

Calcein-AM uptake assay



1. Effect *Citrus hystrix* fruit (flavored, albedo, segment membrane, juice) extract on calcein-AM uptake in Caco-2

Date - 25.3.18, 8.4.18, 20.5.18, 22.7.18, 28.7.18

Passage	RFU					% of control				
	Verapamil (100 μ M)	Extract (80 μ g/ml)			Juice	Verapamil (100 μ M)	Extract (80 μ g/ml)			
		Flavedo	Albedo	Segment membrane			Flavedo	Albedo	Segment membrane	Juice
46	8274	10401	6652	5883	7801	177	222	142	126	167
	7477	11459	6928	5906	7137	160	245	148	126	153
48	14834	23550	10776	9893	12338	198	315	144	132	165
	14690	16696	9991	9073	12385	196	223	133	121	165
50	18898354	25817832				127	174			
	18400469	26122464				124	176			
	18276063	24064855				123	162			
35	42858379	42534538				189	188			
	41297619	42764581				182	189			
	38403787	42993527				169	190			
39	26279446	30163021				154	177			
	26391524	28275124				155	166			
	25124805	28104891				147	165			

2. Effect *Citrus hystrix* fruit (flavedo, albedo, segment membrane, juice) extract on calcein-AM uptake in LLC-PK₁ and LLC-GA5-COL300

Date - 10.7.18, 15.7.18, 22.7.18, 2.8.18, 6.8.18

Passage	RFU				% of control					
	Verapamil (100 μ M)	Extract (80 μ g/ml)			Verapamil (100 μ M)	Extract (80 μ g/ml)				
		Flavedo	Albedo	Segment membrane		Juice	Flavedo	Albedo	Segment membrane	Juice
LLC-PK ₁										
31	17269802	23754287	12375132	14714914	17039901	139	192	100	119	138
	18084008	20058176	11961979	13706273	14806262	146	162	97	111	120
	14172778	23870580	12453234	13538329	12344209	114	137	101	109	100
	7719751	18270526	6262548	6550602	7982213	124	295	101	106	129
32	7000000	10819334	6261677	8291341	7285794	113	174	101	134	118
	25583896	21980846				142	122			
36	25802051	24170877				143	134			
	25707954	21568369				142	119			
	10089533	9867979				176	172			
38	7520538	8969289				131	156			
	8069869	9833117				141	171			
	6125215	7683652				172	216			
40	6062817	7264162				170	204			
	6132745	7506712				172	211			

Passage	RFU					% of control				
	Verapamil (100 μ M)	Extract (80 μ g/ml)			Juice	Verapamil (100 μ M)	Extract (80 μ g/ml)			
		Flavado	Albedo	Segment membrane			Flavado	Albedo	Segment membrane	Juice
LLC-GA5-COL300										
24	4604872	10485886	808273	790843	891989	549	1250	96	94	106
	4324246	8678818	742630	841604	875271	515	1034	88	100	104
	3922152	10519396	773631	823406	912282	467	1254	92	98	109
25	4083227	7663223	600793	623605	613998	660	1239	97	101	99
	4000000	8081031	553435	601993	700588	646	1306	89	97	113
	5645828	12278015				1166	2535			
29	4941374	11788766				1020	2434			
	5317405	12936285				1098	2671			
	3697469	8008699				1050	2273			
31	3702861	8655280				1051	2457			
	3766974	7858189				1069	2231			
	2043515	4498871				1028	2262			
33	2073594	4558161				1043	2292			
	2297214	4586716				1155	2306			

3. Effect of flavedo extract on calcein-AM uptake in Caco-2

Date – 20.5.18, 22.7.18, 28.7.18

Passage	RFU				% of control			
	verapamil (100 μ M)	Flavedo extract (μ g/ml)			verapamil (100 μ M)	Flavedo extract (μ g/ml)		
		8	40	80		8	40	80
50	18898354	19172951	23865059	25817832	127	129	161	174
	18400469	20438587	24545399	26122464	124	138	165	176
	18276063	19822825	22008774	24064855	123	133	148	162
	42858379	26640155	30554754	42534538	189	117	135	188
35	41297619	25161951	29745472	42764581	182	111	131	189
	38403787	23406026	32601065	42993527	169	103	144	190
39	26279446	23165432	26117894	30163021	154	136	153	177
	26391524	21394763	24543778	28275124	155	126	144	166
	25124805	21025952	26358049	28104891	147	123	155	165

4. Effect of flavedo extract on calcein-AM uptake in LLC-PK₁ and LLC-GA5-COL300

Date – 22.7.18, 2.8.18, 6.8.18

Cell lines	Passage	RFU				% of control			
		verapamil (100 μ M)	Flavedo extract (μ g/ml)			verapamil (100 μ M)	Flavedo extract (μ g/ml)		
			8	40	80		8	40	80
LLC-PK ₁	36	25583896	15025496	20643498	21980846	142	83	114	122
		25802051	14233606	18458093	24170877	143	79	102	134
		25707954	15012428	18801828	21568369	142	83	104	119
	38	10089533	5893056	9912997	9867979	176	103	173	172
		7520538	6461814	8355018	8969289	131	113	146	156
		8069869	6198439	7776922	9833117	14	108	136	171
LLC-GA5-COL300	40	6125215	3869316	5661491	7683652	172	109	159	216
		6062817	3965481	5619604	7264162	170	111	158	204
		6132745	3930396	5463191	7506712	172	110	153	211
	29	5645828	1064844	5170876	12278015	1166	220	1068	2534
		4941374	1101556	4878711	11788766	1020	227	1007	2434
		5317405	1205709	5528589	12936285	1098	249	1141	2671
LLC-GA5-COL300	31	3697469	965379	4758707	8008699	1050	274	1351	2273
		3702861	990866	4782249	8655280	1051	281	1357	2457
		3766974	1046436	3814952	7858189	1069	297	1083	2231
	33	2043515	424504	2027314	4498871	1028	213	1019	2262
		2073594	378800	2041822	4558161	1043	190	1027	2292
		2297214	438972	2261571	4586716	1155	221	1137	2306

5. Effect of fractions of flavedo extract on calcein-AM uptake in Caco-2

Date – 27.7.18

Passage	RFU				
	Verapamil (100 µM)	Fraction (30 µg/ml)			
37		E1	E2	E3	E5
	25933630	16338956	17919051	20984783	28418896
	25904800	20469692	14823099	29286736	29651678
	% of control				
37	Verapamil (100 µM)	Fraction (30 µg/ml)			
		E1	E2	E3	E5
	151.35	95	105	122	166
	151.18	119	87	171	173

6. Effect of fractions of flavedo extract on calcein-AM uptake in LLC-PK₁ and LLC-GA5-COL300

Date – 31.7.18

Cell lines	Passage	RFU						
		Verapamil (100 µM)	Fraction (30 µg/ml)					
			E1	E2	E3	E4	E5	
LLC-PK ₁	37	2932565	1322634	1751163	2432299	6908337		2019699
		2638909	1770610	1929107	2633113	3479836		2456889
		868599	134359	307547	1040502	821619		1257667
LLC-GA5-COL300	30	838477	159711	216018	1406371	733838		1311180
% of control								
Cell lines	Passage	Verapamil (100 µM)	Fraction (30 µg/ml)					
			E1	E2	E3	E4	E5	
LLC-PK ₁	37	149	67	89	123	350		102
		134	90	98	133	176		125
		966	149	342	1157	913		1398
LLC-GA5-COL300	30	932	178	240	1563	816		1458

7. Preliminary study of isolated compounds on calcein-AM uptake in Caco-2

Date – 27.7.18, 28.7.18

Passage	RFU					% of control				
	Verapamil (100 μ M)	Compounds (30 μ g/ml)				Verapamil (100 μ M)	Compounds (30 μ g/ml)			
		<u>1</u>	<u>2 + 3</u>	<u>4</u>	<u>5</u>		<u>1</u>	<u>2 + 3</u>	<u>4</u>	<u>5</u>
37	25933630	16338956	19912777	27379925	17076264	151	95	116	160	100
	25904800	20469692	23019725	26903544	21475525	151	119	134	157	125
39	26279446	15901832	19768518	23013952	15515776	154	93	116	135	91
	26391524	15709821	22376141	24526009	19309684	155	92	131	144	113

8. Effect of isolated compounds on calcein-AM uptake in LLC-PK₁ and LLC-GA5-COL300

Date – 31.7.18, 2.8.18

Cell lines	Passage	RFU					% of control				
		Verapamil (100 μM)	Compounds (30 μg/ml)				Verapamil (100 μM)	Compounds (30 μg/ml)			
			<u>1</u>	<u>2 + 3</u>	<u>4</u>	<u>5</u>		<u>1</u>	<u>2 + 3</u>	<u>4</u>	<u>5</u>
LLC-PK ₁	37	2932565	1622634	2322013	1955615	1738238	149	82	118	99	88
		2638909	1770610	2117499	1965190	1974034	134	90	107	100	100
	38	7520538	4696674	9513423	5694856	5242066	131	82	166	99	91
		8069869	4818034	8272304	6295979	6289731	141	84	144	110	110
LLC-GA5-COL300	30	868599	134359	829024	687319	185157	966	149	922	764	206
		838477	159711	839682	617485	151269	932	178	933	686	168
	31	3702861	585505	3703215	2644652	531744	1051	166	1051	751	151
3766974		541271	3501043	2606501	692475	1069	154	994	740	197	

9. Effect of dihydroxybergamottin on calcein-AM uptake in LLC-PK₁ and LLC-GA5-COL300

Date – 18.8.18, 10.10.18, 24.8.18, 3.10.18, 15.10.18, 16.10.18

Passage	RFU						% of control					
	Verapamil (100 μ M)	10 μ M	25 μ M	50 μ M	100 μ M	200 μ M	Verapamil (100 μ M)	10 μ M	25 μ M	50 μ M	100 μ M	200 μ M
LLC-PK ₁												
42	5882341		4929027		7860695	10022652	146		122		195	249
	5842051		5313655		6739695	11093566	145		132		167	275
	12916975		11887612		14679003	17163003	141		130		160	187
	13425035		11538275		14442743	17306258	146		126		158	189
			11143509		15051316	17025096			122		164	186
LLC-GA5-COL300												
41	2622512		352395		1480525	3928901	1136		153		641	1702
	2420453		531999		1570930	4193148	1048		230		680	1816
	2662419	443795	688344	1369670	2197618	5850642	895	149	232	461	739	1968
	3146518	474191	639666	1412409	2260326	5840480	1058	159	215	475	760	1964
44			603849	1267316	2259999	5527403			203	426	760	1859
			457683	1214007	2051923	2710799			154	408	690	912
	5722812	1013659	1289731	2453040	3028692	4719008	1198	212	270	513	634	988
	5951674	1532698	1754701	1951437	2861470	4550953	1246	321	367	408	599	952
25		1800036	1370093	2405084	3033369	4767903		377	287	503	635	998
	6108617	219485	520153	715681	1293177	4703343	1370	154	365	501	906	3296
		229086	323585	554941	1293662	5578084		161	227	389	907	3910
			392227	700196	1296930	5268429			275	491	909	3692
29				670116	1292848	5249878				470	906	3679
	2456933			278687	1224770	5563128	1179			434	588	2669
	1694461			191301	1229001	5230807	813			439	587	2510
	1957996						939					

10. Effect of Oxypeucedanin hydrate on calcein-AM uptake in LLC-PK₁ and LLC-GA5-COL300

Date – 18.8.18, 10.10.18, 24.8.18, 3.10.18, 15.10.18

Cell lines	Passage	RFU						% of control					
		Verapamil (100 μ M)	10 μ M	25 μ M	50 μ M	100 μ M	200 μ M	Verapamil (100 μ M)	10 μ M	25 μ M	50 μ M	100 μ M	200 μ M
LLC-PK ₁	42	5882341		3875747		4306055	4679680	146		96		107	116
		5842051				4410125	4743654	145				109	118
	57	12916975		8213272		92422308	9557888	141		90		101	104
		13425035		7624760		9043624	10277552	146		83		99	112
				7950588		8977409	10173291			87		98	111
LLC-GA5-COL300	44	2662419	269996	248267	365889	483453	554972	895	91	84	123	163	187
		3146518	293679	287248	368503	506631	428489	1058	99	97	124	170	144
				249648	317995	363175	511377			84	107	122	172
				256635	327332	457165	289548			86	110	154	97
					871836	1134282	1182521	1198			182	237	247
	25	5722812						1246					
		5951674											
	29	6108617	145869	158129	191627	221140	316554	1370	102	111	134	155	222
			136383	162389	211600	293549	213112		96	114	148	206	149
				155918	194817	316554	401969			109	137	222	282
				165769	188848	298626	464317			116	132	209	325

11. Effect of bergamottin on calcein-AM uptake in LLC-PK₁ and LLC-GA5-COL300

Date – 18.8.18, 10.10.18, 3.10.18, 16.10.18

Cell lines	Passage	RFU					% of control				
		Verapamil (100 μ M)	10 μ M	25 μ M	50 μ M	100 μ M	Verapamil (100 μ M)	10 μ M	25 μ M	50 μ M	100 μ M
LLC-PK ₁	42	5882341		3950469	4091066	4332216	146		98	102	108
		5842051		3932832	4008005	4295906	145		98	99	107
	57	12916975		8043440	8651590	10057374	141		88	94	110
		13425035		8812738	9117680	9712305	146		96	99	106
				7886303	9117128	9230192			86	99	101
LLC-GA5-COL300	25	5722812	650637	1196265	1206400	1425912	1198	136	250	252	298
		5951674	371249	963114	1200207	1472221	1246	78	202	251	308
			191249	780763	1115350	1452165		40	163	233	304
	29	2456933	130827	352462	357404	479153	1179	63	169	171	230
		1694461	120594	262760	452361	531683	813	58	126	217	255
		1957996	157017	223448	432624	470115	939	75	107	208	226
				282228	398081	419517			135	191	201

12. Effect of Oxypeucedanin on calcein-AM uptake in LLC-PK₁ and LLC-GA5-COL300

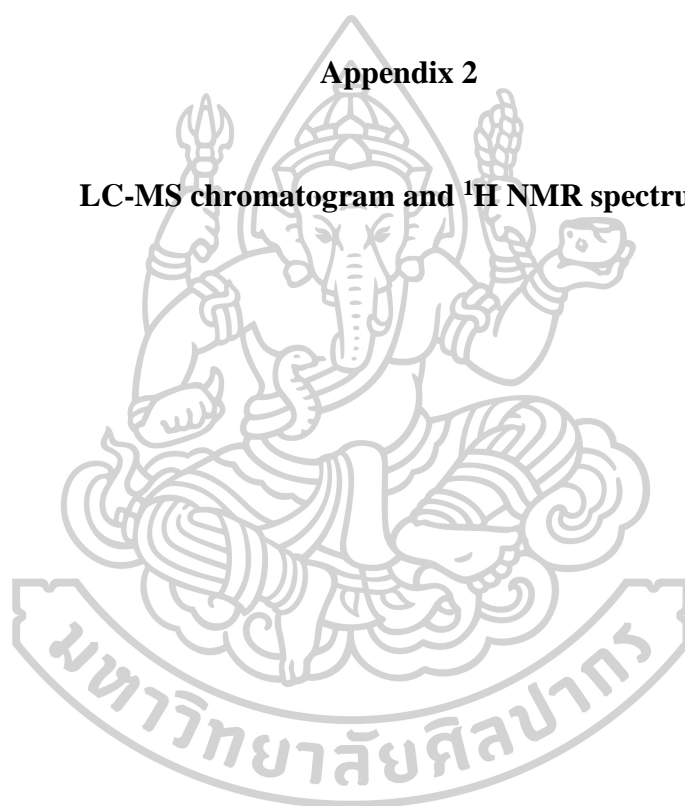
Date – 18.8.18, 10.10.18, 24.8.18, 3.10.18, 15.10.18, 16.10.18

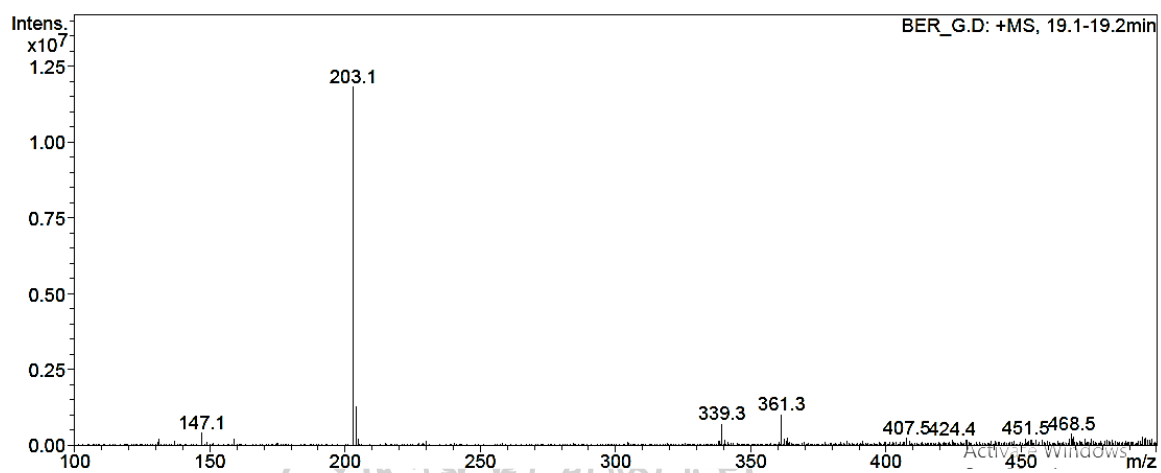
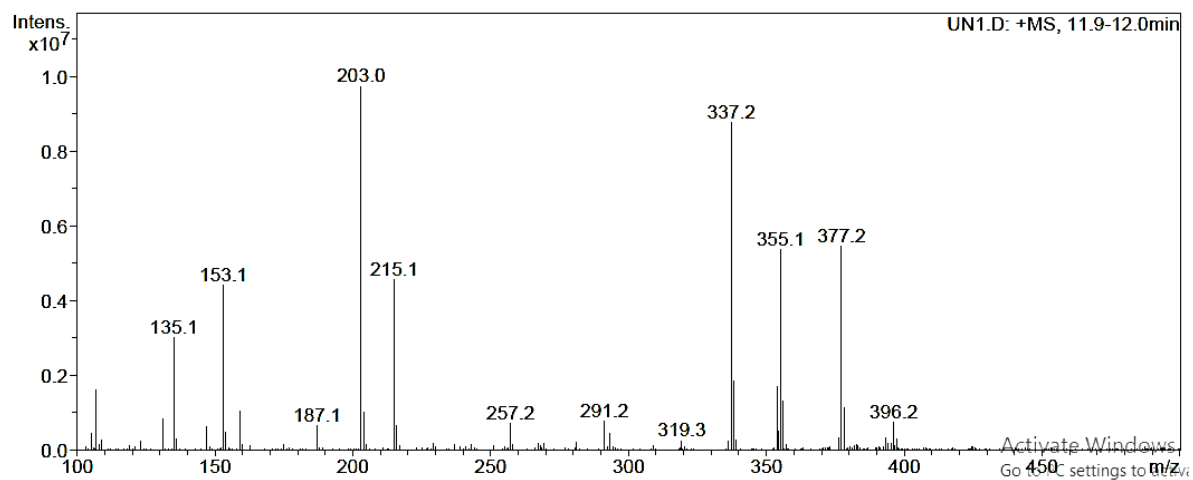
Cell lines	Passage	RFU						% of control					
		Verapamil (100 μ M)	10 μ M	25 μ M	50 μ M	100 μ M	200 μ M	Verapamil (100 μ M)	10 μ M	25 μ M	50 μ M	100 μ M	200 μ M
LLC-PK ₁	42	5882341				5966408		146				148	
		5842051						145					
	57	12916975		8960926		12960926	15353622	141		98		141	168
		13425035		8943796		13235886	15532597	146		98		144	169
LLC-GA5-COL300	41			10110646		12795426	15188365			110		140	166
		2622512						1136					
		2420453						1048					
		2662419	330236	489973	659357	1334410	3605578	895	111	165	222	449	1213
	44	3146518	217345	418768	478805	1290056	2966699	1058	73	141	161	434	998
				482513	576379	1259118	2407841			162	194	423	810
				352166	666146	1151508	3213144			118	224	387	1081
		5722812	1718278	1879600	1456587	1835681	3097285	1198	360	393	305	384	648
	25	5951674	1053196	1792872	1183122	1968008	2603686	1246	220	375	248	412	545
			1546300	1430999	2283362	1943305	2691577		324	299	478	407	563
29		6108617	135581	256971	350436	847047	2200263	1370	95	180	246	594	1542
			170504	213903	554225	917280	2612410		119	150	388	643	1831
				225835	357650	928839	2271167			158	251	651	1592
				313344	389777	580640	2052092			220	273	407	1438
	29	2456933			258677	672593	1152895	1179			124	323	553
		1694461			574327	798252	1225148	813			276	383	588
		1957996						939					

13. Effect of Epoxybergamottin on calcein-AM uptake in LLC-PK₁ and LLC-GA5-COL300

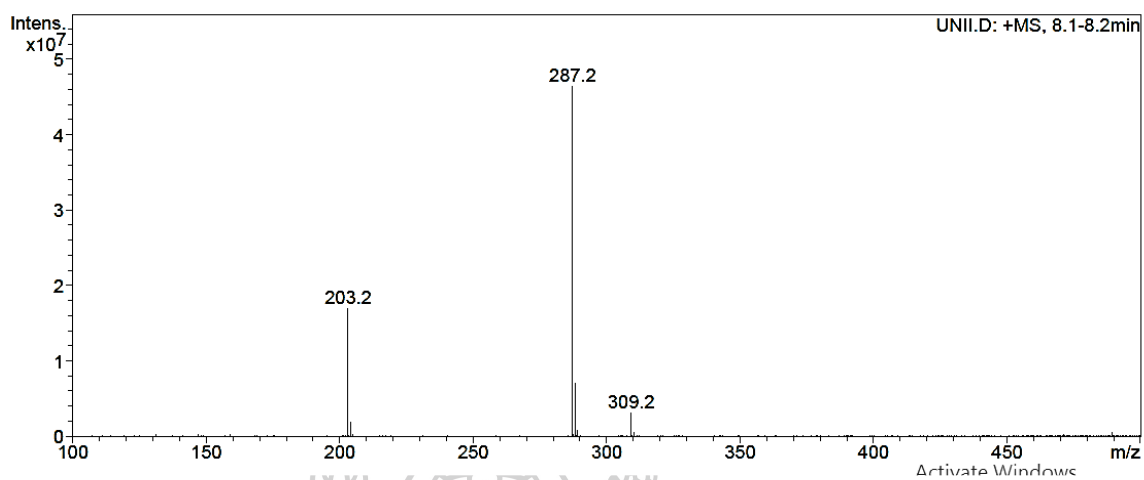
Date – 18.8.18, 10.10.18, 16.10.18

Cell lines	Passage	RFU							% of control				
		Verapamil (100 μ M)	10 μ M	25 μ M	50 μ M	100 μ M	200 μ M	Verapamil (100 μ M)	10 μ M	25 μ M	50 μ M	100 μ M	200 μ M
LLC-PK ₁	42	5882341				3834453		146				95	
		5842051						145					
	57	12916975		7901143		8251336	11138395	141		86		90	122
		13425035		7720390		8494292	10036474	146		84		93	110
LLC-GA5-COL300	41			7935158		8226574	10564957			87		90	115
		2622512	581349	2024679	3066938	2221902	5640924	1136	252	877	1328	962	2443
		2420453	576824	2147104	3416897	3859870	5650851	1048	250	930	1480	1672	2448
	29	2456933	400254	1923823	2641933	3612027	4773132	1179	192	923	1268	1733	2290
		1694461	486256	2110983	3145916	4411749	5418075	813	233	1013	1509	2117	2600
	29	1957996	540030	1808292	3086076	3626185	5034400	939	259	868	1481	1740	2416
			664878	1689734	2833244	3767993	5162866		319	811	1359	1808	2477

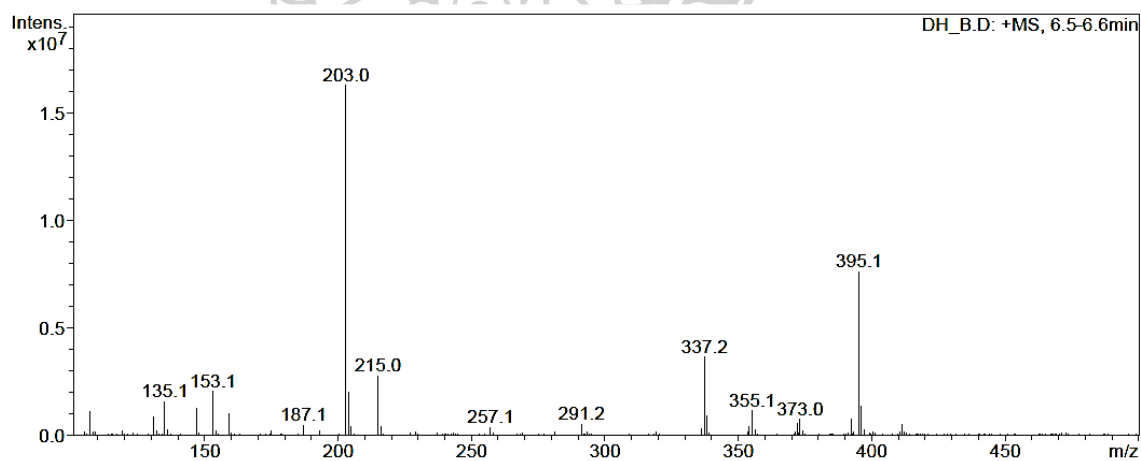
Appendix 2**LC-MS chromatogram and ^1H NMR spectrum**

LC-MS chromatogram**Bergamottin****Epoxybergamottin**

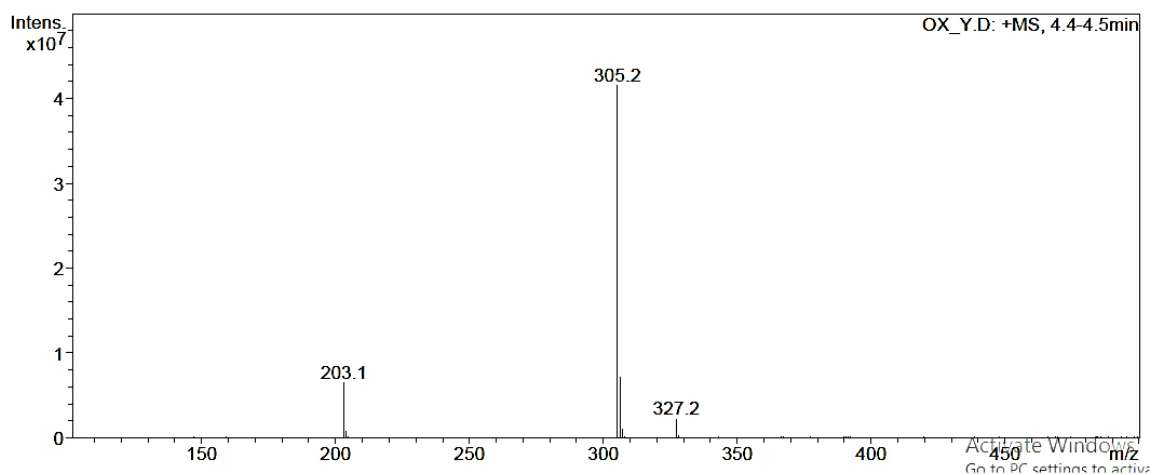
Oxypeucedanin



Dihydroxybergamottin

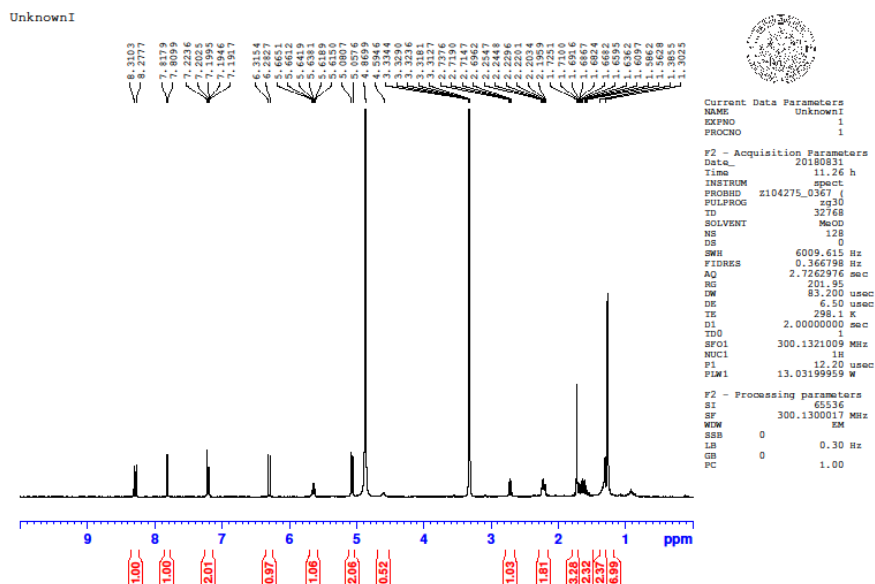


Oxypeucedanin hydrate

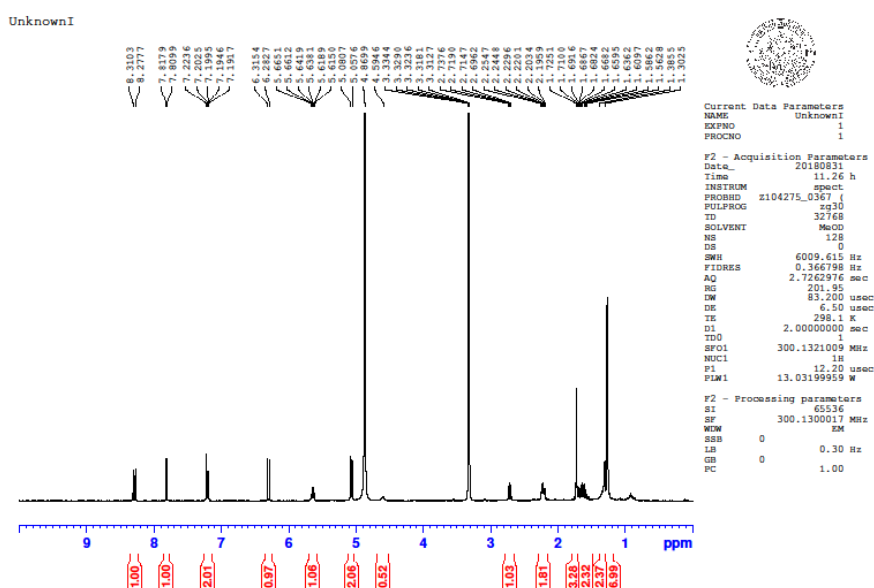


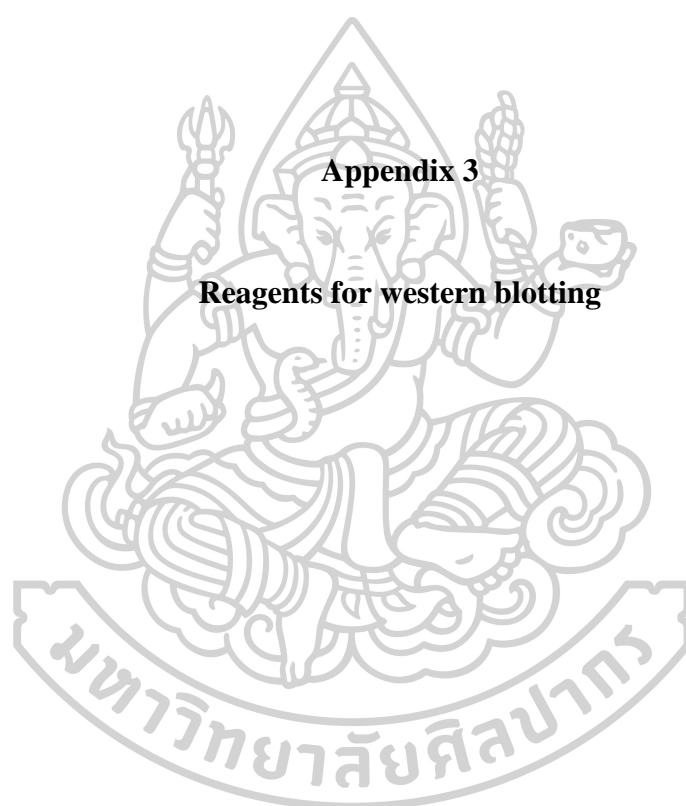
^1H NMR spectrum

Epoxybergamottin



Oxypeucedanin





Reagents for western blotting

1. 1% SDS lysis buffer

Components	Weigh out
1 M Tris HCL, pH 8.0	50 μ l
10% Sodium lauryl sulphate	500 μ l
Ultrapurified water to	5 ml

2. Laemmli sample loading buffer (4X)

Components	Weigh out
0.5 M Tris HCL, pH 6.8	250 μ l
Sodium lauryl sulphate	0.08 g
Glycerol	200 μ l
2-mercaptoethanol	150 μ l
Bromophenol blue dye	20 μ l
Ultrapurified water to	1 ml

3. SDS-polyacrylamide gel

Components	10% Resolving gel (8 ml)	Components	4% Stacking gel (5 ml)
Ultrapurified water	3.2 ml	Ultrapurified water	3 ml
30% Acrylamide	2.67 ml	30% Acrylamide	0.67 ml
1.5M Tris base pH 8.8	2 ml	0.5 M Tris base pH 6.8	1.25 ml
10% SDS	80 μ l	10% SDS	50 μ l
10% APS	80 μ l	10% APS	50 μ l
TEMED	8 μ l	TEMED	5 μ l

Tris base- Tris (hydroxymethyl) aminomethane, SDS- Sodium lauryl sulphate, APS- Ammonium persulphate, TEMED- Tetramethylethylenediamine

4. Tris-glycine running buffer (10X)

Components	Molar	MW	Weigh out (g)
Tris base	250 mM	121.14	30.3
Glycine	1920 mM	75.07	144.1
SDS	1% W/V		10
Ultrapurified water			Add up to 1 L

Tris base- Tris (hydroxymethyl) aminomethane, SDS- Sodium lauryl sulphate

- To make 1X running buffer: add 100 ml of 10X running and make up to 1 L of ultrapurified water (pH should be 8.3).

5. Wet Transfer buffer (10X)

Components	Molar	MW	Weigh out (g)
Tris base	250 mM	121.14	30.3
Glycine	1920 mM	75.07	144.1
Ultrapurified water			Add up to 800 ml

Tris base- Tris (hydroxymethyl) aminomethane

- To make 1X transfer buffer: add 100 ml of 10X transfer buffer and make up to 1 L of ultrapurified water (pH should be 8.3).
- Add 100% methanol and 0.05% v/v SDS to 1X wet transfer buffer freshly before make up to final volume.

6. Tris-buffered saline (TBS) for washing and probing (10X)

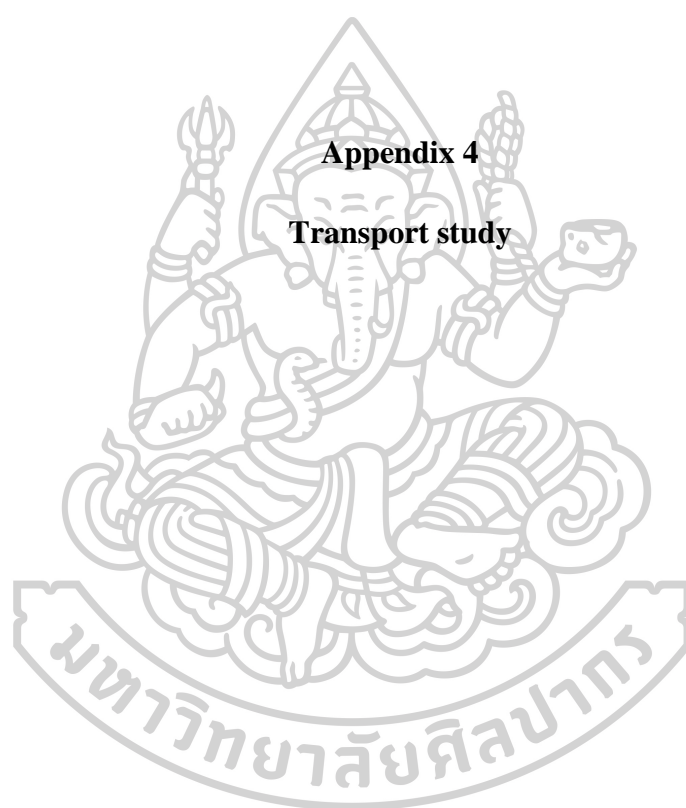
Components	Molar	MW	Weigh out (g)
Tris base	20 mM	121.14	24.23
NaCl	150 mM	58.45	87.67
ddH ₂ O			Add up to 1 L

Tris base- Tris (hydroxymethyl) aminomethane

- To make 1X TBS buffer: add 100 ml of 10X TBS and make up to 1 L of ultrapurified water (pH should be 7.8).
- To make Tris-buffered saline with 0.1% tween 20 (TBST): Add 1 ml of tween 20 to 999 ml of 1X TBS.

7. Blocking solution

- Prepare 5% Skim milk in TBST.



Bidirectional transport study

Passage	dQ/dt (nmol/min)				Passage	dQ/dt (nmol/min)			
	Dihydroxybergamottin		Oxypeucedanin			Dihydroxybergamottin + cyclosporine		Oxypeucedanin + cyclosporine	
	A-B	B-A	A-B	B-A		A-B	B-A	A-B	B-A
P-33	0.0274	0.0711	0.1484	0.4943	P-35	0.0713	0.1013	0.0727	0.1177
P-35	0.0614	0.1177	0.0411	0.1700	P-36	0.0665	0.0781	0.0692	0.1074
P-36	0.0601	0.1126	0.0438	0.154	P-37	0.0624	0.0991	0.069	0.1132

Inhibition study

Passage	dQ/dt (nmol/min)					
	Concentration (μM)					
	0	5	25	50	100	200
Dihydroxybergamottin						
P - 39	0.0394	0.0388	0.031	0.0244	0.0161	0.0125
P - 40	0.0421	0.0408	0.0310	0.0247	0.0183	0.0126
P - 41	0.0428	0.0389	0.0323	0.0240	0.0171	0.0127
Oxypeucedanin						
P - 39	0.0394	0.0413	0.0316	0.0252	0.0218	0.0132
P - 40	0.0421	0.0436	0.0323	0.0262	0.0186	0.0135
P - 41	0.0428	0.0422	0.0329	0.0254	0.0189	0.0138

VITA

NAME	May Phyu Thein Maw
DATE OF BIRTH	2 February 1984
PLACE OF BIRTH	Mandalay, Myanmar
INSTITUTIONS ATTENDED	Faculty of Pharmacy, Silpakorn University
HOME ADDRESS	No. 3 (Sa), Corner of 28th and 64th street, Mandalay, Myanmar
PUBLICATION	<p>Maw MPT, Sukonpan C, Piyapolrunroj N. Possible Intestinal Absorption Enhancers from Citrus hystrix. E3S Web of Conferences. 2020;141:02003.</p> <p>Maw MpT, Sotanaphun U, Piyapolrunroj N. Natural Furanocoumarin as Potential Oral Absorption Enhancer. Key Engineering Materials. 2019;819:63-9.</p> <p>Piyapolrunroj N, Phatanawasin P, Sotanaphun U, Maw MPT. Role of citrus limonoid as a possible bioavailability enhancer. 2020.</p> <p>Maw MPT, Charsangbong K, Kasilerk J, Chavalit P, Piyapolrunroj N. Effect of candelabra bush (Senna alata) herbal infusion tea on the functions of multidrug resistance proteins. Thai Journal of Pharmaceutical Sciences. 2018;42.</p> <p>Maw MPT, Piyapolrunroj N. Effect of Gymnema inodorum on P-glycoprotein Function: an In Vitro Study. Thai Journal of Pharmaceutical Sciences. 2017;41.</p>

